UNIVERSITY OF OKLAHOMA

GRADUATE COLLEGE

# SELECTIVE CONVERSION OF UNSATURATED CARBOXYLIC ACIDS TO OLEFINS OR DIOLEFINS

A THESIS

SUBMITTED TO THE GRADUATE FACULTY

in partial fulfillment of the requirements for the

Degree of

MASTER OF SCIENCE

By

MONICA CHIDURALA
Norman, Oklahoma
2018

Downloaded from SHAREOK. Persistent Handle URL: https://hdl.handle.net/11244/299815

SELECTIVE CONVERSION OF UNSATURATED CARBOXYLIC ACIDS TO OLEFINS OR DIOLEFINS

A THESIS APPROVED FOR THE
SCHOOL OF CHEMICAL, BIOLOGICAL AND MATERIALS ENGINEERING

BY

_____
Dr. Steven Crossley, Chair

_____
Dr. Daniel Resasco

_____
Dr. Bin Wang

© Copyright by MONICA CHIDURALA 2018
All Rights Reserved.

To my caring parents, Sudhakar and Vijaya, and my brother, Rahul.

Thanks for all the love, encouragement, and support.

Dedicated to the memory of my grandfather, Badriah Komakula, who always believed in my ability to succeed. You are no longer with us but your belief in me has made this journey possible.

## Acknowledgements

I would like to thank my advisor, Dr. Steven Crossley, who gave me this wonderful opportunity to pursue a Master of Science degree in Chemical Engineering at the University of Oklahoma. Thank you for your kindness and sharing your knowledge with me during my journey as a student. Your passion and enthusiasm for this work has encouraged me to work hard to reach my potential. Thank you for being patient, motivating, and supporting me the past two years while also enriching my learning experience overall. It was an honor learning from you.

I would also like to thank my committee members, Dr. Resasco and Dr. Wang, for their valuable guidance in this research. Thank you for taking the time to review my results in group meetings and for also evaluating my thesis.

I would like to specially thank all the biofuels group members: Lawrence Barrett, Dr. Nick Briggs, Zheng Zhao, Valeria Herrera, Tania Erazo, Santiago Umbarila, Danny Plus, Felipe Anaya, Dr. Abishek Gumidyala, Nhung Duong, Alejandra Gomez, Ismaeel Alalq, Gap Warakunwit, Michael Zeets, Tong Mou, Tuong Bui, Reda Bababrik, Rajiv Janupala, Cristiane Scaldaferri, Feifei Yang, Camila Abreu, and Carla Herrera. Thank you for your constant help around the lab and for transferring your knowledge. My special thanks to Lawrence for conducting TEM, EDX, and TG of my samples, to Tong for VMD illustrations of the concepts, and to Carla, Feifei, Cristiane, and Camila for valuable discussions to help me improve my experimental methods and analysis. I also want to thank my friends I have met at OU: Jennifer Qiao, Hailey Wang, Wen Yang, Kayla Foley, and Kevin Zhou for your precious friendship and support.

I want to acknowledge my funding source, National Science Foundation, for supporting my work, and the University of Oklahoma for providing me with the opportunity to contribute to academia.

I want to acknowledge my family for moving thousands of miles 15 years ago to give my brother and I a better opportunity to excel in our studies and lives. I am grateful for all that you have done for me.

## Table of Contents

Acknowledgements ..... iv

List of Tables ..... ix

List of Figures ..... x

Abstract ..... xvi

Chapter 1: Introduction ..... 1

1.1 Biomass as an alternative ..... 5

1.1.1 Processing the biomass ..... 5

1.1.2 Production of γ-valerolactone (GVL), an important platform molecule ..... 7

1.1.3 Ring opening of γ-valerolactone (GVL) to produce pentenoic acids ..... 10

1.1.4 Motivation and scope of work ..... 12

Chapter 2: Enhancing pentanol production rate by cofeeding alcohols in the presence of pentanoic acid in the liquid phase ..... 15

Abstract ..... 15

2.1 Introduction ..... 16

2.2 Experimental ..... 21

2.2.1 Catalyst preparation ..... 21

2.2.2 Catalyst characterization ..... 21

2.2.3 Catalytic activity measurement ..... 23

2.3 Results and discussion ..... 24

2.3.1 Catalyst characterization results ..... 24

2.3.2 Catalytic results and discussion ..... 27

2.3.3 Equilibrium test ..... 41

2.3.4 Effect of water on the hydrogenation of PEA and esters to alcohols ..... 41
2.3.5 Mechanism and location of the active site ..... 43
2.4 Conclusion ..... 46
2.5 Future Directions ..... 47
Chapter 3: Enhancing propanol production rate by cofeeding alcohols in the presence of propionic acid in the gas phase ..... 48
Abstract ..... 48
3.1 Introduction ..... 49
3.2 Experimental ..... 53
3.2.1 Catalyst preparation ..... 53
3.2.2 Catalyst characterization ..... 53
3.2.3 Catalytic activity measurement ..... 55
3.3 Results and Discussion ..... 56
3.3.1 Catalyst characterization results ..... 56
3.3.2 Catalytic results and discussion ..... 59
3.4 Conclusion & Future Direction ..... 66
Chapter 4: Identification of the active site on copper chromite ..... 68
Abstract ..... 68
4.1 Introduction ..... 69
4.2 Experimental ..... 70
4.2.1 Catalyst preparation ..... 70
4.2.2 Catalyst characterization ..... 71
4.3 Results and Discussion ..... 73

4.3.1 Catalyst characterization results ..... 73
4.3.2 Catalyst activity results ..... 77
4.4 Conclusion & Future Direction ..... 79
Chapter 5: Concluding Remarks ..... 81
Chapter 6: Future Direction ..... 83
References ..... 85
Appendix A1: Preliminary Studies ..... 94
A1.1 Literature Review ..... 94
A1.2 Preliminary Results and Discussion ..... 96
Appendix A2: Supporting information for Chapter 1: Enhancing pentanol production rate by cofeeding alcohols in the presence of pentanoic acid in the liquid phase ..... 102
Appendix A3: Supporting information for Chapter 2: Enhancing propanol production rate by cofeeding alcohols in the presence of propionic acid in the gas phase 108
Appendix References ..... 109

## List of Tables

Table 1: Yields of ethylene, propylene, 1,3-butadiene (BTD), and C4 olefins from different feedstocks[5] ..... 4

Table 2: Summary of PEA parameters, reaction rate constant (k) and activation energy ($E_a$) for PEA → pentanol + pentyl-pentanoate ..... 35

Table 3: Results at longer reaction times when no alcohol was present ..... 41

Table 4: Summary of PrA parameters, reaction rate constant (k) and activation energy ($E_a$) for PrA → propanol + propyl-propanoate ..... 66

## List of Figures

Figure 1: Methods of producing olefins and diolefins in the industry[2] ..... 1

Figure 2: Octane cracks into pentane and propylene in the presence of a catalyst[3] ..... 2

Figure 3: Catalytic dehydrogenation (reforming) of butane to produce butene and 1,3-butadiene[3] ..... 2

Figure 4: Ethylene and Butadiene prices (thousands of $/tonnes) from 1988-2011[5] ..... 3

Figure 5: Reaction pathway to produce γ-valerolactone (GVL) from lignocellulosic biomass (hemicellulose and cellulose)[16] ..... 8

Figure 6: Conversion of biomass (green) to chemicals (orange) and fuels (yellow) from sugars (blue)[17] ..... 8

Figure 7: Pathways to produce GVL from LA[16] ..... 10

Figure 8: Conversion of GVL to pentenoic acids and 1-butene via proton-mediated elementary steps[43] ..... 12

Figure 9: Motivation of the project ..... 13

Figure 10: Scope of the project ..... 14

Figure 11: Order of the polarizability of the carbonyl group from most reactive to least reactive[52] ..... 18

Figure 12: Temperature programmed reduction (TPR) of the copper chromite ..... 24

Figure 13: The X-ray diffraction data for the copper chromite samples: 1 - fresh copper chromite, 2 - spent catalyst after reaction ..... 25

Figure 14: Energy-dispersive X-ray spectroscopy (EDX) of copper chromite ..... 26

Figure 15: Reaction pathway showing the reduction of pentanoic acid, 3-methylphenyl valerate, and pentyl pentanoate to pentanol ..... 27

Figure 16: Reaction pathway showing the reduction of pentanoic acid, ethyl-valerate, and pentyl-pentanoate to pentanol ..... 27

Figure 17: Yield of pentanol product on copper chromite catalyst using various feeds. Reduction: 100 mg $2CuO{\cdot}Cr_2O_3$ at 280 °C under 300 psi $H_2$ for 2 hrs. Reaction: 250 °C for 2 hrs under 450 psi $H_2$. Feeds include: 0.421 M Ethyl-Valerate, 0.453 M Pentanoic Acid + excess ethanol (1:5 molar ratio), 0.424 M Pentanoic Acid, and 0.465 M Pentyl-Pentanoate ..... 28

Figure 18: Rate of formation of pentanol on copper chromite catalyst using various feeds. Reduction: 100 mg $2CuO{\cdot}Cr_2O_3$ at 280 °C under 300 psi $H_2$ for 2 hrs. Reaction: 250 °C for 2 hrs under 450 psi $H_2$. Feeds include: 0.421 M Ethyl-Valerate, 0.453 M Pentanoic Acid + excess ethanol (1:5 molar ratio), 0.424 M Pentanoic Acid, and 0.465 M Pentyl-Pentanoate ..... 29

Figure 19: Rate appearance of products when 0.1 M PEA is cofed with various molar ratios of water ($H_2O$), glycerol, m-cresol, and ethanol (EtOH) in decalin solvent. Reduction: 100 mg $2CuO{\cdot}Cr_2O_3$ at 280 °C under 300 psi $H_2$ for 2 hrs. Reaction: 250 °C for 1 hr under 450 psi $H_2$. Carbon balances wrt PEA: >90%. ..... 31

Figure 20: Rate appearance of pentanol when 0.103 M Pentanoic Acid (PEA) is co-fed with various molar ratios of ethanol and 1-dodecanol in decalin solvent, and m-cresol in n-dodecane solvent. Reduction: 100 mg $2CuO{\cdot}Cr_2O_3$ at 280 °C under 300 psi $H_2$ for 2 hrs. Reaction: 250 °C for 1 hr under 450 psi $H_2$. Carbon balances with respect to PEA: >90% ..... 32

Figure 21: Reaction pathway showing the reduction of pentanoic acid, dodecyl-valerate, and pentyl-pentanoate to pentanol ..... 33

Figure 22: Zeroth order regime with respect to pentanoic acid..... 34

Figure 23: Rate appearance of esters when 0.103 M Pentanoic Acid (PEA) is co-fed with various molar ratios of ethanol and 1-dodecanol in decalin solvent, and m-cresol in n-dodecane solvent. Reduction: 100 mg $2CuO{\cdot}Cr_2O_3$ at 280 °C under 300 psi $H_2$ for 2 hrs. Reaction: 250 °C for 1 hr under 450 psi $H_2$. Carbon balances with respect to PEA: >90%..... 40

Figure 24: Effect of water on product distributions at 0.33 molar ratio of EtOH to PEA ..... 42

Figure 25: Proposed mechanism for the reduction of esters to alcohols[89] ..... 45

Figure 26: Order of the polarizability of the carbonyl group from most reactive to least reactive[52] ..... 50

Figure 27: Temperature programmed reduction (TPR) of the copper chromite ..... 57

Figure 28: The X-ray diffraction data for the copper chromite samples: 1 - fresh copper chromite, 2 - spent catalyst after reaction..... 58

Figure 29: Energy-dispersive X-ray spectroscopy (EDX) of copper chromite..... 59

Figure 30: Reaction pathway showing the reduction of propionic acid, butyl propanoate, and propyl propanoate to propanol..... 60

Figure 31: Yield of products (%) when flowing 0.0013 mol/hr of propionic acid. Reduction: 50 mg of copper chromite, 400 °C, 1 hour, 100 stcm $H_2$..... 61

Figure 32: Yield of propanol (%) when flowing 0.0013 mol/hr of propionic acid alone and when flowing 0.0013 mol/hr of propionic acid and 0.00067 mol/hr 1-butanol (1:0.5 molar ratio). Reduction: 50 mg of copper chromite, 400 °C, 1 hour, 100 stcm $H_2$. Reaction: 300 °C, 100 stcm $H_2$..... 62

Figure 33: Zeroth order regime with respect to Propionic Acid (PrA) at 32 min. ..... 64

Figure 34: Arrhenius Plot, PrA = 0.000102 mol/hr, Reduction: 5 mg of copper chromite, 400 °C, 1 hour, 100 stcm $H_2$. Reaction: 250, 280, and 300 °C, 100 stcm $H_2$..... 65

Figure 35: Temperature programmed reduction (TPR) of the copper chromite and 10% $Cu/SiO_2$..... 74

Figure 36: The X-ray diffraction data for the copper chromite samples: 1 - fresh copper chromite, 2 - spent catalyst after reaction..... 75

Figure 37: Energy-dispersive X-ray spectroscopy (EDX) of copper chromite..... 76

Figure 38: Particle size effect of copper on pentanol production rate. Reduction: 300 mg x wt.% $Cu/SiO_2$ at 280 °C under 300 psi $H_2$ for 2 hrs. Reaction: 250 °C for 1 hr under 450 psi $H_2$. Feed: 0.101 M PEA. Carbon balances with respect to PEA: >90%..... 77

Figure 39: Comparing activity of 10% Cu/SiO2 vs. copper chromite. Reduction: 300 mg 10% $Cu/SiO_2$ or 100 mg copper chromite at 280 °C under 300 psi $H_2$ for 2 hrs. Reaction: 250 °C for 1 hr under 450 psi $H_2$. Feed: 0.101 M PEA. Carbon balances with respect to PEA: >90%. ..... 78

Figure 40: Yield of products and conversion of pentanoic acid (indicated in the bars) over different amounts of zeolite H-Beta. Reaction conditions: 0.5 M pentanoic acid, 6 M m-cresol, 250 °C, 3 hours, under 500 psi $N_2$ ..... 96

Figure 41: Selectivity of products over different amounts of zeolite H-Beta. Reaction conditions: 0.5 M pentanoic acid, 6 M m-cresol, 250 °C, 3 hours, under 500 psi $N_2$.... 97

Figure 42: Yield of ethyl-valerate and conversion of pentanoic acid (indicated in the bars) from the esterification of pentanoic acid and ethanol on various Lewis acidic

catalysts. 50 mg of catalyst, 0.569 M pentanoic acid, 0.381 M ethanol (1:1.5 acid to alcohol molar ratio) in decalin. Reaction conditions: 250 °C for 1 hour ..... 98

Figure 43: Selectivity to products on 5% Ru on various supports. 100 mg of catalyst, reduced at 280 °C under 300 psi $H_2$ for 3 hours, and 0.4 M ethyl-valerate reacted at 250 °C for 4 hours. ..... 98

Figure 44: Solvent effects on the reduction of ethyl-valerate on 100 mg 5% Ru/TiO2. Reduced at 280 °C under 300 psi $H_2$ for 2 hours, and 0.4 M ethyl-valerate reacted at 250 °C for 1 hour. ..... 99

Figure 45: Comparing selectivity of products on 5% $Ru/TiO_2$ to a copper chromite catalyst. 100 mg 5% $Ru/TiO_2$ reduced at 280 °C under 300 psi $H_2$ for 2 hours, reacted at 250 °C for 30 min. 100 mg $2CuO{\cdot}Cr_2O_3$ reduced at 280 °C under 300 psi $H_2$ for 2 hours, reacted at 250 °C for 30 min. ..... 100

Figure 46: Product distribution on copper chromite catalyst using various feeds. Reduction: 100 mg $2CuO{\cdot}Cr_2O_3$ at 280 °C under 300 psi $H_2$ for 2 hrs. Reaction: 250 °C for 2 hrs under 450 psi $H_2$. Feeds include: 0.421 M Ethyl-Valerate, 0.453 M Pentanoic Acid + excess ethanol (1:5 molar ratio), 0.424 M Pentanoic Acid, and 0.465 M Pentyl-Pentanoate ..... 102

Figure 47: Selectivity of products on copper chromite catalyst using various feeds. Conversion of reactants are shown in Section 2.3. 100 mg $2CuO{\cdot}Cr_2O_3$ reduced at 280 °C under 300 psi $H_2$ for 2 hours, reacted at 250 °C for 2 hours. Feeds include: 0.421 M Ethyl-Valerate, 0.453 M Pentanoic Acid + excess ethanol (1:5 molar ratio), 0.424 M Pentanoic Acid, 0.465 M Pentyl-Pentanoate ..... 103

Figure 48: Yield of products and conversion of PEA (%) at various molar ratios of m-cresol to PEA ..... 103
Figure 49: Yield of products and conversion of PEA (%) at various molar ratios of ethanol to PEA ..... 104
Figure 50: Yield of products and conversion of PEA (%) at various molar ratios of 1-dodecanol to PEA ..... 104
Figure 51: Rate disappearance of PEA vs. concentration of PEA, zeroth order regime, reaction rate = k ..... 105
Figure 52: Rate appearance of products vs. concentration of PEA at various concentrations of PEA, zeroth order regime with respect to PEA ..... 105
Figure 53: Yield of products and conversion of PEA (%) at various concentrations of PEA, zeroth order regime with respect to PEA ..... 106
Figure 54: Effect of various ratios of water to PEA on pentanol production rates ..... 106
Figure 55: Effect of various ratios of water to PEA on product yields and PEA conversion ..... 107
Figure 56: Yield of products (%) when flowing 0.0013 mol/hr of propionic acid and 0.00067 mol/hr 1-butanol (1:0.5 molar ratio). Reduction: 50 mg of copper chromite, 400 °C, 1 hour, 100 stcm $H_2$. Reaction: 300 °C, 100 stcm $H_2$ ..... 108
Figure 57: Yield of propyl-propionate (%) when flowing 0.0013 mol/hr of propionic acid alone and yield of butyl-propionate (%) when flowing 0.0013 mol/hr of propionic acid and 0.00067 mol/hr 1-butanol (1:0.5 molar ratio). Reduction: 50 mg of copper chromite, 400 °C, 1 hour, 100 stcm $H_2$. Reaction: 300 °C, 100 stcm $H_2$ ..... 108

## Abstract

Biomass is composed of pentosans and hexosans that can be converted to γ-valerolactone (GVL) via an acid-catalyzed dehydration and metal-catalyzed hydrogenation reactions.[16,17] Through acid catalysis, GVL can undergo ring-opening to produce isomers of pentenoic acids.[43] These pentenoic acids can be converted to olefins or diolefins such as butadiene or pentadiene, both of which are petrochemical intermediates used in the industry. This research focuses on converting pentanoic acid, the hydrogenated form of pentenoic acid, to alcohols so they can be dehydrated to produce alkenes and alkynes.

Direct conversion of carboxylic acids to olefins and diolefins is difficult due to the low electrophilicity of the carbonyl carbon.[51,52,72,90-92] This can be intercepted by creating an ester intermediate, which has a lower activation energy than its carboxylic acid counterpart.[51] Various molar ratios of alcohols (m-cresol, ethanol, and 1-dodecanol) were cofed with pentanoic acid to increase the pentanol production rate in the liquid phase. The effect of partial pressures of carboxylic acids on the alcohol production rate was also investigated. Finally, a mechanism and the location of the active site for these reactions was discussed using characterization techniques and literature.

# Chapter 1: Introduction

Light olefins and diolefins have many diverse applications in the petrochemical industry. They are used as starting materials in the syntheses of alcohols, plastics, detergents, and fuels. They are typically produced via processes involving endothermic alkane activation at elevated temperatures to overcome large kinetic barriers and to achieve favorable equilibrium products. The products are also more functionalized and more reactive than their parent alkanes, making the product selectivity difficult to control. Since the process requires a high energy demand, attaining high product yields is also challenging. Thus, the cost of these petrochemical intermediates is always higher than their parent alkanes and increases with functionality.[1]

As mentioned above, industrial methods of preparing olefins or diolefins entails hydrocarbon or steam cracking.[2]

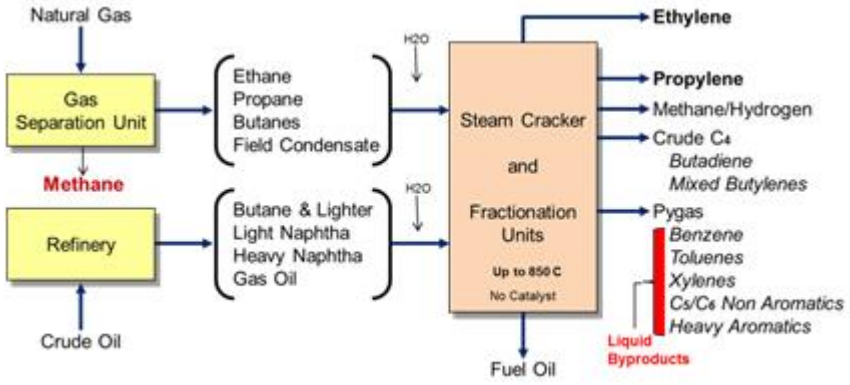



**Figure 1: Methods of producing olefins and diolefins in the industry[2]**

A hydrocarbon feed enters the reactor and the alkanes are broken apart at elevated temperatures in the presence of a catalyst to produce a mix of aliphatic alkenes and low molecular weight alkanes. See Figure 2 below.[3]

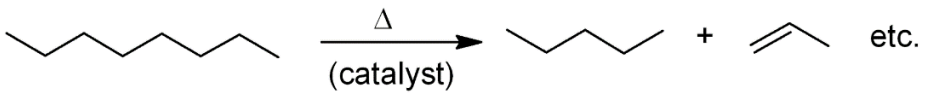



**Figure 2: Octane cracks into pentane and propylene in the presence of a catalyst[3]**

After separation, the products undergo catalytic dehydrogenation, also known as reforming, to produce olefins and diolefins.[3]

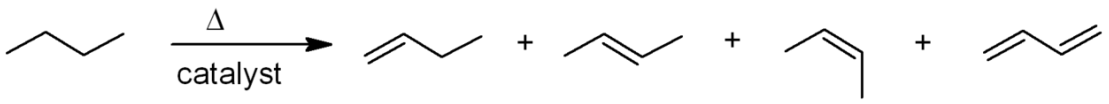



**Figure 3: Catalytic dehydrogenation (reforming) of butane to produce butene and 1,3-butadiene[3]**

Light hydrocarbon feeds such as ethane give product streams rich in light alkenes, while heavier hydrocarbon feeds such as naphtha give product streams rich in heavy alkenes.[3] 1,3-Butadiene is one of the largest commodity chemicals produced in the United States. Most of it is obtained from a mix of butenes stream that is a by-product of ethylene production. Butadiene has a major use in the manufacturing of synthetic rubber and other polymers. It is also used to manufacture a nonpolymeric compound called adiponitrile, an intermediate in nylon production. In addition, it is also used in a small-scale production of an industrial solvent called sulfolane.[4]

Prior to 2003, there was a sufficient supply of butadiene and the need was satisfied from the cracking of naphtha and other heavy hydrocarbon feeds in steam cracking operations. From 2003 to 2008, both ethylene and butadiene prices increased at a similar rate (Figure 4). After 2008, as a consequence of the global financial crisis (GFC), butadiene prices doubled to over $2000/ton. By 2011, butadiene prices have skyrocketed to over $4000/ton. This is due to the industry shifting towards lighter feedstocks such as ethane,

instead of the traditional feedstock naphtha. The shift in the feedstock is due to the expansion of natural gas production and the recent shale gas boom where the heavier feedstocks can be used as fuels in their own right. This clearly benefited the ethylene production and has kept the ethylene prices low; however, propylene, butene, and butadiene productions suffered tremendously. Figure 4 shows the sored prices of butadiene in comparison with ethylene by 2011.[5]

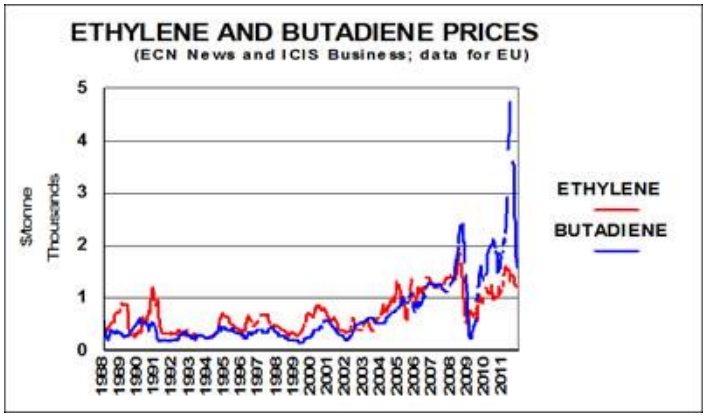



**Figure 4: Ethylene and Butadiene prices (thousands of $/tonnes) from 1988-2011[5]**

Table 1 shows the yields of various olefins from various feedstocks. As discussed above, heavier feedstocks such as naphtha and gas oil have a butadiene or C4 olefins yield of approximately 8% compared to lighter feedstocks such as ethane and propane, which have a butadiene yield of around 3-4%. This not only justifies the reason for a low supply of butadiene in the recent years but also explains how the shift in feedstocks (from heavy to light) can have a profound impact on butadiene production.[5]

As long as ethane is a cheaper feedstock compared to the rest, supply of butadiene and heavier olefins will continue to be limited and expensive.

| | ETHANE | PROPANE | BUTANE | NAPHTHA | GAS OIL |
|---|---|---|---|---|---|
| **Ethylene** | 76.80% | 44.29% | 44.33% | 30.19% | 20.17% |
| **Propylene** | 2.61% | 13.73% | 14.89% | 15.46% | 14.48% |
| **BTD/C4 olefins** | 2.61% | 3.99% | 6.65% | 7.67% | 7.95% |

**Table 1: Yields of ethylene, propylene, 1,3-butadiene (BTD), and C4 olefins from different feedstocks[5]**

Currently, there is an opportunity to satisfy the need for butadiene and/or heavier diolefins. In order to meet the demand for heavier olefins and diolefins, alternative technologies can be explored and studied. Although we can increase butadiene dehydrogenation using the butane streams, this may be an expensive route to explore since it requires complex steps such as distillation and extraction.[6] Some of the other alternative technologies involve using acetylene from coal or natural gas as a feedstock.[5] In a process known as the Lebedev process[7], ethanol can be used as a feedstock to dehydrate to acetaldehyde followed by aldol condensation and dehydration to butadiene. Ethanol can be derived from bio-based resources, which is cost-effective, renewable and a simple alternative. However, the metal oxide catalyst used in this process undergoes quick deactivation due to coke deposition. Thus, regenerating the catalyst takes time and energy, increasing the cost of the process.[7,8] In the Reppe process, aqueous formaldehyde and gaseous acetylene are combined to produce 1,4-butanediol in the presence of a copper (II) oxide supported on silica with 3%-6% bismuth oxide. 1,4-Butanediol can undergo dehydration to make 1,4-butadiene. Although this is a dominant process in the industry,

acetylene and formaldehyde have serious environmental, safety, and economic implications.[9]

Although these processes already exist, a novel approach can be created using bio-based technologies that can avoid all such consequences. It is because bio-based technologies are cheaper, environmentally friendly, tremendously abundant, and renewable.

## 1.1 Biomass as an alternative

As the world population is increasing and the economies of various countries are developing, energy consumption has been escalating despite the limited availability of fossil fuels. Biomass is a promising alternative feedstock that can be explored in further detail. It has low Sulphur content; therefore, it would have low emissions of $SO_2$. It also consists of less nitrogen and ash; thus, the $NO_x$ and soot emissions would also be lower compared to the combustion of fossil fuels. Since the carbon dioxide released from plants will be recycled into the biomass via photosynthesis, there should also be a carbon dioxide net emission of zero. Thus, biomass is an extremely promising alternative because it is clean, environmentally friendly, renewable, and greatly abundant.[10,11]

Biomass can be used to compensate for the low supply of petrochemical intermediates caused by the shift towards using lighter feedstocks. Since it is difficult to produce olefins selectively at elevated temperatures, it may be likely to accomplish this using biomass at lower temperatures.[11]

### *1.1.1 Processing the biomass*

The three main components of the lignocellulosic biomass are: lignin (10-25 wt.%), cellulose (40-60 wt.%), and hemicellulose (20-40 wt.%). Typically, studies involving pyrolysis of biomass is broken down into four parts: lignin decomposition, cellulose

decomposition, hemicellulose decomposition, and evolution of moisture.[11] In a process known as the fast pyrolysis, the biomass is rapidly heated at elevated temperatures in anaerobic conditions, producing a lot of vapor products and charcoal. In addition, short vapor residence times and reactor temperatures below 400 °C can produce liquid products. Cooling and condensing the products result in a dark-brown bio-oil and can be attained in the yields of up to 75 wt.% of the dry-feed. The liquid product yields depend on the type of biomass feedstock used, reaction temperature, vapor residence times, catalysts used, and ash content.[11-14] While this process can be more economical since everything can be done in one step, it would be very expensive to separate the products from the complex bio-oil mixture with high yields and selectivities.[15,18]

While there are alternative ways, one of the effective ways to prevent this problem and to isolate the organic compounds is to process the biomass in two steps. The first step is to breakdown the biomass into its three main components.[16-17] This can be done by pretreating biomass using steam, hot water, ammonia fiber explosion, or ionic liquid pretreatments. Acidic treatments are usually efficient and cost-effective.[17,19-24]

The second step is to fractionate each component separately to obtain products of interest.[16-17] Cellulose is made up of glucose monomers linked by β-(1,4)-glycosidic bonds. Hemicellulose is made up of xylose monomers, $C_5$ sugars, and $C_6$ sugars. Dilute acids such as oxalic, sulfuric, and phosphoric acid, can separate hemicellulose from the other components while slightly separating lignin from cellulose, making it easier to hydrolyze cellulose for the next step. Cellulose can be hydrolyzed using a mineral acid catalyst to release the glucose monomers.[17,23,25-27]

Biomass processing (pyrolysis, torrefaction, pre-treatment steps, etc.) is currently an active area of research. However, the details of such topic are outside the scope of this project. Nevertheless, it is still important to mention and requires attention because it is the initial step in obtaining the valuable platform molecules and intermediates that are used to accomplish the goals of this project.

### *1.1.2 Production of γ-valerolactone (GVL), an important platform molecule*

As mentioned in the previous section, upon decomposing lignin, cellulose, and hemicellulose, a variety of chemical compounds are obtained. Hemicellulose is composed of xylose, $C_5$, and $C_6$ sugar monomers while cellulose is composed of glucose ($C_6$ sugar) monomers. These sugars can be converted to intermediate organic compounds shown in Figure 5 under mild conditions. While these intermediate molecules are less reactive than their parent sugars, they are functional enough to be converted into chemicals that have a practical purpose in the industry shown in yellow in Figure 6.[16-17]

While there are many chemicals that can be produced, the compound of interest for the purposes of this project is γ-valerolactone (GVL). GVL is an important platform molecule that can be produced from a metal-catalyzed reaction of levulinic acid or ethyl levulinate in the presence of hydrogen. These intermediate molecules can be obtained from hemicellulose and cellulose as shown in Figure 5. GVL is an excellent precursor to many fuels and chemicals that have a high demand in the industry (Figure 6). Upgrading cellulose and hemicellulose to levulinic acid or ethyl levulinate and further upgrading these compounds to GVL is an active area of research that can have an enormous impact on the economics and feasibility of biomass conversion.[16,17,28-31]

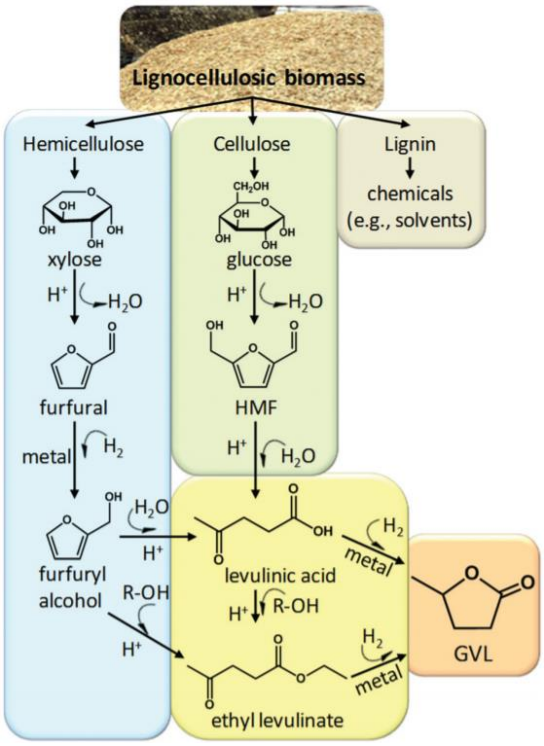



**Figure 5: Reaction pathway to produce γ-valerolactone (GVL) from lignocellulosic biomass (hemicellulose and cellulose)[16]**

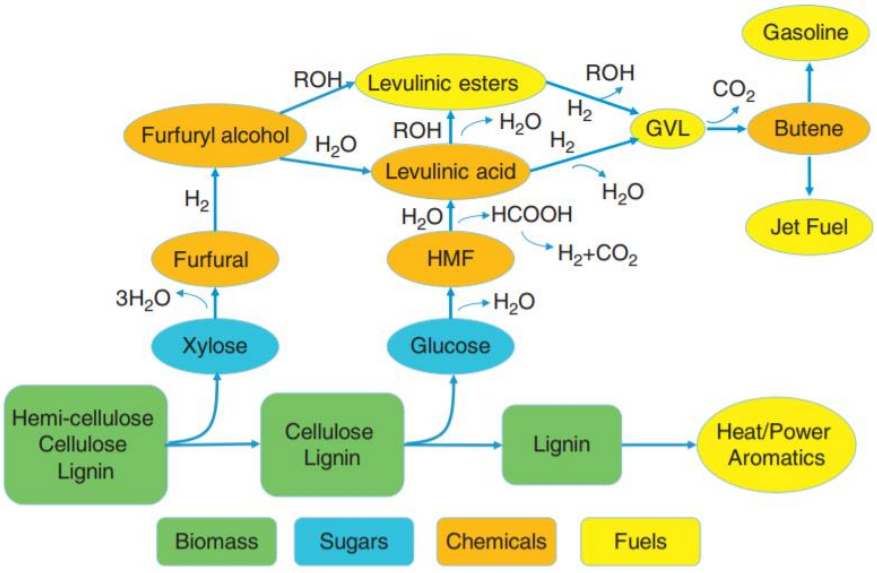



**Figure 6: Conversion of biomass (green) to chemicals (orange) and fuels (yellow) from sugars (blue)[17]**

GVL is a five-carbon cyclic ester that is very stable. There are many ways in which levulinic acid (LA) can be converted into GVL as shown in Figure 7. Hydrogenation of LA produces γ-hydroxyvaleric acid which undergoes dehydration and ring-closure to form GVL.[32] In another pathway, LA can be dehydrated to form α-angelica or β-angelica lactone, which can be hydrogenated to produce GVL. However, this pathway produces GVL in lower yields due to coking of the acid catalysts by the lactones.[33] In the third pathway, LA can be dehydrated and reacted with an alcohol to form levulinic esters which can be hydrogenated to form hydroxy levulinic esters. This compound undergoes ring-closure via intramolecular transesterification to release GVL and alcohol.[34,35] In the last pathway, olefinic acids can undergo ring-closure to also form GVL. These olefinic acids are usually 5-carbon unsaturated acids such as 4-petenoic acids.[16,36,37]

Studies have explored the use of both heterogeneous and homogeneous catalysts for this reaction. Ruthenium[38] based catalysts showed the most promise in producing GVL at high yields while platinum[39] and palladium[39] catalysts hydrogenated both LA and GVL, forming side products. Some studies have shown that adding acidity or phosphine ligands to the Ru-based catalysts showed improvement in GVL yields.[40,41] However, noble metal catalysts are extremely expensive and may or may not be available in the future. Therefore, it is not feasible to scale-up the process for industrial purposes.[16]

Some researchers studied copper-based catalysts, hoping to replace noble metal catalysts; however, they observed a prominent level of sintering, coking, and low selectivity towards GVL.[42] While it may be difficult to replace the use of noble metal catalysts, perhaps it will be an important research topic in the future to find alternative catalysts that are cost-effective and will allow the scale-up in the production of GVL.[16]

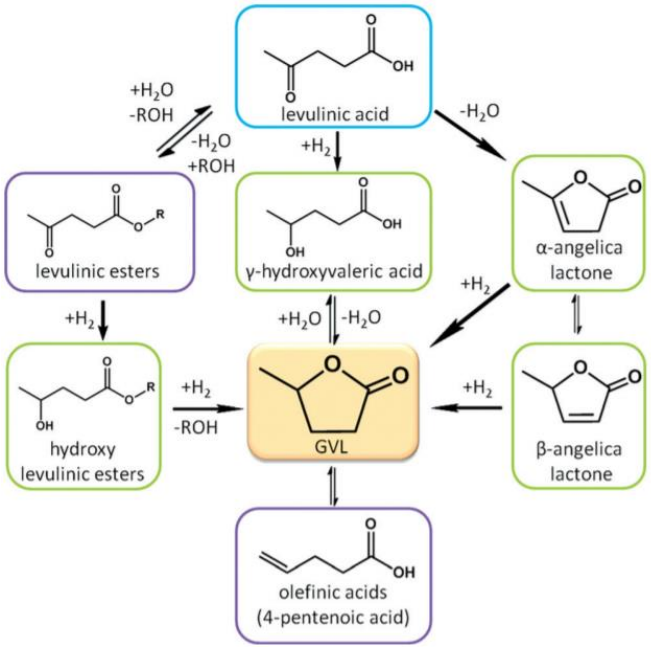



**Figure 7: Pathways to produce GVL from LA[16]**

*1.1.3 Ring opening of γ-valerolactone (GVL) to produce pentenoic acids*

In one pathway, GVL can undergo ring-opening to produce pentenoic acids in the presence of a heterogeneous acid catalyst. In another pathway, GVL can decarboxylate to produce butene and $CO_2$. The ring-opening could occur on bifunctional catalysts such as $Pt/SiO_2$ on H-ZSM-5, which have both acidic and hydrogenation characteristics. The reaction depends on the acidity and hydrogenation function of the catalyst, thus various ratios of H-ZSM-5 would lead to different yields of pentenoic acids. Having too much metal on the support would excessively hydrogenate GVL to methyl-tetrahydrofuran (mTHF), alkanes, and other alcohols. The catalyst also tends to hydrogenate the pentenoic acids to valeric acid. On a platinum catalyst supported on H-ZSM-5, selectivity of pentenoic acids was as high as 90% under the following reaction conditions: weight hourly space velocity of 2 $h^{-1}$, 10 bar $H_2$, and 523 K. Despite the use of zeolites, the reaction itself is not structure-selective.[30]

Bond *et al.*[43] performed microkinetic analysis on the ring opening of GVL to produce pentenoic acids. The study considered the kinetics of the reaction, the interconversion between GVL and pentenoic acids, and the thermochemistry of the compounds on a silica alumina catalyst in the gas phase. The ring opening of GVL and olefinic acids (pentenoic acids) ring closure occurs at the surface of the Bronsted sites via proton-mediated elementary steps.[43-45] Figure 8 shows the sequence of proton-mediated elementary steps: 1) ring opening, 2) hydride shift, 3) deprotonation, and 4) decarboxylation. The ring-opening and decarboxylation occur in parallel and are responsible for the observed products.[43]

Looking at the mechanism in Figure 8, GVL ring-opening should form a carbenium ion intermediate in the $C_4$ position. Then, through the process of hydride shifts, the intermediates can convert into isomers of pentenoic acids. These isomers can deprotonate to form stable pentenoic acid isomers.[43]

Furthermore, in the decarboxylation pathway, 1-butene is the primary product while isobutene is a secondary product. Bond *et al.*[43] suggest that the precursors to the decarboxylation pathways are also the carbenium ion species. When heterolytic cleavage occurs between $C_1$-$C_2$, electron density shifts into $C_2$-$C_3$ while stabilizing the carbenium at $C_3$, producing 1-butene and $CO_2$. These products are responsible in regenerating the Bronsted sites. If the decarboxylation is occurring via a different mechanism on the surface, then 1-butene and 2-butene are probably re-adsorbed and re-protonated due to longer contact times, causing hydride and alkyl shifts, producing various butene isomers.[43,44]

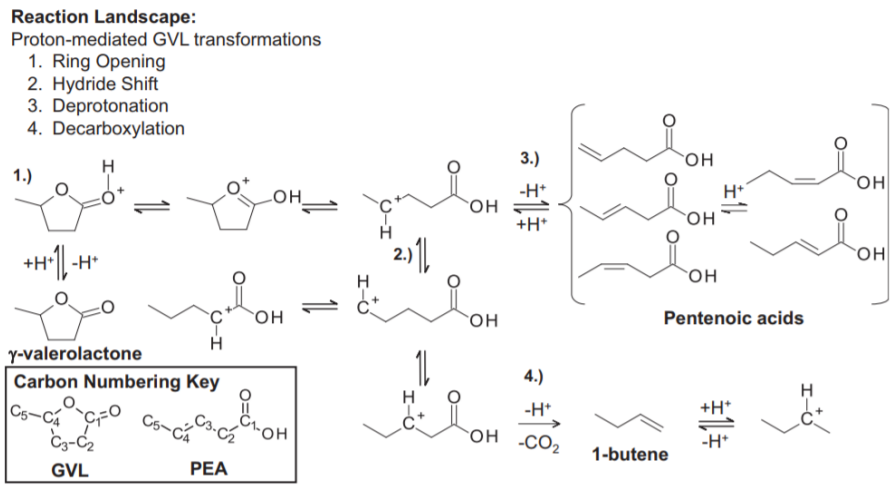



**Figure 8: Conversion of GVL to pentenoic acids and 1-butene via proton-mediated elementary steps[43]**

The pentenoic acid and valeric acid formed from the GVL ring-opening are important platform molecules for this project. They are not only the building blocks of various chemicals and fuels, but also the future of the biomass.

### *1.1.4 Motivation and scope of work*

Since heavy hydrocarbon feeds can be used as fuels in their own right, there is a shift to lighter feedstocks in the industry. While this may seem positive, the shift in feedstocks is impacting the production of heavier olefins and diolefins. The industry is not able to keep up with the needs of the growing populations and economy, resulting in soaring prices.[5] To satisfy this demand for olefins and diolefins, biomass can be used as an effective alternative source. It is clean, environmentally friendly, abundant, and still an active area of research. However, it can be extremely beneficial in the long run.[10,11]

Biomass is composed of cellulose, hemicellulose, and lignin. Hemicellulose is made up of xylose, $C_5$ (pentosan) sugars, and $C_6$ (hexosan) sugars, while cellulose is composed of $C_6$ (hexosan) sugars. After pre-treating and fractionating the biomass, these sugars can be

isolated.[11-18] Conversion of pentosans and hexosans to γ-valerolactone (GVL) can occur through an acid-catalyzed dehydration and metal-catalyzed hydrogenation reactions.[16,17] Through acid catalysis, GVL can undergo ring-opening to produce isomers of pentenoic acids.[43] These pentenoic acids can be converted to olefins or diolefins such as butadiene or pentadiene, both of which are petrochemical intermediates used in the industry.

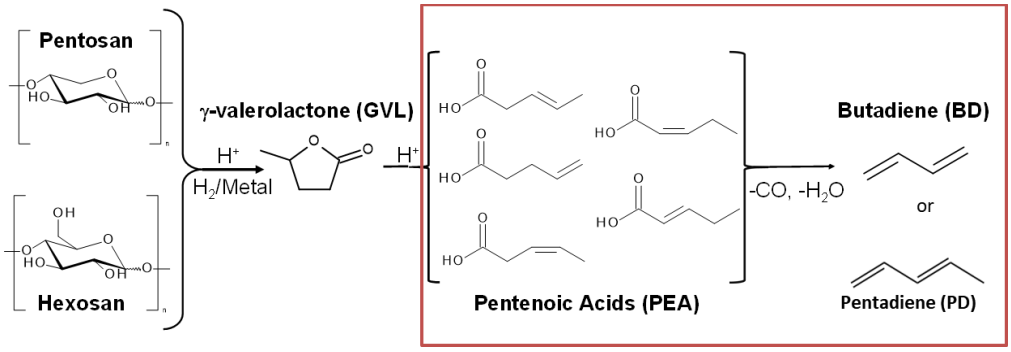



**Figure 9: Motivation of the project**

Dr. Jesse Q. Bond and his research team at the Syracuse University, College of Engineering and Computer Science, are working on the GVL ring-opening to produce pentenoic acids. The motivation of the project to convert these pentenoic acids to butadiene (BD) or pentadiene (PD).

Pentadiene, also known as piperylene, is a five-carbon diolefin. It is typically obtained from ethylene production from crude oil after several extractions, making it an expensive chemical to produce. Similar to BD, this heavier diolefin also has a high demand in the industry because it can be used as a monomer to manufacture adhesives, plastics, and resins. The conjugated system created by alternating double bonds make the molecules such as BD and PD extremely reactive, thus making them valuable commodities in the industry. They can undergo polymerization reactions to form various polymers.[4,5,46]

The scope of this project involves efficiently converting the pentanoic acids (PEA) to pentanol using a heterogeneous catalyst in the liquid and gas phase so that they can be dehydrated to form olefins or diolefins. Pentanoic acid (PEA), without the double bond, will be used for cost-saving measures.

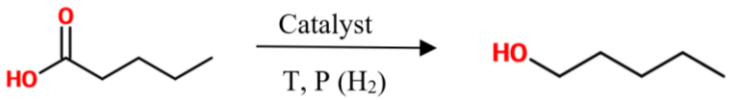
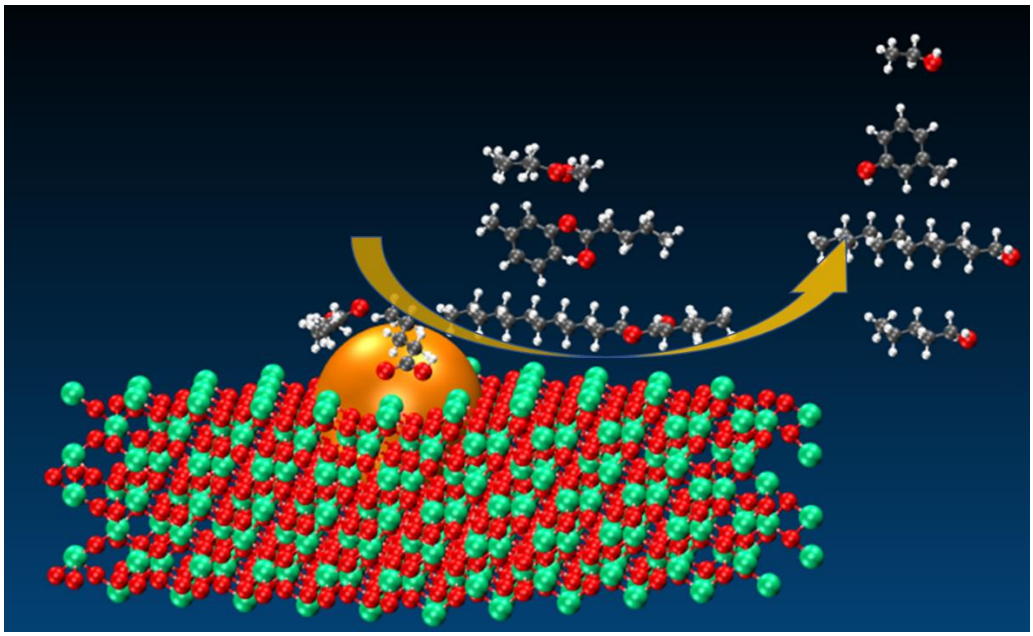



**Figure 10: Scope of the project**

## Chapter 2: Enhancing pentanol production rate by cofeeding alcohols in the presence of pentanoic acid in the liquid phase

### Abstract



Tong Mou created this illustration of the concepts covered in this manuscript.

Due to an increasing energy demand in our society, heavier hydrocarbon feedstocks are being used as fuels in their own right. This shift has caused the petrochemical industry to suffer from a low supply of petrochemical intermediates.[5] Biomass can be used to compensate for the low supply of petrochemical intermediates.[11] It is composed of cellulose, hemicellulose, and lignin. Hemicellulose is made up of xylose, $C_5$ (pentosan) sugars, and $C_6$ (hexosan) sugars, while cellulose is composed of $C_6$ (hexosan) sugars. After pre-treating and fractionating the biomass, these sugars can be isolated.[11-18] Conversion of pentosans and hexosans to γ-valerolactone (GVL) can occur through an acid-catalyzed dehydration and metal-catalyzed hydrogenation reactions.[16,17] Through acid catalysis, GVL can undergo ring-opening to produce isomers of pentenoic acids.[43]

These pentenoic acids can be converted to olefins or diolefins such as butadiene or pentadiene, both of which are petrochemical intermediates used in the industry. This study focuses on converting pentanoic acid, the hydrogenated form of pentenoic acid, to alcohols so they can be dehydrated to produce alkenes and alkynes.

Direct conversion of carboxylic acids to olefins and diolefins is difficult due to the low electrophilicity of the carbonyl carbon.[51,52,72,90-92] This can be intercepted by creating an ester intermediate, which has a lower activation energy than its carboxylic acid counterpart.[51] In this study, various molar ratios of alcohols (m-cresol, ethanol, and 1-dodecanol) were cofed with pentanoic acid to increase the pentanol production rate. The basis for this study came from Santiago *et al.*[51] and experiments that compared the yields of pentanol when pentanoic acid was directly injected versus when esters were directly fed. The results of this study indicate that at small molar ratios of alcohol to pentanoic acid, there is a slight enhancement in pentanol production rates due to an efficient production and adsorption of the ester. However, at high molar ratios of alcohol to pentanoic acid, all the species begin to compete for active sites and inhibit the reaction. These results can further be explained by Langmuir-Hinshelwood kinetics at zeroth order saturation conditions. Optimum pentanol production is important in producing alkenes and alkynes efficiently in the future as these can be selectively removed in a biphasic system.

## 2.1 Introduction

As the world population is increasing and economies are developing, energy consumption has been escalating despite the limited availability of fossil fuels. In addition, combustion of fossil fuels requires a lot of energy, releases a lot of heat, and increases the emissions

of greenhouse gases. Biomass is receiving increasing attention in the energy sector because it is a promising sustainable feedstock.[28] Biomass derived energy is clean, environmentally friendly, abundant, and renewable. Biofuels have maximum benefits in that they do not compete with food, do not cause "land grabbing," and lower greenhouse gas emissions if used correctly.[47] They also have less Sulphur content; therefore, $SO_2$ emissions would be lower. They also consist of less nitrogen and ash; thus, the $NO_x$ and soot emissions would be lower compared to the combustion of fossil fuels. Since the carbon dioxide released from plants will be recycled into the biomass via photosynthesis, there should also be a carbon dioxide net emission of zero.[10,11,28] Despite needing some policy changes to protect the environment, biofuels can be extremely beneficial in the sustainable development of our future.[47,48]

Currently in the industry, hydrocarbons feedstocks are used to produce petrochemical intermediates. Biorefining can produce the same petrochemical intermediates except in that biomass is used as an energy source rather than petroleum.[28,49,50] Biomass can also be used to compensate for the low supply of petrochemical intermediates caused by the shift towards using lighter hydrocarbon feedstocks as the heavier hydrocarbon feedstocks can be used as fuels in their own right.[11]

Lignocellulosic biomass, the most abundant feedstock[28], is composed of cellulose, hemicellulose, and lignin. Hemicellulose consists of xylose, $C_5$ (pentosan) sugars, and $C_6$ (hexosan) sugars, while cellulose is composed of $C_6$ (hexosan) sugars. After pre-treating and fractionating the biomass, these sugars can be isolated.[11-18] Conversion of pentosans and hexosans to γ-valerolactone (GVL) can occur through an acid-catalyzed dehydration and metal-catalyzed hydrogenation reactions.[16,17] Through acid catalysis, GVL can

undergo ring-opening to produce isomers of pentenoic acids.[43] These pentenoic acids can be converted to olefins or diolefins such as butadiene (BD) or pentadiene (PD), both of which are valued petrochemical intermediates in the industry. For the purposes of cost-saving measures, the experiments in this study utilized pentanoic acid (PEA).

Direct conversion of carboxylic acids to olefins and diolefins is difficult due to the low electrophilicity of the carbonyl carbon. Their low reactivity is associated with low polarizability of the carbonyl group. The order of polarizability of the carbonyl group in various functional groups is shown in the figure below. [51,52,72,90-92]

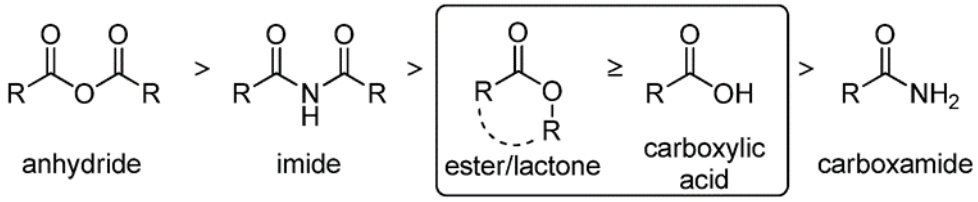



**Figure 11: Order of the polarizability of the carbonyl group from most reactive to least reactive[52]**

An ester can be more reactive than a carboxylic acid based on the -R group attached.[52] In addition, Santiago *et al.*[51] performed DFT calculations to obtain activation energies for dissociative adsorption of various carbonyl species on copper supported on silica. Copper is a great metal because it is low in oxophilicity.[51,81] It avoids decarbonylation and supports hydrogenation. Acetic acid had a high activation energy of 90-100 kJ/mol while the esters presented a much lower barrier. The barrier for methyl acetate was 70-80 kJ/mol and the barrier for ethyl acetate was 50-60 kJ/mol. Since carboxylic acids require a high activation energy for dissociative adsorption, they are more difficult to adsorb and react on the surface of copper.[51]

To reduce carboxylic acids and esters to alcohols, the C-O bond adjacent to the carbonyl group must be cleaved according to the following equation where the R-groups represent different alkyl groups.[51]

$$R_ACOOR_B + 2H_2 \leftrightarrow R_ACH_2OH + R_BOH^{51}$$

Many studies have shown that impregnating hydrogenation metals such as Zn, Co, Ni, Fe, and Cu on oxides such as $Cr_2O_3$, $ZrO_2$, $V_2O_5$, and $WO_3$, was effective in reducing esters and carboxylic acids to alcohols.[51,54-61] Turek *et al*[53] has shown that copper-based catalysts reduce carboxylic acids and esters to alcohols a lot more efficiently than some of the other hydrogenation catalysts.[53]

Individual studies regarding hydrogenolysis of monoesters have been performed in the mid to late 1900s. Lazier was the first to propose a copper oxide/zinc oxide catalyst to convert butyl butyrate to butanol. Schmidt proposed the use Ni, Co, and Cu for the reaction conditions: temperature range of 200 °C to 400 °C at atmospheric pressure. Barium-promoted copper chromite was used in several hydrogenolysis studies, and most showed that these catalysts can produce transesterification products. The hydrogenolysis of esters rate increased with increasing size of the -R groups. In addition, a lower rate was observed when the alkoxyl carbon had a methyl group, but a high rate was observed when the second alkoxyl carbon was branched. Overall, copper-based catalysts were shown in literature to be effective in cleaving the C-O bond adjacent to the carbonyl group of esters and carboxylic acids.

Copper chromite catalyst is one of the most widely used copper-based catalysts.[51,62] Adkins-type catalysts such as CuO and copper chromite ($CuCr_2O_4$) were discovered in the 1930s.[54] These catalysts are still used in the industry to manufacture alcohols even

though they exhibit low activity and require harsh operating conditions. This is because their catalytic structure is resistant to the free fatty acids.[55] Thus, the composition of these catalysts has remained unchanged since they were discovered.[72] In addition, copper supported on silica and Raney copper showed just as much promise as copper chromite in reducing esters.[51,63-71]

In this paper, we present results from experiments applying similar concepts from Clayden *et al*[52] and Santiago *et al*[51], that pentanoic acid's carbonyl carbon has low electrophilicity and polarizability[52]. The low reactivity of pentanoic acid can be overcome by first converting the carboxylic acid into an ester, which can then be reduced to its corresponding alcohols.[51] These alcohols can then be dehydrated to form olefins or diolefins. However, the main goal of this study is to understand the reduction of pentanoic acid to pentanol via an ester intermediate. Reactions were performed in a liquid phase batch reactor and the reaction species were quantified using a gas chromatography equipped with a flame ionization detector (GC-FID). Using the copper chromite catalyst, temperature programmed reduction (TPR), X-ray diffraction (XRD), and transmission electron microscopy (TEM) characterizations were performed. This study will show that forming an ester intermediate with the help of an alcohol, increases the reactivity of the pentanoic acid and enhances the rate of pentanol production. The importance of reducing carboxylic acids to alcohols lies in converting the biomass-derived pentanoic acids to alkenes or alkynes by dehydrating the alcohols. This will be conducted in a biphasic reactor in the future.

## 2.2 Experimental

### *2.2.1 Catalyst preparation*

The copper chromite ($2CuO \cdot Cr_2O_3$) catalyst was purchased from Sigma Aldrich. It was prepared via the industrial combustion method.

### *2.2.2 Catalyst characterization*

a. Temperature programmed-reduction (TPR)

TPR of the catalyst was performed in a custom-made system. A ¼" quartz tube packed with quartz wool and 50.0 mg of copper chromite catalyst was mounted vertically in a furnace. The tube and the sample were purged with nitrogen flow rate of 30 stcm for 30 minutes. After the signal stabilized, a flow rate of 35 sccm (5% hydrogen in argon) was passed through the sample. The thermal conductivity detector (TCD, SRI 110), measured the effluent gas that passed through the sample before entering the TCD. This was analyzed using 35 sccm of 5% hydrogen in argon mixture. The temperature was then ramped to 900 °C at 10 °C/minute.

b. Transmission electron microscopy (TEM)

Lawrence Barret performed TEM analysis at the Microbiology Department at OU.

The catalyst was pre-reduced at 280 °C for 2 hours under 100 stcm of hydrogen. After cooling it down to room temperature, a small sample was dispersed in heptane and sonicated to achieve a uniform suspension. A few drops of the suspension were then placed on TEM grids (polymer-coated copper). The TEM (ZEISS 10 model) was used to take images of the samples.

c. X-ray diffraction (XRD)

The XRD analysis was performed by the Geology Department at OU.

A small amount of fresh copper chromite catalyst was placed flat on a plastic slide. A curved crystal monochromator Rigaku automatic diffractor (model D-Max A) was used to analyze the sample. The equipment utilized 40 kV, 35 mA, and Cu Kα radiation source. After reaction, the reaction mixture was filtered via vacuum filtration. The catalyst in the Buchner funnel on the filtered paper was washed with pure acetone multiple times. This catalyst was then removed from the funnel and placed on a plate in an oven. The catalyst was dried over night at 80 °C and then cooled to room temperature before performing the XRD. The above parameters were used to analyze the sample.

d. Energy-dispersive X-ray spectroscopy (EDX)

Lawrence Barret performed EDX analysis at the Microbiology Department at OU.

A small sample of the copper chromite catalyst was pressed against the carbon tape on the stud. NEON ZEISS 40ESB was used to scan the sample for all elements of the periodic table. High, moderate, and low-resolution images were taken at various frames.

e. Thermogravimetric analysis (TGA)

Lawrence Barret performed TGA at the Chemical Engineering department at OU.

This technique was performed using STA 449 F1 Jupiter®, Netzsch and Quadrupole Mass Spectrometer (QMS) 403 C Aeolos®. Approximately 15 mg of copper chromite catalyst was reduced in hydrogen at 400 °C at a heating rate of 3 °C/min. The sample was then cooled down and passivated with nitrous oxide ($N_2O$) at 60 °C under constant flow of 60 mL/min for 4 hours. Afterwards, the sample was heated in hydrogen from 80 °C to 400 °C using the ramp rate of 3 °C/min.

*2.2.3 Catalytic activity measurement*

Approximately 100 mg of the copper chromite ($2CuO \cdot Cr_2O_3$, Sigma Aldrich) was placed into a 160 mL stainless-steel autoclave vessel (Parr Corporation) along with 60 mL of solvent. The experiments with m-cresol and benzyl-alcohol used n-dodecane (Alfa Aesar, 99.9%) as a solvent. The remainder of the studies used decahydronaphthalene, mixture of cis + trans, (Sigma Aldrich anhydrous, ≥ 99%) as a solvent. The reactor consisted of a pressure gauge, temperature controller, stirring impeller, sampling port, and a feeding cylinder. The catalyst was initially reduced at 280 ºC for 2 hours under 300 psig of $H_2$ at a stirring speed of 500 rpm. After reduction, a known concentration of pentanoic acid (Sigma Aldrich, 99%) and a particular molar ratio of alcohol [m-cresol (Sigma Aldrich, 99%), ethyl-alcohol (Sigma Aldrich, 200 proof, anhydrous, ≥ 99.5%), benzyl-alcohol (Sigma Aldrich anhydrous, 99.8%), or 1-dodecanol (Sigma Aldrich, 99%)] were diluted in the solvent and fed into the reactor with an additional 150 psi of $H_2$ at 250 ºC. The reaction was run at 250 ºC for 1 hour under 500 rpm stirring speed. After the reaction, the reactor was cooled to 15 ºC using an ice bath. A 10 mL liquid sample from each experiment was filtered and mixed with 50.0 mg of Phenol (Sigma ACS reagent, ≥ 99.0%), an internal standard. The reactants and products were quantified in a gas chromatography with flame ionization detector (Agilent GC-FID) equipped with a ZB-5 column (Agilent, 60 m x 250 μm x 0.25 μm). Mass spectrometry (Shimadzu) was used for liquid products identification. Another mass spectrometry that was custom-built was used to identify gaseous products, which were negligible for these experiments.

## 2.3 Results and discussion

### *2.3.1 Catalyst characterization results*

In order to find the reduction temperature of copper chromite, temperature programmed reduction (TPR) was performed. Results are shown in Figure 12. The bulk CuO is expected to reduce between 200-300 ºC[73]. For the reaction conditions used in this study, at 280 ºC, 300 psig $H_2$, 2 hours, a complete reduction of copper must have occurred.

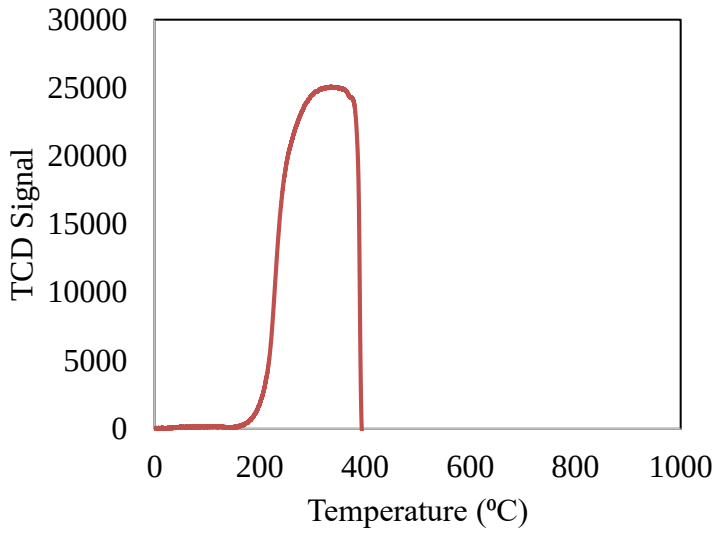



**Figure 12: Temperature programmed reduction (TPR) of the copper chromite**

Transmission electron microscopy (TEM) was performed to calculate the copper particle diameters after reduction. However, the results showed extreme sintering of the copper particles and were not viable to calculate particle diameters.

To further confirm that under reaction conditions, there will be a complete reduction of copper, X-ray diffraction (XRD) analysis was performed. It was also done to understand the crystalline nature of the catalyst and the size of the copper particles in copper chromite. The resulting peaks in Figure 13 were identified according to XRD data obtained from literature.[74,78,79] The metallic copper peaks significantly increase in height

after reduction and reaction, suggesting that there is a low dispersion and that the catalytic particles are not stable under reaction conditions. Therefore, the metallic copper particle size is higher due to sintering. $Cu^{2+}$ from CuO peak disappeared after reaction, suggesting that CuO was no longer present in the active phase of the reaction and does not play a role. Because there is a large amount of metallic copper (due to sintering, etc.) at high particle diameters, this is likely the active site. More calculations are necessary to determine the exact plane where the reaction is taking place. However, planes (111) and (400) can be identified in Figure 13 according to literature[74,78,79].

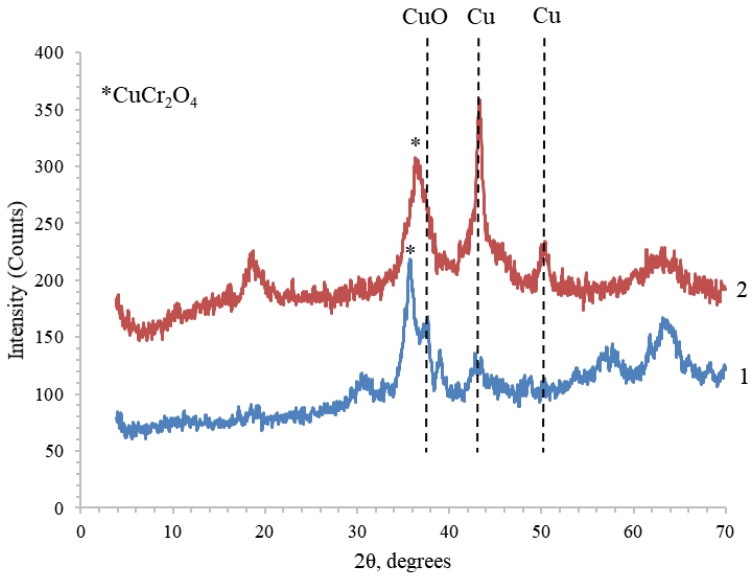



**Figure 13: The X-ray diffraction data for the copper chromite samples: 1 - fresh copper chromite, 2 - spent catalyst after reaction**

Applying the Scherrer equation (1)[75]:

$$D = \frac{K\lambda}{B\cos\theta} \quad (1)$$

Where, $K$ (dimensionless shape factor) = 0.89, $\lambda$ (X-ray wavelength) = 0.1542 nm, $B$ (line broadening at half the maximum intensity) = 0.680°, 2θ (Bragg angle) = 43.356°,

the metallic copper particle diameter was calculated to be 12.44 nm. This value is comparable to the value accepted in literature (13.3 nm).[76]

Many commercial copper chromite catalysts were known to have promoters such as barium.[77,79] Thus, an energy-dispersive X-ray spectroscopy (EDX) was performed to scan for various elements, impurities, or promoters in the sample for further confirmation. The results are shown below.

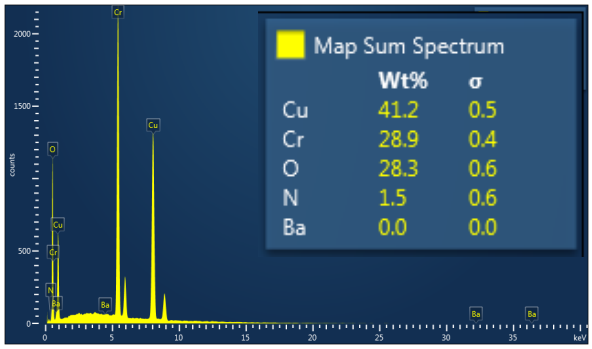



**Figure 14: Energy-dispersive X-ray spectroscopy (EDX) of copper chromite**

The copper chromite consists of 41 wt.% Cu, 29 wt.% Cr, and 28 wt.% O. Thus, the EDX further proved that the activity of the catalyst is only related to the copper and chromium mixed oxides present in the sample.

The TGA results for copper chromite were not viable in calculating particle diameters. Our current experimental conditions must be altered because the weight loss of the sample showed a very high dispersion of copper particles with extremely low particle diameters. It is likely that the nitrous oxide may have penetrated deeper than simply the surface layer of the sample. Perhaps if the nitrous oxide was diluted and the passivation time was decreased, it would lead to more realistic results.

*2.3.2 Catalytic results and discussion*

According to Clayden *et al*[52] and Santiago *et al*[51], esters are more reactive than carboxylic acids.[72,90-92] To confirm this theory, same concentrations of esters and carboxylic acids were fed into a batch reactor in the presence of copper chromite catalyst. Reaction pathways are shown in Figures 15 & 16.

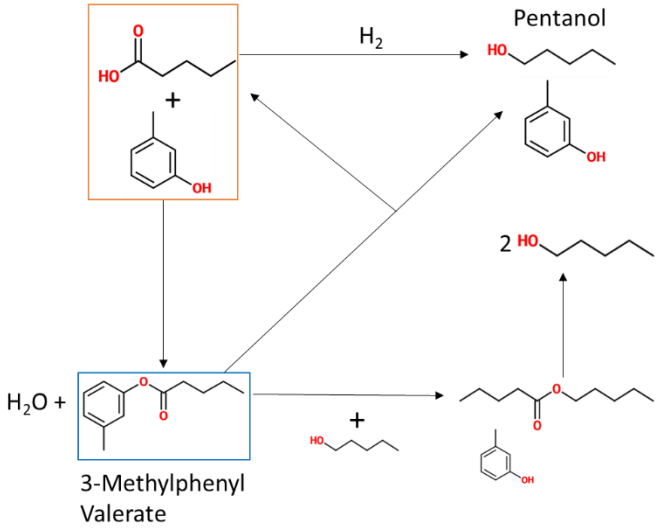



**Figure 15: Reaction pathway showing the reduction of pentanoic acid, 3-methylphenyl valerate, and pentyl pentanoate to pentanol**

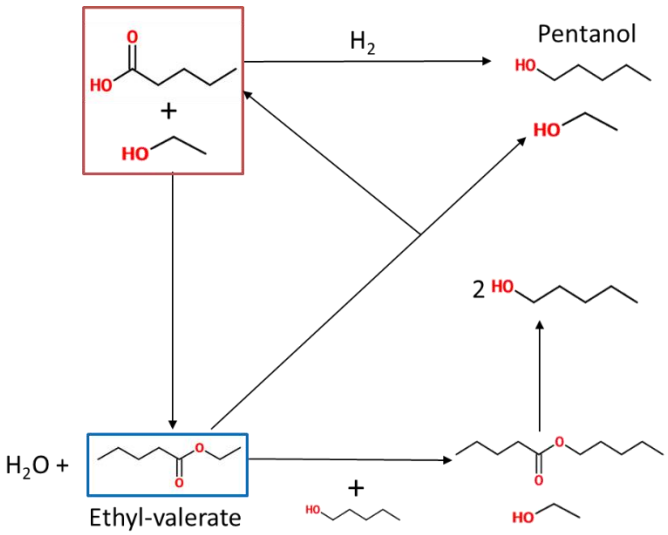



**Figure 16: Reaction pathway showing the reduction of pentanoic acid, ethyl-valerate, and pentyl-pentanoate to pentanol**

Ester and water are formed when a carboxylic acid reacts with an alcohol. Although m-cresol is considered a phenolic compound, it still consists of an alcoholic -OH group, which is the functional group of interest for the purposes of these studies. Pentanoic acid can be reduced directly to form pentanol or can go through an ester intermediate, pentyl-pentanoate, which then reduces to form two moles of pentanol (Figures 15 & 16). Pentyl-pentanoate can be formed when pentanoic acid ester reacts with pentanol that is produced from the reduction of the acid or the ester. In the presence of excess ethanol, pentanoic acid reacts with it to form ethyl-valerate ester (Figure 16). This ester can be reduced to form one mole ethanol and one mole of pentanol. Pentyl-pentanoate ester is also formed as a side product which can further be reduced to form two moles of pentanol.

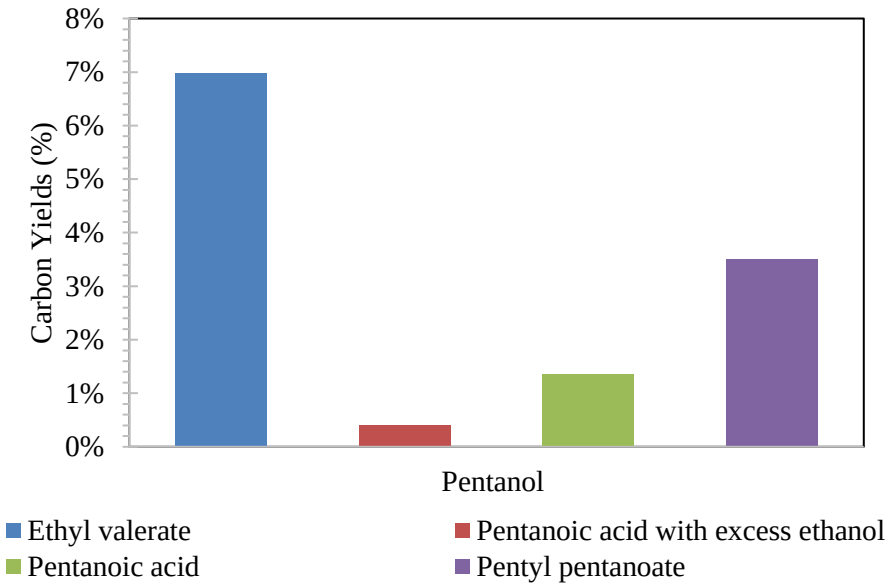



**Figure 17: Yield of pentanol product on copper chromite catalyst using various feeds. Reduction: 100 mg $2CuO{\cdot}Cr_2O_3$ at 280 °C under 300 psi $H_2$ for 2 hrs. Reaction: 250 °C for 2 hrs under 450 psi $H_2$. Feeds include: 0.421 M Ethyl-Valerate, 0.453 M Pentanoic Acid + excess ethanol (1:5 molar ratio), 0.424 M Pentanoic Acid, and 0.465 M Pentyl-Pentanoate**

After reducing the copper chromite catalyst, initial experiments were performed using

various feeds of 0.4 M of pentanoic acid (PEA), ethyl-valerate (EV), pentyl-pentanoate (PP), and pentanoic acid with excess ethanol (1:5 molar ratio). The yields and rate of formation of pentanol are shown in Figures 17 & 18 respectively. Selectivity and a complete distribution of products are shown in Figures 46 & 47. The carbon balances for the following reactions with respect to the pentanoic acid are above 90%. Conversion of reactants are the following: ethyl valerate (14%), pentanoic acid (9%), pentanoic acid with excess ethanol (100%), and pentyl pentanoate (4%).

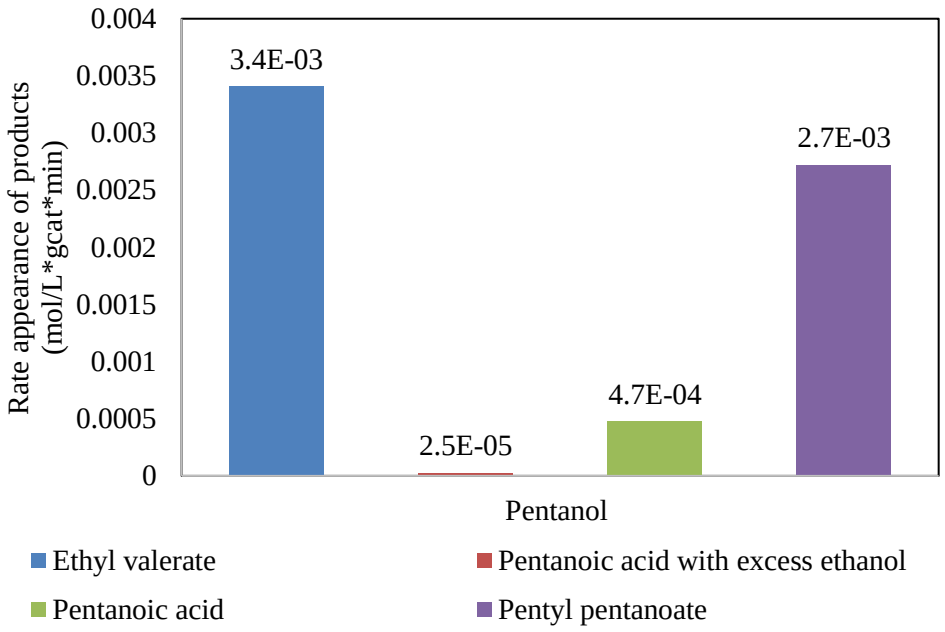



**Figure 18: Rate of formation of pentanol on copper chromite catalyst using various feeds. Reduction: 100 mg $2CuO{\cdot}Cr_2O_3$ at 280 °C under 300 psi $H_2$ for 2 hrs. Reaction: 250 °C for 2 hrs under 450 psi $H_2$. Feeds include: 0.421 M Ethyl-Valerate, 0.453 M Pentanoic Acid + excess ethanol (1:5 molar ratio), 0.424 M Pentanoic Acid, and 0.465 M Pentyl-Pentanoate**

Reduction of ethyl-valerate ester and pentyl-pentanoate ester produced a higher yield of pentanol (7% and 4% respectively) compared to the reduction of PEA alone or PEA with excess ethanol. This further proves the theory that carboxylic acids have a high activation energy and a low degree of reduction to produce alcohols compared to the esters[51,52].

Although we observe a 100% conversion of PEA in the presence of excess ethanol, a high yield of ethyl-valerate is produced (not shown in the figure), while a very small amount of the ethyl-valerate reduces to ethanol and pentanol. This may be because ethanol adsorbs more strongly onto copper than the ethyl-valerate ester. Ethanol has a high heat of adsorption on copper, 140 kJ/mol.[51] Perhaps the copper surface is saturated with alcohol, while slowly reacting with pentanoic acid or ethyl-valerate. When only PEA is fed, there is a high yield of pentyl-pentanoate. Pentyl-pentanoate accumulates because its rate of formation is higher than its rate of reduction to pentanol. However, its rate of reduction to pentanol occurs at a much faster rate than pentanoic acid converting to pentanol. When only ethyl-valerate is fed, there is a high yield of pentanol. Cleaving the C-O bond adjacent to the carbonyl group should release one mole of ethanol and one mole of pentanol for every ethyl-valerate converted. The carbon yields are not equivalent in Figure 46 due to the volatile nature of ethanol going from the reaction mixture to analysis. Pentanol is produced in the yields of 4% when PP is fed alone. The difference in yields of pentanol when EV or PP were fed is due to the type of -R group attached to the ester. Having a bulky hydrocarbon chain, such as $C_5$ in the case of PP, reacts at a much slower rate than having a light hydrocarbon chain, $C_2$, in the case of EV. Therefore, the size of the molecule and the type of -R group attached to the ester are extremely important in converting to alcohols. From Figure 18, we can conclude that the rate of formation of pentanol from pentanoic acid is much smaller than the rate of pentanol produced from the esters. Therefore, if a small amount of alcohol is added to pentanoic acid, this can create a slight enhancement in pentanol production rates. To test this hypothesis, various conditions were tested as shown in Figure 19.

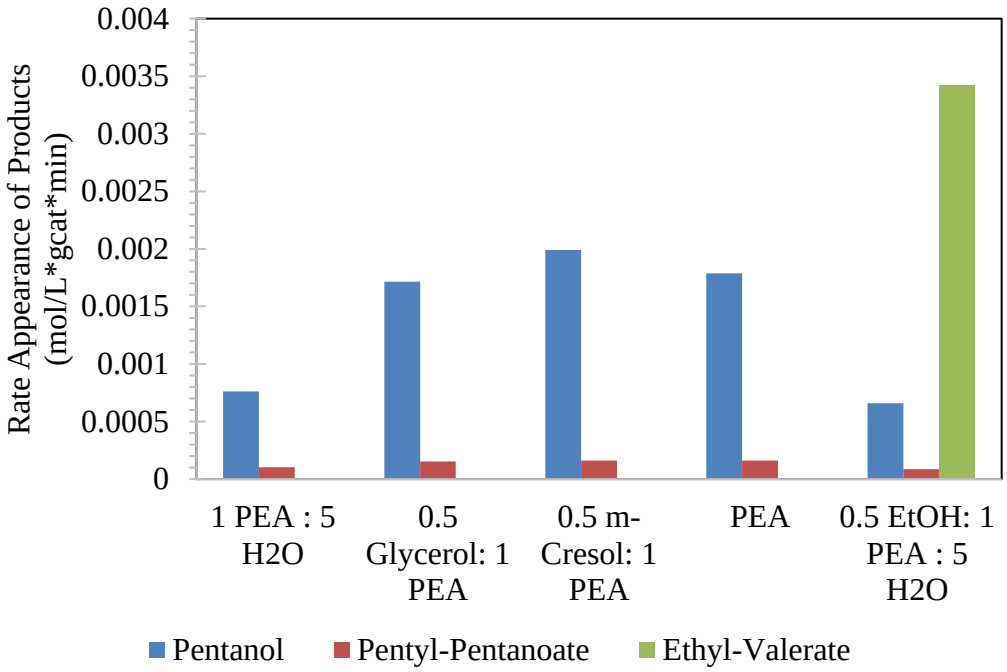



**Figure 19: Rate appearance of products when 0.1 M PEA is cofed with various molar ratios of water ($H_2O$), glycerol, m-cresol, and ethanol (EtOH) in decalin solvent. Reduction: 100 mg $2CuO{\cdot}Cr_2O_3$ at 280 $^oC$ under 300 psi $H_2$ for 2 hrs. Reaction: 250 $^oC$ for 1 hr under 450 psi $H_2$. Carbon balances wrt PEA: >90%.**

According to the data presented in Figure 19, water inhibits the reaction rate. While m-cresol slightly enhanced the reaction rate, glycerol had no effect. It was difficult to quantify the amount of glycerol converted due to its incompatibility in the GC-FID column. Adding water in the presence of excess ethanol inhibited the reaction rate even more. Thus, to further investigate the role of esters in the pentanol production rates, various molar ratios of alcohol was added to PEA feed. The results are shown in Figure 20. For a clear understanding of the pentanol appearance rates presented in Figure 20, yields of products as well as conversion of the reactants are presented in the Figures 48-50.

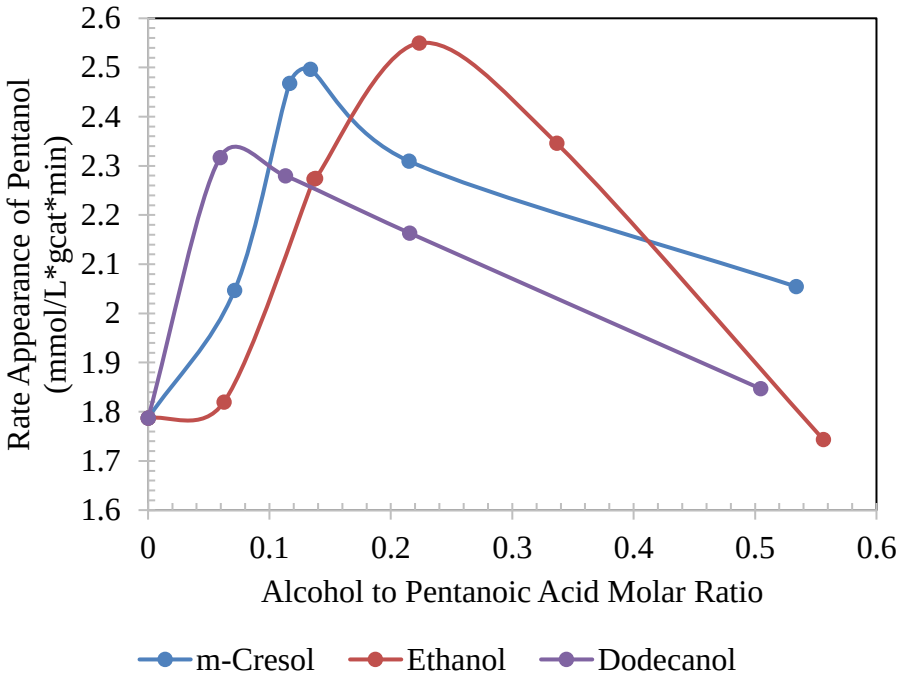



**Figure 20: Rate appearance of pentanol when 0.103 M Pentanoic Acid (PEA) is co-fed with various molar ratios of ethanol and 1-dodecanol in decalin solvent, and m-cresol in n-dodecane solvent. Reduction: 100 mg $2CuO{\cdot}Cr_2O_3$ at 280 °C under 300 psi $H_2$ for 2 hrs. Reaction: 250 °C for 1 hr under 450 psi $H_2$. Carbon balances with respect to PEA: >90%.**

Reaction pathways are shown in Figures 15, 16, & 21. As seen in Figure 20, there is an enhancement in pentanol production rates when different molar ratios of alcohols were added compared to when there was no alcohol. Each achieve an optimum pentanol yield at various molar ratios, depending on the type of alcohol. After attaining the optimum, the rate of pentanol formation decreases as the molar ratios of alcohol to PEA are further increased.

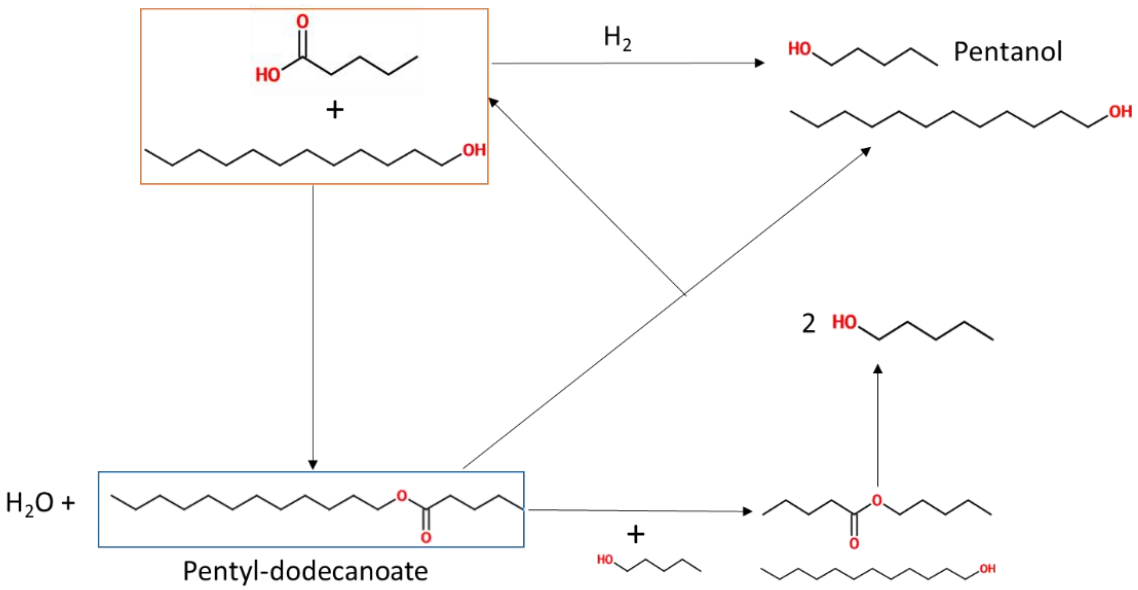



**Figure 21: Reaction pathway showing the reduction of pentanoic acid, dodecyl-valerate, and pentyl-pentanoate to pentanol**

Under the reaction conditions shown in Figure 20, the PEA is in a zeroth order regime where the reaction rate does not vary with changing reactant concentrations.[82] When only pentanoic acid is fed into the reactor, without the presence of alcohol, pentanol and pentyl-pentanoate are produced. Therefore, the reaction rate in Figure 22 only accounts for the conversion of PEA producing these products. In the case of zeroth order, the surface of the catalyst is always saturated with pentanoic acid regardless of the concentration of pentanoic acid fed into the reactor.

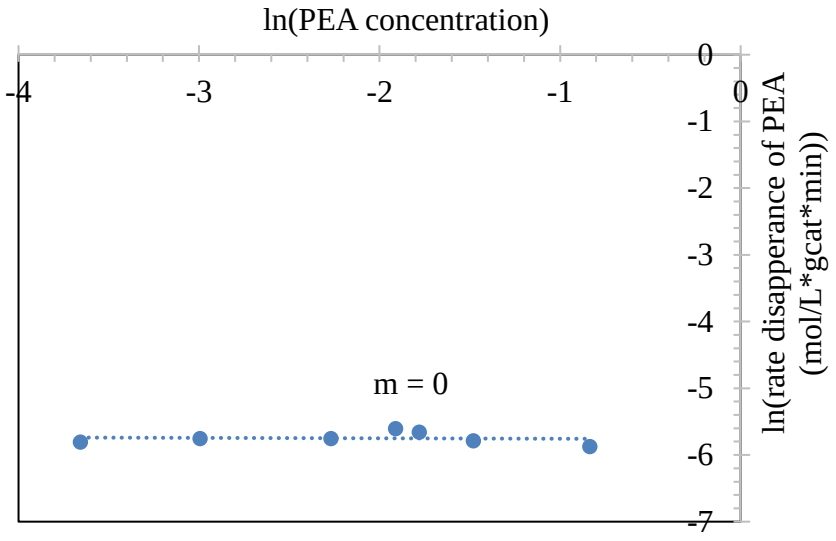



**Figure 22: Zeroth order regime with respect to pentanoic acid**

$$Rate = -\frac{d[C_{PEA}]}{dt} = k[C_{PEA}^{0}] = k = constant \quad [82] \tag{2}$$

In Equation (2), rate (reaction rate) is equivalent to k (reaction rate coefficient) usually in the units of mol/L*min. [82] The slope in Figure 22 represents the reaction order, which is zero. Since we know the reaction rate at various PEA concentrations, we can estimate the reaction rate coefficient of PEA using the graph presented in Appendix Figure 51. The average rate of disappearance of PEA is equivalent to the reaction rate constant, k, 0.0032 mol/L*gcat*min. The same analysis procedure was followed as Figure 22 but at a higher reaction temperature of 280 °C by feeding different concentrations of PEA. These experiments were useful in calculating the activation energy for PEA converting to pentanol and PP. Reaction rates $r_1$ and $r_2$ are equivalent to the reaction rate constants $k_1$ and $k_2$. Applying the Arrhenius equation for zeroth order conditions[82]:

$$\ln\left(\frac{r_2}{r_1}\right) = \frac{E_a}{R}\left(\frac{1}{T_1} - \frac{1}{T_2}\right) \tag{3}$$

Where, $T_1$ (reaction temperature) = 250 °C = 523 K, $T_2$ (reaction temperature) = 280 °C = 553 K, $r_1$ (reaction rate at $T_1$) = 0.0032 mol/L*gcat*min, $r_2$ (reaction rate at $T_2$) = 0.0081 mol/L*gcat*min, and R (ideal gas constant) = 8.314 J/mol*K.

The pre-exponential factor, $A$, can be estimated by applying the following equation[82]:

$$A = \frac{k}{e^{-\frac{E_a}{RT}}} \quad (4)$$

Where, the pre-exponential factor $A$ has the same units as the reaction rate constant $k$ (mol/L*gcat*min). The following table summarizes an approximation of the rate constants and activation energy.

| ***Parameters*** | **$T_1$ = 250 °C** | **$T_2$ = 280 °C** |
|---|---|---|
| *k (mol/L*gcat*min)* | 0.0032 | 0.0081 |
| *A (mol/L*gcat*min)* | 87,912 | 87,852 |
| *$E_a$ (kJ/mol)* | 74.48 | |

**Table 2: Summary of PEA parameters, reaction rate constant (k) and activation energy ($E_a$) for PEA → pentanol + pentyl-pentanoate**

To understand the general trend that is seen in Figure 20, we can model the zeroth order saturation kinetics using a Langmuir-Hinshelwood model. This model has the following assumptions: 1) all surface sites are identical 2) one adsorbate per site 3) no adsorbate-adsorbate interactions 4) equilibrium between surface and gas phase species.[82] Using the procedure outlined in Chapter 10, the subsequent rate equations can be obtained.[82] At low molar ratios of alcohol to PEA (low coverage), the rate of pentanol formed from PEA is given by:

$$rate_{PEA/POH} = \frac{k_1 K_{PEA} C_{PEA}}{1 + K_{PEA} C_{PEA}} \quad (5)$$

At saturated zeroth order conditions, this reduces to $rate_{PEA/POH} = k_1$ calculated in Table 2. The rate of ester formed from PEA and alcohol is given by:

$$rate_{ester} = \frac{k_{ester}K_{ester}C_{PEA}C_{alcohol}}{1+K_{PEA}C_{PEA}} \quad (6)$$

The rate of pentanol formed from reducing the above ester is given by:

$$rate_{ester/POH} = \frac{k_2K_{ester}C_{ester}}{1+K_{PEA}C_{PEA}} \quad (7)$$

Very small amounts of added alcohol create an ester (6) that decomposes to produce pentanol (7). Since the rate production of ester will not be dominating at low feeds of alcohol, the rate of pentanol produced will increase until it plateaus. The plateau or the optimum will occur when the coverage is the highest of all the species and has enough molecules to convert. This optimum is seen in Figure 20 for all added alcohols.

After the optimum number of ester molecules are cleaved, at higher molar ratios of alcohols/PEA, more molecules will begin to compete for sites as shown in Equations (8), (9), and (10). At intermediate to high molar ratios of alcohol to PEA (high coverage), assuming the rate-liming step is the decomposition of PEA, the rate of pentanol formed from PEA is given by:

$$rate_{PEA/POH} = \frac{k_1K_{PEA}C_{PEA}}{1 + K_{PEA}C_{PEA} + K_{alcohol}C_{alcohol} + K_{H_2O}C_{H_2O} + K_{ester}C_{ester}} \quad (8)$$

Rate of formation of the ester is given by:

$$rate_{ester} = \frac{k_{ester}K_{ester}C_{PEA}C_{alcohol}}{1 + K_{PEA}C_{PEA} + K_{alcohol}C_{alcohol} + K_{H_2O}C_{H_2O} + K_{ester}C_{ester}} \quad (9)$$

Assuming the rate-liming step is the decomposition of the ester, the rate of pentanol formed from the ester is given by:

$$rate_{ester/POH} = \frac{k_2K_{ester}C_{ester}}{1 + K_{PEA}C_{PEA} + K_{alcohol}C_{alcohol} + K_{H_2O}C_{H_2O} + K_{ester}C_{ester}} \quad (10)$$

Considerable amounts of added alcohol create an ester (9) that decomposes to produce pentanol (10); however, the high concentration of alcohol in the denominator begins to inhibit the reaction rate by competing with the ester for active sites. Producing more ester may not necessarily be advantageous because it leads to creation of more water, which will also compete for sites and lower the reaction rate. Any addition of the species in the denominator will further lower the rate of pentanol produced due to a competition for active sites. Looking at Equations 8 and 10, $k_1 < k_2$ because pentanoic acid reacts slower (yields less pentanol) than esters (high yield of pentanol) as seen in Figures 17 and 18. The rate constant of ester formation (9) is expected to be faster than the decomposition of PEA to pentanol: $k_1 < k_2 \leq k_{ester}$. The rate of formation of the ester may or may not be faster than its decomposition as it depends on the -R group that is attached to the alcohol.

Both m-cresol/PEA and 1-dodecanol/PEA reach an optimum in pentanol production at a molar ratio of 0.1 compared to EtOH/PEA molar ratio of 0.2 (Figure 20). The shifts in these optimums are possibly due to the following: 1) the equilibrium adsorption constants of one ester is larger than the other, and/or 2) one ester competes more strongly for active sites compared to the other.

Expanding on the first reason, the equilibrium adsorption constants can play a vital role in understanding these shifts in optimum pentanol production rates. The 3-methylphenylvalerate has a bulky aromatic -R group and dodecyl-valerate has a long 12C -R group compared to the ethyl-valerate's short 2C chain. In the case of m-cresol, the 3-methylphenylvalerate ester adsorbs on the metallic copper surface at the carbonyl oxygen, the oxygen adjacent to the carbonyl, and the aromatic ring.[80] If the m-cresol was

hydrogenating, the aromatic ring will adsorb flat on the surface and will adsorb more strongly than alkanols.[80] However, hydrogenation products are never seen for these reactions, suggesting that m-cresol does not adsorb flat on the surface. It may still have a high equilibrium adsorption constant compared to ethanol. This leads to the weakening of the C-O bond adjacent to the carbonyl group. The cleavage of this group yields pentanol and m-cresol. Dodecyl-valerate adsorbs at the carbonyl oxygen and the oxygen adjacent to the carbonyl group. However, it has an extremely long -R group that donates electrons at a much larger extent compared to 3-methylphenylvalerate. Thus, shifting its optima to the left. In the case of ethanol, the ethyl-valerate ester adsorbs on the metallic copper surface at the carbonyl oxygen and the oxygen adjacent to the carbonyl. However, the 2C -R group does not weaken the C-O bond to the same extent as 3-methylphenylvalerate or dodecyl-valerate. Thus, the C-O bond adjacent to the carbonyl group is not as weakened and it is cleaved at a slower rate. Therefore, the equilibrium adsorption constants are expected to have the following trends: $K_{dodecanol} > K_{mcresol} > K_{ethanol}$. Since dodecyl-valerate adsorbs more strongly and has a higher $K_{dodecanol}$, the optimum pentanol production rate occurs at a much lower dodecanol concentration compared to other alcohols. Because ethyl-valerate adsorbs less strongly, the optimum pentanol rate shifted to the right.

It was suggested that the strength of the bond formed between the alkoxy group (RO-) and the surface of the catalyst depends on the type of -R group attached. This is because the -R group can affect the electron density of the oxygen atom and/or contribute to the steric hindrance of the molecule, which can influence reaction rates. The O-Cu chemisorption bond length increases as the electron-withdrawing properties of the -R

group increases. Thus, their adsorption energy decreases. The aromatic ring in the 3-methylphenylvalerate donates electron density to the alkoxy oxygen and makes the Cu-O bond strong, increasing the adsorption. Ethyl-valerate donates electrons at a smaller extent, so the Cu-O bond is weaker with lower adsorption constant. The data further suggests that dodecyl-valerate donates electrons at a larger extent compared to 3-methylphenylvalerate or ethyl-valerate, so the Cu-O bond is the strongest with the highest adsorption constant.[89]

Expanding on the second reason, some of the esters may compete more strongly with the species compared to other esters depending on how quickly they are made (9). The 3-methylphenylvalerate ester is difficult to make compared to the ethyl-valerate ester due to steric hindrance. Also, the dodecyl-valerate ester is the most difficult to make due to its long hydrocarbon chain. The faster the reaction rate to produce the ester, the more it will build up in the system. This is further supported by the figure below.

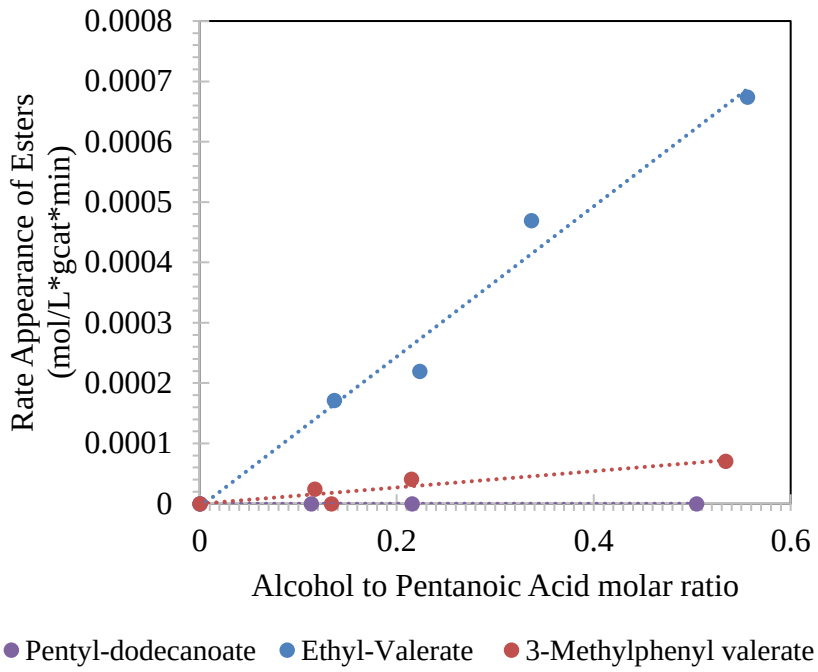



**Figure 23: Rate appearance of esters when 0.103 M Pentanoic Acid (PEA) is co-fed with various molar ratios of ethanol and 1-dodecanol in decalin solvent, and m-cresol in n-dodecane solvent. Reduction: 100 mg $2CuO{\cdot}Cr_2O_3$ at 280 °C under 300 psi $H_2$ for 2 hrs. Reaction: 250 °C for 1 hr under 450 psi $H_2$. Carbon balances with respect to PEA: >90%.**

Figure 23 suggests that $k_{ethylvalerate} > k_{methylphenylvalerate} > k_{pentyldodecanoate}$. Results from Figure 23 and the reaction rate constants correlate with the results seen in Figure 20. Dodecyl-valerate reduction to pentanol is slow because the ester itself is produced at a slower rate.

Similar experiments were also performed using benzyl alcohol (BA) and it produced a high yield of pentanol with increasing molar ratios of BA. However, the carbon balances for these reactions were not reasonable and therefore the results were omitted from Figures 20 and 23.

*2.3.3 Equilibrium test*

To test if the data collected in Figures 20 and 23 are true enhancements in pentanol production rates, equilibrium tests were performed. The reaction was run for 2 hours when no alcohol was present using the conditions: 0.103 M Pentanoic Acid (PEA) in decalin solvent, reduction: 100 mg $2CuO{\cdot}Cr_2O_3$ at 280 ºC under 300 psi $H_2$ for 2 hrs, reaction: 250 ºC under 450 psi $H_2$. Carbon balances with respect to PEA: >90%. The results are below:

| Rxn time (min) | Conversion/Yield (%) | | | Rates (mol/L*gcat*min) | | |
|---|---|---|---|---|---|---|
| | PEA Converted | Pentanol | Pentyl-Pentanoate | PEA disappeared | Pentanol | Pentyl-Pentanoate |
| 60 | 18.52% | 10.44% | 1.89% | -0.00317 | 0.001787 | 0.00016 |
| 120 | 34.52% | 34.52% | 5.92% | -0.00297 | 0.002022 | 0.00026 |

**Table 3: Results at longer reaction times when no alcohol was present**

Since the conversion of PEA and yields of products nearly doubled at twice the reaction times, it is very likely that the data collected is a true representation of increase in pentanol production rates. In other words, the enhancements are not caused by equilibrium. In addition, the rate of pentanol produced at twice the reaction time is still less than when a small amount of alcohol is added. Thus, the addition of alcohols increased the pentanol rate by almost two-folds.

*2.3.4 Effect of water on the hydrogenation of PEA and esters to alcohols*

Figures 54 & 55 show the effect of water on pentanol production rates when only PEA is fed into the reactor. At molar ratios of water to PEA below 0.8, water slightly enhanced the reaction rate. At higher molar ratios of water to PEA, water inhibited the reaction rate as modeled by equations 8-10.

To investigate the effect of water when alcohols are cofed with PEA, 200 mg of copper chromite was initially reduced at 280 ºC for 2 hours under 300 psi of $H_2$. The reduction

process is expected to produce approximately 0.0232 mL of water. In one case after reduction, the reactor was cooled down to 100 °C and purged with $N_2$ to remove the water. At this temperature, all the water is expected to be in the gas phase according to the bubble point calculations using Clausius-Clapeyron equation[83]. In another case, water was not removed after reduction. The reactions in both cases were carried out normally at 250 °C, 1 hour, under 450 psi of $H_2$. The resulting product distributions are shown below.

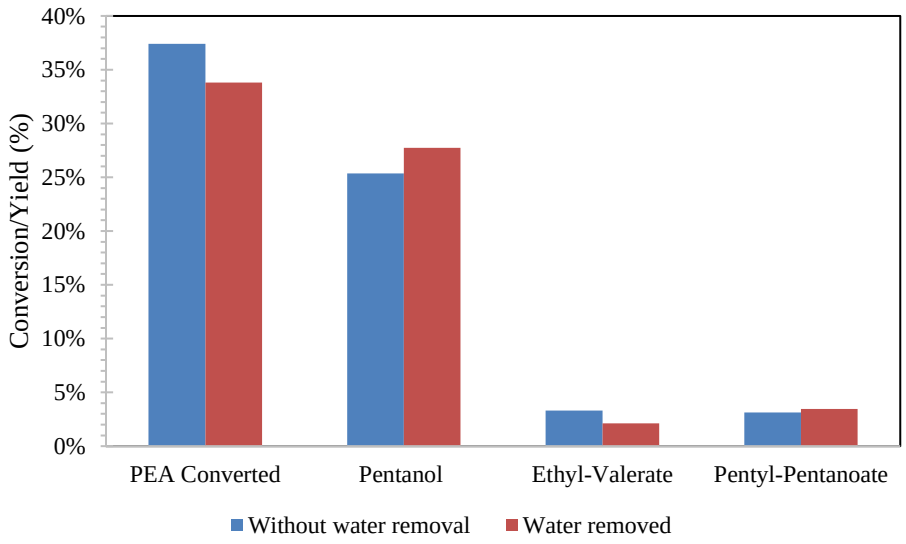



**Figure 24: Effect of water on product distributions at 0.33 molar ratio of EtOH to PEA**

Keeping the water in the system slightly lowered the pentanol yield. This is because water tends to occupy the active sites and prevent the reactants from reacting. It has an inhibitory effect as discussed above. Ethyl-valerate yield is lower after removing the water. This is possibly due to that fact that water is no longer present in the system, so more of it is reacting on the catalyst surface to produce pentanol. As a result, we see an increase in pentanol yield when water is removed from the system.

*2.3.5 Mechanism and location of the active site*

There have been several studies regarding carboxylic acid and ester hydrogenolysis to alcohols. Previous literature indicates that the esters adsorb dissociatively on to the metallic copper surface.[11,51,53,84]

$$RCOOR' + 2^* \rightarrow RCO^* + R'O^*$$

Here, * is the catalytic site on the surface of the catalyst. The alkoxy fragment reacts quickly to form R'OH while the acyl group, RCO*, is adsorbed longer.[69] Therefore, the rate-limiting step is the hydrogenation of the adsorbed acyl group during ester hydrogenolysis.[53] Furthermore, this acyl group can either be hydrogenated directly to form an alcohol or it could form an aldehyde intermediate that can be hydrogenated to form the alcohol.[84,85] However, the aldehyde intermediate may not be observed after the reaction because it reacts three times more faster than any of the acids or esters, especially at higher pressures.[70] This supports my results as none of my products were identified as aldehydes by the mass-spectrometry. Isotopic labeling and in-situ infrared spectroscopy studies further concluded that esters are adsorbed dissociatively onto the catalyst surface.[68,69] Using this theory as a basis[70,71,84,85], many other researchers afterwards were able to successfully explain their results regarding the ester hydrogenolysis.[51,86] Thus, it became established that the mechanism for ester hydrogenolysis requires dissociative adsorption of the species.

Some groups also hypothesized that the mechanism for reduction of ester to alcohols may go through a hemiacetal intermediate.[84,87] However, Mutzall and van den Berg[88] were unable to confirm this intermediate under a wide range of reaction conditions, concluding that it is not possible for this intermediate to occur.

Turek *et al.*[53] and Santiago *et al.*[51] suggest that the reduction of carboxylic acids and esters happen mostly on the metallic copper particles. The amount of $Cu^{2+}$ or $Cu^{+}$ does not affect the reaction rates. According to my results and literature, it is likely that the active site for this reaction is most likely on the metallic copper of the copper chromite; however, more studies are needed to verify this claim. See Figure 13 for XRD results. In addition, this was further tested by impregnating various weight loadings of copper on different oxide supports. The activity of all the catalysts were low and not many achieved the high yields of pentanol on copper chromite. However, they all showed some form of activity including in the case of $Cu/SiO_2$, which further supports the evidence indicated by Turek *et al.*[53] and Santiago *et al.*[51] that metallic copper is the active site.

Zhang *et al.*[89] also proposed a mechanism of hydrogenolysis of amino acid esters on copper-based catalysts via an aldehyde intermediate. This mechanism is redrawn to propose the reaction mechanism for this research using pentanoic acid acyl group and an alcohol alkoxy group in Figure 25. The first step requires the adsorption of the ester, formed from feeding PEA and various alcohols, onto the catalyst surface. The carbonyl oxygen and alkoxy oxygen are adsorbed onto Cu using their lone pair of electrons.[89]

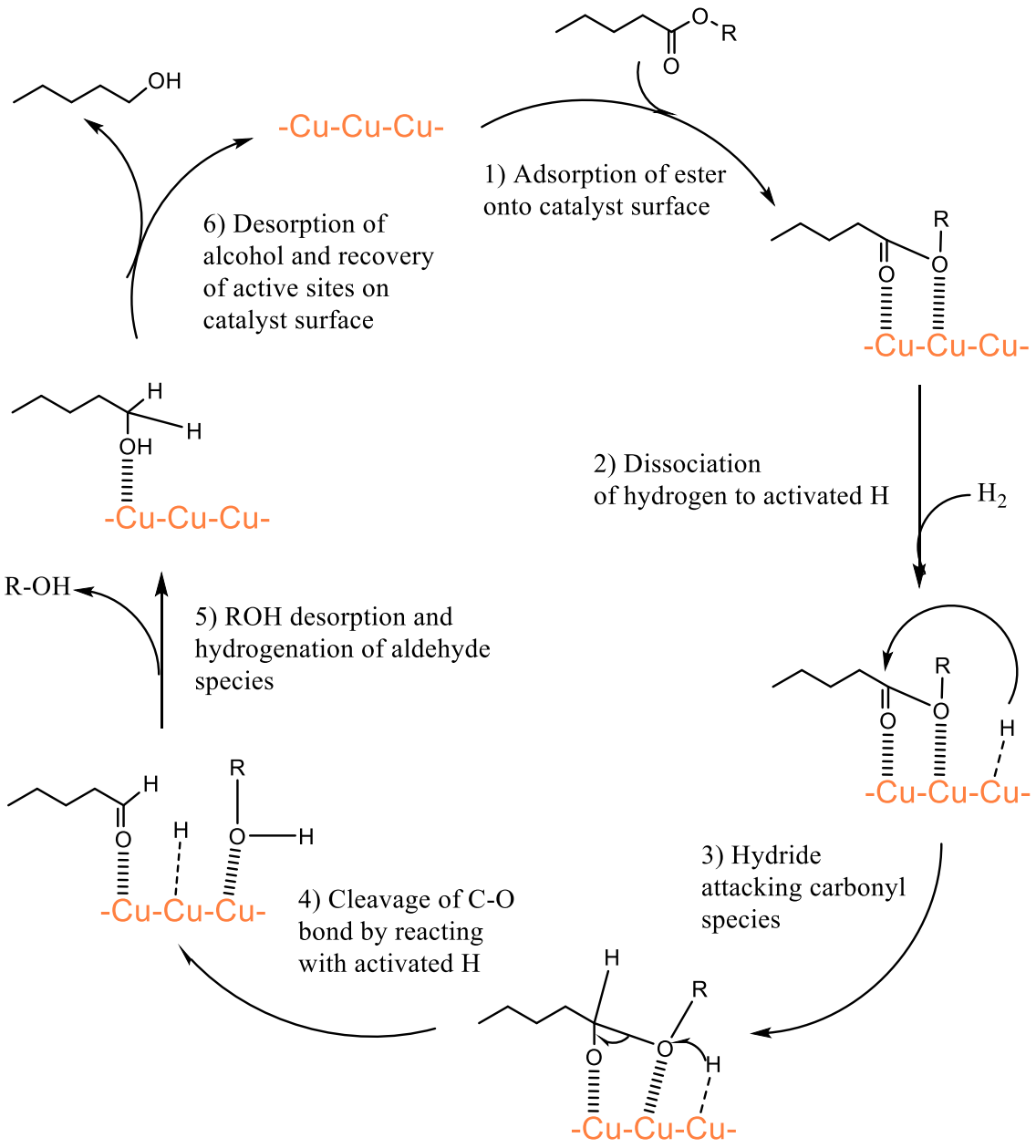



**Figure 25: Proposed mechanism for the reduction of esters to alcohols[89]**

The second step requires the dissociation of hydrogen to activated H. Then, this H attacks the carbonyl group (3) and weakens its bond, further weakening the C-O bond adjacent to the carbonyl group. The C-O bond is cleaved by reacting with activated H (4) and this forms an intermediate aldehyde. The alkoxy alcohol is desorbed and then the aldehyde is

further hydrogenated (5). The aldehyde converts to an alcohol and desorbs, regenerating the active sites on the catalyst surface (6).[89]

The role of $Cr_2O_3$ is interesting to postulate because when various loadings of copper were prepared on different oxide supports, none of them had the same high activity as the copper chromite. While it is common to think that there may be promoters present in this sample, the EDX in Figure 14 proved that this was not the case. Therefore, it is possible that the $Cr_2O_3$ may play a role in increasing the adsorption strength of the esters and PEA, but this needs to be confirmed with more studies. Perhaps, Cr may even be playing a role in increasing the dispersion of Cu, so it can adsorb or dissociate hydrogen more effectively. It is also possible that Cr is simply decorating the sintered copper particles and allows the ester formation to occur more efficiently before passing the ester to the copper. Regardless, more studies need to be performed to find the role of chromia in copper chromite.

**2.4 Conclusion**

Cofeeding small amounts of alcohols with pentanoic acid (PEA) accelerated the rate of pentanol produced. This is because the esters formed from these cofeeds have a much lower activation energy compared to carboxylic acids (PEA) alone.[51,52,72,90-92] While smaller molar ratios of alcohols to PEA accelerated the rate, high molar ratios had the opposite effect due to inhibition and species competing for sites. The results can be explained by using Langmuir-Hinshelwood kinetics and the competition for sites at zeroth order saturation conditions. Excessive amounts of water, alcohol, and heavy esters have an inhibitory effect. The reaction rate constants in Equations (8), (9), and (10) are expected to have the following trends: $k_1 < k_2 \leq k_{ester}$, where $k_1$ is for PEA → pentanol,

$k_{ester}$ is for the formation of ester, and $k_2$ is for ester → pentanol. The equilibrium adsorption constants are expected to have the following trends: $K_{dodecanol} > K_{mcresol} > K_{ethanol}$. The rate constants for ester formations are expected to have the following trends: $k_{ethylvalerate} > k_{methylphenylvalerate} > k_{pentyldodecanoate}$. From equilibrium tests, it was proved that the enhancements observed in pentanol production rates are kinetic in nature and are not measured at equilibrium. Overall, it was possible to accelerate pentanol production rates with small addition of alcohol to the pentanoic acid feed on a copper chromite catalyst.

**2.5 Future Directions**

More experiments are required to understand what is happening between the data points collected in Figure 25. Furthermore, the role of the $Cr_2O_3$ in the mixed oxide copper chromite catalyst should be investigated in detail to understand the mechanism of this reaction. More studies need to be performed to verify that the metallic copper is the active site and that it is formed through an aldehyde intermediate. For strong support to explain the trends seen in Figure 25, DFT studies may be necessary to find the reaction rate constants and equilibrium adsorption constants to generate a working kinetic model.

Enhancing the pentanol production rates is just the beginning of this project. Future outlooks include modifying the liquid phase batch reactor to accommodate biphasic reactions. A biphasic reactor can be utilized to selectively remove pentanol from the oil phase as it is produced to increase the yield of pentanol even more. In the future, this pentanol will be dehydrated to form pentadiene to satisfy the goal of this project.

# Chapter 3: Enhancing propanol production rate by cofeeding alcohols in the presence of propionic acid in the gas phase

## Abstract

Due to an increasing energy demand in our society, heavier hydrocarbon feedstocks are being used as fuels in their own right. This shift has caused the petrochemical industry to suffer from a low supply of petrochemical intermediates.[5] Biomass can be used to compensate for this low supply of petrochemical intermediates.[11] It is composed of cellulose, hemicellulose, and lignin. Hemicellulose is made up of xylose, $C_5$ (pentosan) sugars, and $C_6$ (hexosan) sugars, while cellulose is composed of $C_6$ (hexosan) sugars. After pre-treating and fractionating the biomass, these sugars can be isolated.[11-18] Conversion of pentosans and hexosans to γ-valerolactone (GVL) can occur through an acid-catalyzed dehydration and metal-catalyzed hydrogenation reactions.[16,17] Through acid catalysis, GVL can undergo ring-opening to produce isomers of pentenoic acids.[43] These pentenoic acids can be converted to olefins or diolefins such as butadiene or pentadiene, both of which are petrochemical intermediates used in the industry. This study focuses on converting propanoic acid, a model molecule to mimic the behavior of pentanoic acid, to propanol so it can be dehydrated to produce propene and/or propyne. This is a continuation of the previous study, but this study mainly focuses on studying the effect of partial pressures of propionic acid on the propanol production rate while cofeeding alcohol in the gas phase.

Direct conversion of carboxylic acids to olefins and diolefins is difficult due to the low electrophilicity of the carbonyl carbon.[51,52,72,90-92] This can be intercepted by creating an ester intermediate, which has a lower activation energy than its carboxylic acid

counterpart.[51] In this study, 1-butanol was cofed with propionic acid to increase the propanol production rate. The results of this study indicate that there is a slight enhancement in propanol production rate due to an efficient production and adsorption of the ester when 1-butanol was injected.

### 3.1 Introduction

As the world population is increasing and economies are developing, energy consumption has been escalating despite the limited availability of fossil fuels. In addition, combustion of fossil fuels requires a lot of energy, releases a lot of heat, and increases the emissions of greenhouse gases. Biomass is receiving increasing attention in the energy sector because it is a promising sustainable feedstock.[28] Biomass derived energy is clean, environmentally friendly, abundant, and renewable. Biofuels have maximum benefits in that they do not compete with food, do not cause "land grabbing," and lower greenhouse gas emissions if used correctly.[47] They also have less Sulphur content; therefore, $SO_2$ emissions would be lower. They also consist of less nitrogen and ash; thus, the $NO_x$ and soot emissions would be lower compared to the combustion of fossil fuels. Since the carbon dioxide released from plants will be recycled into the biomass via photosynthesis, there should also be a carbon dioxide net emission of zero.[10,11,28] Despite needing some policy changes to protect the environment, biofuels can be extremely beneficial in the sustainable development of our future.[47,48]

Currently in the industry, hydrocarbons feedstocks are used to produce petrochemical intermediates. Biorefining can produce the same petrochemical intermediates except in that biomass is used as an energy source rather than petroleum.[28,49,50] Biomass can also be used to compensate for the low supply of petrochemical intermediates caused by the

shift towards using lighter hydrocarbon feedstocks as the heavier hydrocarbon feedstocks can be used as fuels in their own right.[11]

Lignocellulosic biomass, the most abundant feedstock[28], is composed of cellulose, hemicellulose, and lignin. Hemicellulose consists of xylose, $C_5$ (pentosan) sugars, and $C_6$ (hexosan) sugars, while cellulose is composed of $C_6$ (hexosan) sugars. After pre-treating and fractionating the biomass, these sugars can be isolated.[11-18] Conversion of pentosans and hexosans to γ-valerolactone (GVL) can occur through an acid-catalyzed dehydration and metal-catalyzed hydrogenation reactions.[16,17] Through acid catalysis, GVL can undergo ring-opening to produce isomers of pentenoic acids.[43] These pentenoic acids can be converted to olefins or diolefins such as butadiene (BD) or pentadiene (PD), both of which are valued petrochemical intermediates in the industry. For the purposes of reaction conditions in the gas phase, the experiments in this study utilized propanoic acid, a light model molecule to mimic the behavior of pentanoic acid, so that it does not plug the reactor lines.

Direct conversion of carboxylic acids to olefins and diolefins is difficult due to the low electrophilicity of the carbonyl carbon. Their low reactivity is associated with low polarizability of the carbonyl group. The order of polarizability of the carbonyl group in various functional groups is shown in the figure below. [51,52,72,90-92]

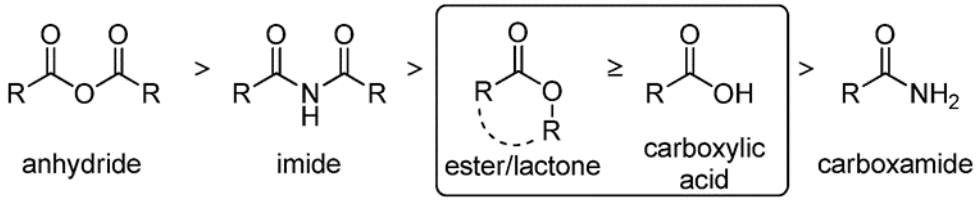



**Figure 26: Order of the polarizability of the carbonyl group from most reactive to least reactive[52]**

An ester can be more reactive than a carboxylic acid based on the -R group attached.[52] In addition, Santiago *et al.*[51] performed DFT calculations to obtain activation energies for dissociative adsorption of various carbonyl species on copper supported on silica. Copper is a great metal because it is low in oxophilicity.[51,81] It avoids decarbonylation and supports hydrogenation. Acetic acid had a high activation energy of 90-100 kJ/mol while the esters presented a much lower barrier. The barrier for methyl acetate was 70-80 kJ/mol and the barrier for ethyl acetate was 50-60 kJ/mol. Since carboxylic acids require a high activation energy for dissociative adsorption, they are more difficult to adsorb and react on the surface of copper.[51]

To reduce carboxylic acids and esters to alcohols, the C-O bond adjacent to the carbonyl group must be cleaved according to the following equation where the R-groups represent different alkyl groups.[51]

$$R_ACOOR_B + 2H_2 \leftrightarrow R_ACH_2OH + R_BOH^{51}$$

Many studies have shown that impregnating hydrogenation metals such as Zn, Co, Ni, Fe, and Cu on oxides such as $Cr_2O_3$, $ZrO_2$, $V_2O_5$, and $WO_3$, was effective in reducing esters and carboxylic acids to alcohols.[51,54-61] Turek *et al*[53] has shown that copper-based catalysts reduce carboxylic acids and esters to alcohols a lot more efficiently than some of the other hydrogenation catalysts.[53]

Individual studies regarding hydrogenolysis of monoesters have been performed in the mid to late 1900s. Lazier was the first to propose a copper oxide/zinc oxide catalyst to convert butyl butyrate to butanol. Schmidt proposed the use Ni, Co, and Cu for the reaction conditions: temperature range of 200 °C to 400 °C at atmospheric pressure.

Barium-promoted copper chromite was used in several hydrogenolysis studies, and most showed that these catalysts can produce transesterification products. The hydrogenolysis of esters rate increased with increasing size of the -R groups. In addition, a lower rate was observed when the alkoxyl carbon had a methyl group, but a high rate was observed when the second alkoxyl carbon was branched. Overall, copper-based catalysts were shown in literature to be effective in cleaving the C-O bond adjacent to the carbonyl group of esters and carboxylic acids.

Copper chromite catalyst is one of the most widely used copper-based catalysts.[51,62] Adkins-type catalysts such as CuO and copper chromite ($CuCr_2O_4$) were discovered in the 1930s.[54] These catalysts are still used in the industry to manufacture alcohols even though they exhibit low activity and require harsh operating conditions. This is because their catalytic structure is resistant to the free fatty acids.[55] Thus, the composition of these catalysts has remained unchanged since they were discovered.[72] In addition, copper supported on silica and Raney copper showed just as much promise as copper chromite in reducing esters.[51,63-71]

In this paper, we present results from experiments applying similar concepts from Clayden *et al*[52] and Santiago *et al*[51], that propionic acid's carbonyl carbon has low electrophilicity and polarizability[52]. The low reactivity of propionic acid can be overcome by first converting the carboxylic acid into an ester, which can then be reduced to its corresponding alcohols.[51] These alcohols can then be dehydrated to form olefins or diolefins. However, the main goal of this study is to enhance the rate of propanol production via an ester intermediate. Reactions were performed in a gas phase flow reactor and the reaction species were quantified using an online gas chromatography

equipped with a flame ionization detector (GC-FID). Using the copper chromite catalyst, temperature programmed reduction (TPR), X-ray diffraction (XRD), and transmission electron microscopy (TEM) characterizations were performed. This study will show that forming an ester intermediate with the help of an alcohol, increases the reactivity of the propionic acid and enhances the rate of propanol production.

## 3.2 Experimental

### *3.2.1 Catalyst preparation*

The copper chromite ($2CuO \cdot Cr_2O_3$) catalyst was purchased from Sigma Aldrich. It was prepared via the industrial combustion method. The composition was defined as 30% CuO and 70% $Cr_2O_3$.

### *3.2.2 Catalyst characterization*

a. Temperature programmed-reduction (TPR)

TPR of the catalyst was performed in a custom-made system. A ¼" quartz tube packed with quartz wool and 50.0 mg of copper chromite catalyst was mounted vertically in a furnace. The tube and the sample were purged with nitrogen flow rate of 30 stcm for 30 minutes. After the signal stabilized, a flow rate of 35 sccm (5% hydrogen in argon) was passed through the sample. The thermal conductivity detector (TCD, SRI 110), measured the effluent gas that passed through the sample before entering the TCD. This was analyzed using 35 sccm of 5% hydrogen in argon mixture. The temperature was then ramped to 900 °C at 10 °C/minute.

b. Transmission electron microscopy (TEM)

Lawrence Barret performed TEM analysis at the Microbiology Department at OU.

The catalyst was pre-reduced at 280 °C for 2 hours under 100 stcm of hydrogen. After cooling it down to room temperature, a small sample was dispersed in heptane and sonicated to achieve a uniform suspension. A few drops of the suspension were then placed on TEM grids (polymer-coated copper). The TEM (ZEISS 10 model) was used to take images of the samples.

c. X-ray diffraction (XRD)

The XRD analysis was performed by the Geology Department at OU.

A small amount of fresh copper chromite catalyst was placed flat on a plastic slide. A curved crystal monochromator Rigaku automatic diffractor (model D-Max A) was used to analyze the sample. The equipment utilized 40 kV, 35 mA, and Cu Kα radiation source. After reaction from the liquid phase batch reactor, the reaction mixture was filtered via vacuum filtration. The catalyst in the Buchner funnel on the filtered paper was washed with pure acetone multiple times. This catalyst was then removed from the funnel and placed on a plate in an oven. The catalyst was dried over night at 80 °C and then cooled to room temperature before performing the XRD. The above parameters were used to analyze the sample.

d. Energy-dispersive X-ray spectroscopy (EDX)

Lawrence Barret performed EDX analysis at the Microbiology Department at OU.

A small sample of the copper chromite catalyst was pressed against the carbon tape on the stud. NEON ZEISS 40ESB was used to scan the sample for all elements of the periodic table. High, moderate, and low-resolution images were taken at various frames.

e. Thermogravimetric analysis (TGA)

Lawrence Barret performed TGA at the Chemical Engineering department at OU.

This technique was performed using STA 449 F1 Jupiter®, Netzsch and Quadrupole Mass Spectrometer (QMS) 403 C Aeolos®. Approximately 15 mg of copper chromite catalyst was reduced in hydrogen at 400 ºC at a heating rate of 3 ºC/min. The sample was then cooled down and passivated with nitrous oxide ($N_2O$) at 60 ºC under constant flow of 60 mL/min for 4 hours. Afterwards, the sample was heated in hydrogen from 80 ºC to 400 ºC using the ramp rate of 3 ºC/min.

*3.2.3 Catalytic activity measurement*

Catalytic activity was measured using a 0.25 in OD quartz tube reactor. Approximately 5 mg of the copper chromite ($2CuO \cdot Cr_2O_3$, Sigma Aldrich) particles were mixed with 195 mg acid washed glass beads (212 – 300 μm, 50 – 70 U.S. sieve, Sigma Aldrich). The copper chromite was pelletized to 90 – 250 μm size particles. The catalyst mixture and the bed remained the same height (~1 inch) for all experiments. The mixture was placed between the quartz wool inside the quartz tube reactor, and the reactor was mounted at the inlet and outlet and placed in an oven. It was well-insulated at both ends and was checked for leaks using a hydrogen gas detector. A 2.5 mL Hamilton syringe was filled with a well-mixed mixture of 1:10 molar ratio of propionic acid (Sigma Aldrich ACS reagent, ≥99.5%) to n-heptane (Sigma Aldrich anhydrous, 99%). The syringe was placed in a kdScientific syringe pump and the reactant flow rate was set to 0.15 mL/hr. It took approximately 1 hour for the flow to stabilize. For some experiments, 1-butanol (Sigma Aldrich anhydrous, ≥99.5%) was cofed at the same flowrate. The system consisted of the reactor oven, pressure gauge, pressure relief valve, temperature controller, and an online gas chromatography with flame ionization detector (Agilent GC-FID). The catalyst was initially reduced at 400 ºC for 1 hour under atmospheric pressure using 100 stcm of $H_2$.

After reduction, the oven cooled to the reaction temperature of 250 °C and the feed was injected into the reactor at an inlet temperature of 100 °C. The reaction was run at 250 °C for a couple of hours under the same flowrate of hydrogen and the gas samples were taken every 25 minutes at ambient pressure using the online GC-FID. After the reaction, the reactor was cooled to room temperature and purged with 100 stcm of nitrogen. A small sample from the liquid trap was analyzed for various experiments in a mass spectrometry (Shimadzu) for identification.

The reactants and products were quantified using a gas chromatography with flame ionization detector (Agilent GC-FID, 7890B) equipped with an INNOWAX column (Agilent, 30 m x 320 μm x 0.32 μm). The GC-FID is connected to the reactor outlet line via a 6-port valve. The areas of the peaks were used to correlate with the number of moles of carbon to quantify the data. A liquid trap with ethanol or acetone were used to trap gas products to identify the compounds using a mass spectrometry (Agilent GC-MS).

## 3.3 Results and Discussion

### *3.3.1 Catalyst characterization results*

In order to find the reduction temperature of copper chromite, temperature programmed reduction (TPR) was performed. Results are shown in Figure 27. The bulk CuO is expected to reduce between 200-300 °C[73]. For the reaction conditions used in this study, at 400 °C, 100 stcm of atmospheric $H_2$ for 1 hour, a complete reduction of copper must have occurred.

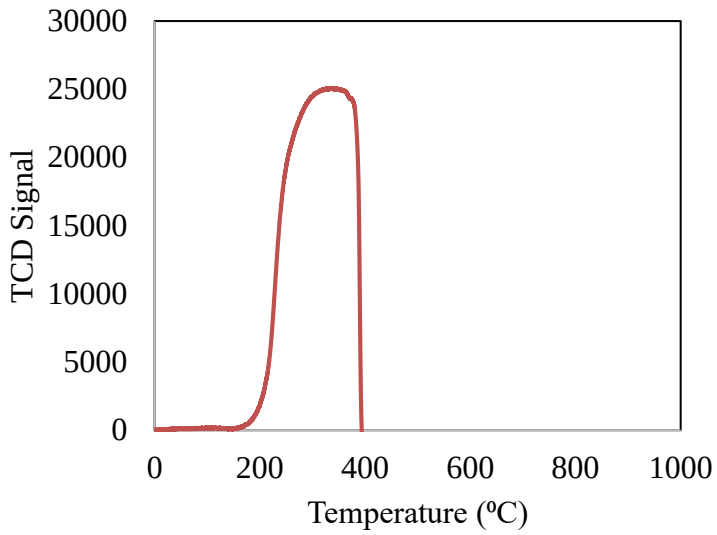



**Figure 27: Temperature programmed reduction (TPR) of the copper chromite**

Transmission electron microscopy (TEM) was performed to calculate the copper particle diameters after reduction. However, the results showed extreme sintering of the copper and were not viable to calculate particle diameters.

To further confirm that under reaction conditions, there will be a complete reduction of copper, X-ray diffraction (XRD) analysis was performed after a liquid phase reaction. It was also done to understand the crystalline nature of the catalyst and the size of the copper particles in copper chromite. The resulting peaks in Figure 28 were identified according to XRD data obtained from literature.[74,78,79] The metallic copper peaks significantly increase in height after reduction and reaction, suggesting that there is a low dispersion and that the catalytic particles are not stable under reaction conditions. Therefore, the metallic copper particle size is higher due to sintering. $Cu^{2+}$ from CuO peak disappeared after reaction, suggesting that CuO was no longer present in the active phase of the reaction and does not play a role. Because there is a large amount of metallic copper (due to sintering, etc.) at high particle diameters, this is likely the active site. More calculations

are necessary to determine the exact plane where the reaction is taking place. However, planes (111) and (400) can be identified in Figure 28 according to literature[74,78,79].

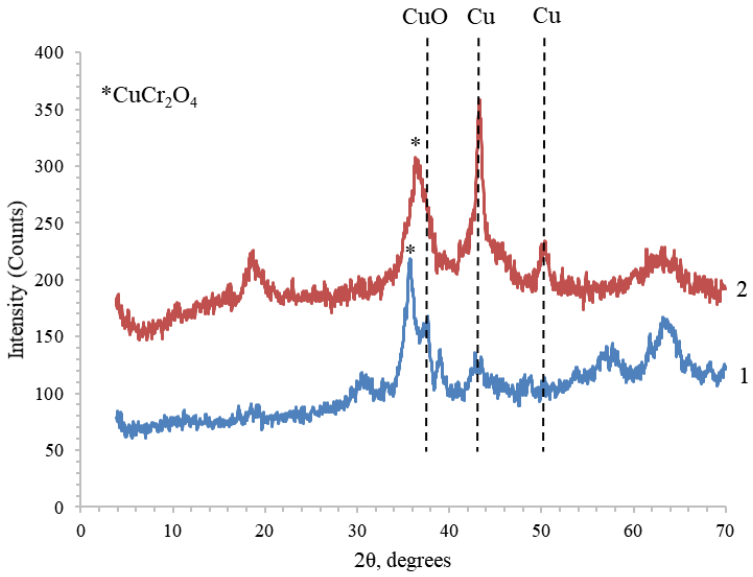



**Figure 28: The X-ray diffraction data for the copper chromite samples: 1 - fresh copper chromite, 2 - spent catalyst after reaction**

Applying the Scherrer equation (1)[75]:

$$D = \frac{K\lambda}{B\cos\theta} \quad (1)$$

Where, $K$ (dimensionless shape factor) = 0.89, $\lambda$ (X-ray wavelength) = 0.1542 nm, $B$ (line broadening at half the maximum intensity) = 0.680°, 2θ (Bragg angle) = 43.356°, the metallic copper particle diameter was calculated to be 12.44 nm. This value is comparable to the value accepted in literature (13.3 nm).[76]

Many commercial copper chromite catalysts were known to have promoters such as barium.[77,79] Thus, an energy-dispersive X-ray spectroscopy (EDX) was performed to scan for various elements, impurities, or promoters in the sample for further confirmation. The results are shown below.

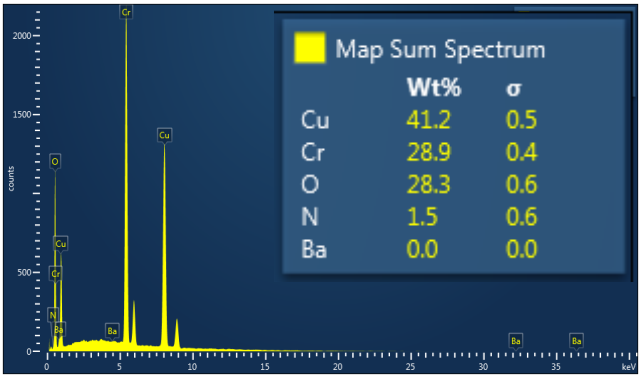



**Figure 29: Energy-dispersive X-ray spectroscopy (EDX) of copper chromite**

The copper chromite consists of 41 wt.% Cu, 29 wt.% Cr, and 28 wt.% O. Thus, the EDX further proved that the activity of the catalyst is only related to the copper and chromium mixed oxides present in the sample.

The TGA results for copper chromite were not viable in calculating particle diameters. Our current experimental conditions must be altered because the weight loss of the sample showed a very high dispersion of copper particles with extremely low particle diameters. It is likely that the nitrous oxide may have penetrated deeper than simply the surface layer of the sample. Perhaps if the nitrous oxide was diluted and the passivation time was decreased, it would lead to more realistic results.

*3.3.2 Catalytic results and discussion*

According to Clayden *et al*[52] and Santiago *et al*[51], esters are more reactive than carboxylic acids.[72,90-92] To confirm this theory, same concentrations of esters and carboxylic acids were fed into a batch reactor in the presence of copper chromite catalyst. The results are shown in Figure 17 and the reaction pathways are shown in Figures 15 & 16. On the basis of these experiments, 1-butanol will be cofed with propionic acid in the gas phase flow reactor to enhance propanol production rate. The reaction pathway is shown below.

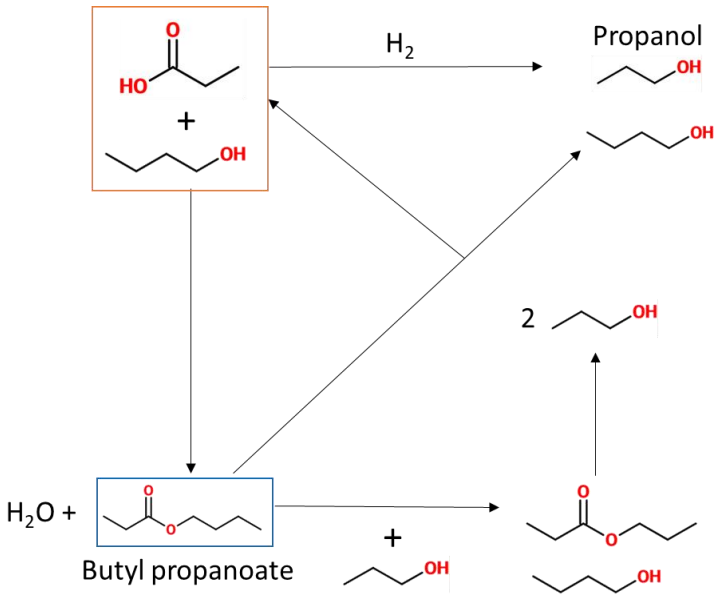



**Figure 30: Reaction pathway showing the reduction of propionic acid, butyl propanoate, and propyl propanoate to propanol**

Ester and water are formed when a carboxylic acid reacts with an alcohol. Propionic acid can be reduced directly to form propanol. In the presence of 1-butanol, propionic acid reacts with it to form butyl propanoate ester. This ester can be reduced to form one mole butanol and one mole of propanol. Propyl propanoate can be formed when butyl propionate reacts with propanol that is produced from the reduction of the acid or the ester. Propyl propanoate can further be reduced to form two moles of propanol.

After reducing the copper chromite catalyst, initial experiments were performed using a pure feed of propionic acid. The yield of products over time on stream are shown in Figure 31. The carbon balances for the following reaction with respect to propionic acid range from 88% to 97%.

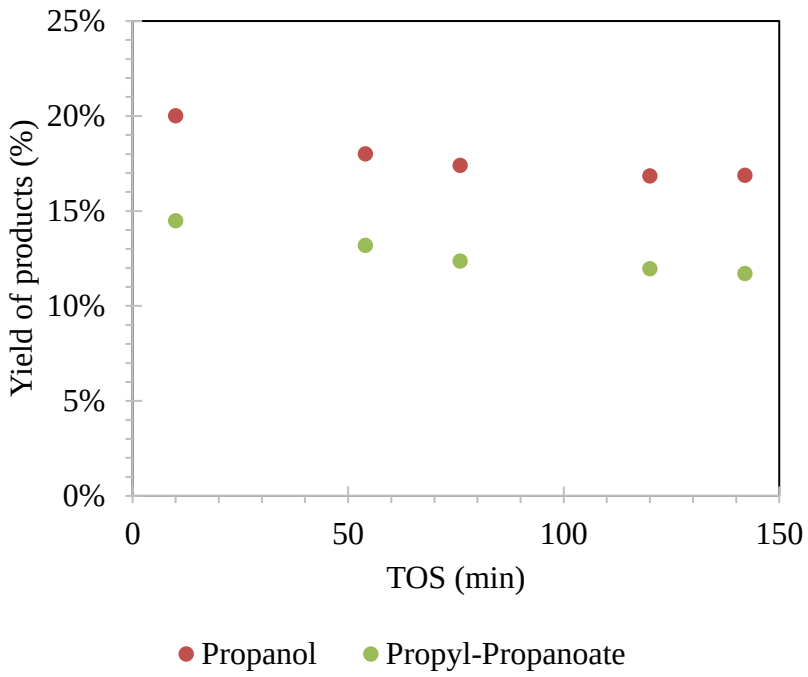



**Figure 31: Yield of products (%) when flowing 0.0013 mol/hr of propionic acid. Reduction: 50 mg of copper chromite, 400 °C, 1 hour, 100 stcm $H_2$. Reaction: 300 °C, 100 stcm $H_2$**

When 1:0.5 molar ratio of propionic acid to 1-butanol is mixed and fed at 0.0013 mol/hr propionic acid and 0.00067 mol/hr 1-butanol, the following is observed. See the figure below. Carbon balances with respect to propionic acid are within the range of 90% to 100%.

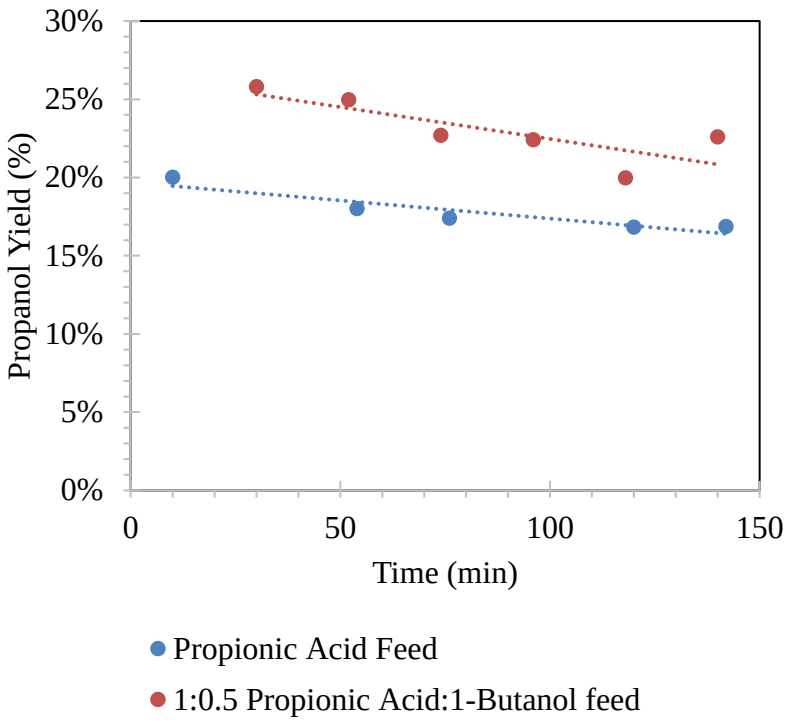



**Figure 32: Yield of propanol (%) when flowing 0.0013 mol/hr of propionic acid alone and when flowing 0.0013 mol/hr of propionic acid and 0.00067 mol/hr 1-butanol (1:0.5 molar ratio). Reduction: 50 mg of copper chromite, 400 °C, 1 hour, 100 stcm $H_2$. Reaction: 300 °C, 100 stcm $H_2$**

With the addition of 1-butanol (BuOH), there is a slight increase in propanol product yield compared to when no alcohol was co-fed. When BuOH was cofed, propyl propionate was no longer observed (Appendix 3); however, butyl propionate is produced at a much higher yield. Although it is easier to form a propyl propionate ester due to its stability, there is not much propanol available to form this ester immediately. The propanol must come from the reduction of propionic acid and that occurs at a much slower rate. Therefore, a high yield of butyl propionate is observed when butanol is cofed because there was more alcohol available (Appendix 3). The enhancement seen in Figure 32 can be explained by the fact that more butyl propionate ester is being formed with the butanol cofeed that is cleaved at a much faster rate to yield propanol compared to when propionic acid was fed

by itself. From this it can be concluded that the conversion of propionic acid to propanol is slower compared to the conversion of butyl propionate ester to propanol. Also, butyl propionate formation from propionic acid and butanol is faster than propionic acid conversion to propanol. The reaction rate constants are expected to have the following trends: $k_1 < k_2 \leq k_{ester}$, where $k_1$ is for PrA → propanol, $k_{ester}$ is for the formation of ester (butyl propionate), and $k_2$ is for ester → propanol. The rate of formation of the ester may or may not be faster than its decomposition as it depends on the -R group that is attached to the alcohol.

Under the reaction conditions shown in Figure 32, the propionic acid is in a zeroth order regime where the reaction rate does not vary with changing reactant concentrations.[82] When only propionic acid is fed into the reactor, without the presence of alcohol, propanol and propyl propanoate are produced. The reaction rates presented in Figure 33 only account for the conversion of propionic acid producing these products. The rates plotted are the disappearance rates of propionic acid or rate appearance of products at 32 minutes. In the case of zeroth order, the surface of the catalyst is always saturated with propionic acid regardless of the concentration of propionic acid fed into the reactor[82].

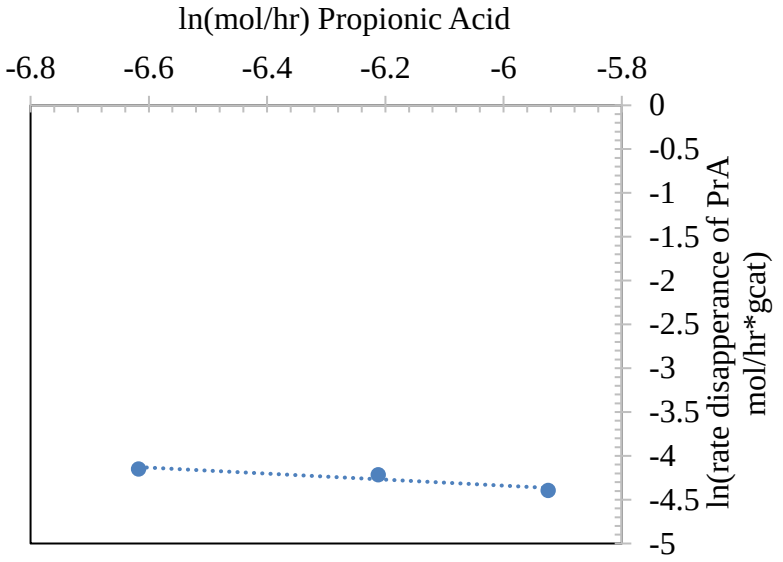



**Figure 33: Zeroth order regime with respect to Propionic Acid (PrA) at 32 min.**

$$Rate = -\frac{d[C_{PEA}]}{dt} = k[C_{PEA}^{0}] = k = constant^{82} \quad (2)$$

In Equation (2), rate (reaction rate) is equivalent to k (reaction rate coefficient) usually in the units of mol/L*min. [82] The slope in Figure 33 represents the reaction order, which is zero. Therefore, if the reaction rates at various PrA concentrations are known, the reaction rate coefficient can be estimated.

Applying the Arrhenius equation for zeroth order conditions[82]:

$$k = Ae^{-\frac{E_a}{RT}} \quad (3)$$

This equation can be expressed in the straight-line form:

$$lnk = -\frac{E_a}{R}\left(\frac{1}{T}\right) + lnA \quad (4)$$

Where, $T$ is the reaction temperature (K), $k$ is the kinetic rate constant (mol/hr*gcat), $A$ is the pre-exponential factor, $E_a$ is the activation energy (J/mol), and R is the ideal gas constant 8.314 J/mol*K. Plotting $lnk$ versus $\left(\frac{1}{T}\right)$ will produce a slope equivalent to $-\frac{E_a}{R}$

and intercept equivalent to $lnA$. In order to find the activation energy of PrA converting to propanol and propyl propanoate, the same procedure was followed as Figure 33 but PrA was diluted in heptane (1:10 molar ratio) and the reaction was run at different temperatures ranging from 250 °C to 300 °C. The PrA molar flow rate, 0.000102 mol/hr, remained the same for all experiments. The initial rates and reaction rate constants were obtained at 32 minutes of reaction. See the figure below for the Arrhenius plot.

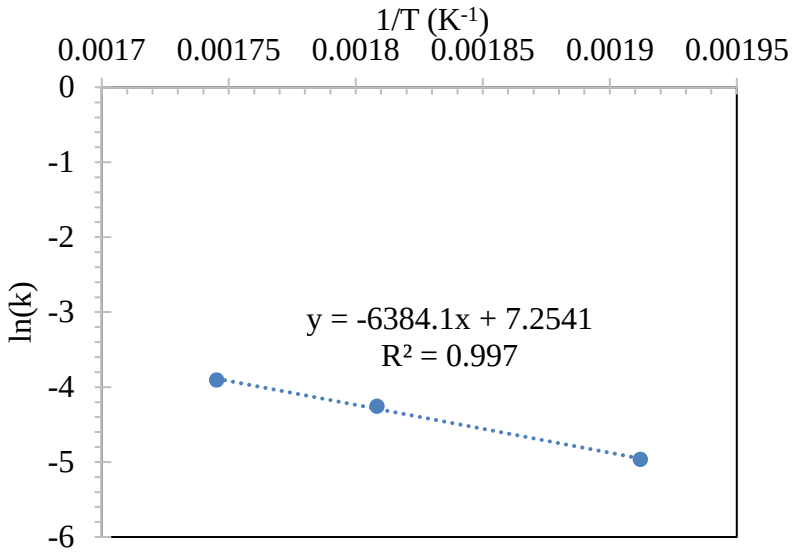



**Figure 34: Arrhenius Plot, PrA = 0.000102 mol/hr, Reduction: 5 mg of copper chromite, 400 °C, 1 hour, 100 stcm $H_2$. Reaction: 250, 280, and 300 °C, 100 stcm $H_2$**

Since slope is equivalent to $-\frac{E_a}{R}$, the activation energy for this reaction is calculated to be 53 kJ/mol. The conversions of propionic acid are 35%, 67%, and 100% at 250 °C, 280 °C, and 300 °C, respectively. Therefore, this may not be an accurate estimation of the activation energy. But, it is lower than the activation energy calculated for pentanoic acid in Chapter 2 due to physical differences in compounds, 3-carbon versus 5-carbon carboxylic acids. While their thermodynamics are different, both molecules have the same chemistry, which is sufficient for this study.

The pre-exponential factor, $A$, has the same units as the reaction rate constant $k$ (mol/hr*gcat) and can be estimated by taking the exponent of the intercept.

The following table summarizes an approximation of the rate constants and activation energy.

| ***Parameters*** | **$T_1$ = 250 °C** | **$T_2$ = 280 °C** | **$T_3$ = 300 °C** |
|---|---|---|---|
| *k (mol/hr*gcat)* | 0.00698 | 0.0142 | 0.0201 |
| *A (mol/hr*gcat)* | 1414 | | |
| *$E_a$ (kJ/mol)* | 53 | | |

**Table 4: Summary of PrA parameters, reaction rate constant (k) and activation energy ($E_a$) for PrA → propanol + propyl-propanoate**

### 3.4 Conclusion & Future Direction

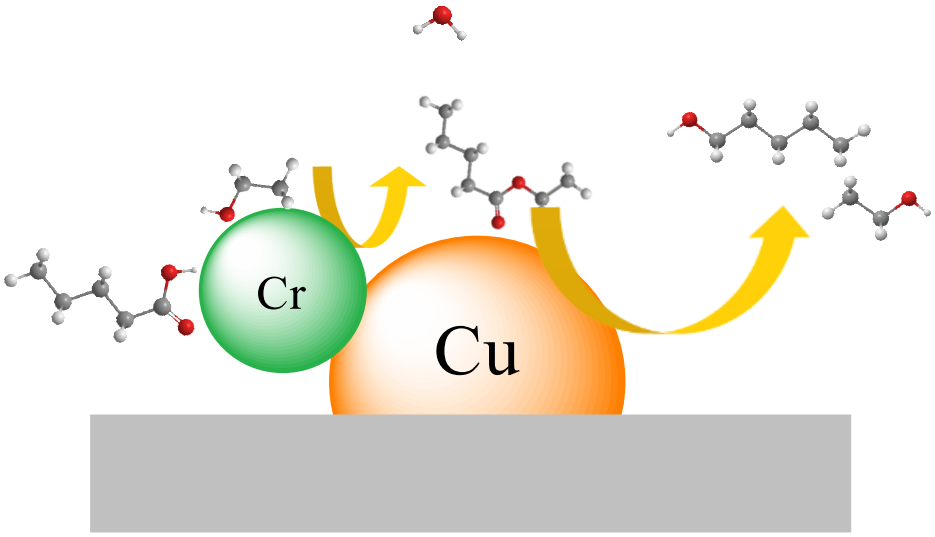
Cofeeding small amount of butanol with propionic acid (PrA) accelerated the rate of propanol produced. This is because the ester formed from this cofeeds have a much lower activation energy compared to carboxylic acids (PEA) alone.[51,52,72,90-92] While the activation energy for PrA to propanol was calculated to be 53 kJ/mol, the activation energy for butyl propionate ester to propanol still needs to be calculated to verify this claim. Although a formal kinetic model was not introduced in this study, the reaction rate constants are expected to have the following trends: $k_1 < k_2 \leq k_{ester}$, where $k_1$ is for PrA → propanol, $k_{ester}$ is for the formation of ester (butyl propionate), and $k_2$ is for ester → propanol. The rate of formation of the ester may or may not be faster than its decomposition as it depends on the -R group that is attached to the alcohol. Overall, it was possible to accelerate propanol production by adding a small amount of butanol to the propionic acid feed on a copper chromite catalyst in the gas phase.

The role of the $Cr_2O_3$ in the mixed oxide copper chromite catalyst should be investigated in detail to understand the mechanism of this reaction. More studies need to be performed to verify that the metallic copper is the active site and that it is formed through an aldehyde intermediate. DFT studies may be necessary to find the reaction rate constants and equilibrium adsorption constants to generate a working kinetic model in the future.

All of the results presented above are preliminary results. The main goal of this study was to understand the effect of changing partial pressures of propionic acid on propanol production with alcohol cofeeds. However, the data presented above has been under zeroth order conditions where the catalyst surface is always saturated with the acid. To truly understand the effect of changing concentrations of acid, the reactant needs to be in a first order regime. After finding the first order regime with respect to the propionic acid, butanol can be added to enhance the rate while changing the concentration of the acid feed. Enhancing the propanol production rates is just the beginning of this project. Future outlooks include dehydrating the propanol to form propene or propyne to satisfy the goal of this project.

# Chapter 4: Identification of the active site on copper chromite

## Abstract




Copper chromite is considered an Adkins-type catalyst that has been in-use in the industry since the 1930s.[54,79] Several studies were performed on the crystalline nature for the location of the active site on this catalyst.[93-95] This study investigates the unique ability of copper chromite to reduce carboxylic acids and esters to alcohols. Specifically, pentanoic acid, a biomass derived compound, is converted to pentanol on copper chromite in the liquid phase batch reactor. The results for copper chromite are compared with 10% $Cu/SiO_2$ prepared via the incipient-wetness impregnation method. Drastic disparities in results suggest that there is an interaction of the support and/or mixed oxide with metallic copper in copper chromite. When copper chromite is initially reduced at 280 °C under 350 psi of $H_2$ for 2 hours, the metallic copper migrates to the surface of the oxide support.[93-95,102-104] In addition to this, we propose that some of the chromia also reduces and migrates to the surface, decorating the largely sintered metallic of copper.

## 4.1 Introduction

Adkins-type catalysts such as CuO and $CuCr_2O_4$ were discovered in the 1930s. They were known for hydrogenating esters and fatty acids to alcohols. These catalysts are still used in the industry to manufacture alcohols even though they exhibit low activity and require harsh operating conditions.[54,79] Previous studies indicated that this catalyst consists of a "tetragonally distorted normal spinel with c/a < 1".[93,95] The distortion is caused by the $Cu^{2+}$ ions that occupy the tetrahedral sites trying to form four square coplanar bonds.[62,93-95] When the catalyst is reduced at high temperatures under hydrogen, the copper undergoes reduction reaction: $Cu^{2+} \rightarrow Cu^0$. The reduced metallic copper atoms are released onto the spinel surface while $H^+$ enters the tetrahedral interstices that were previously occupied by $Cu^{2+}$ ions. Some of the $Cu^+$ ions move into the octahedral interstices.[98-100] Therefore, the bulk oxygen structure in the spinel is not altered.[101,104] The metallic copper atoms that were released on the spinel surface form a flat layer that is epitaxially bound to the surface of the oxide (particle sizes of ~100 angstroms).[101,104] In other words, the resulting copper metal particles sinter and come to the surface of the oxide.[96] The oxide support is composed of copper (II) chromite.[102] The $Cr^{3+}$ ions always occupy octahedral sites.[104] Some studies indicate that prior to reduction of the catalyst, it is a tetragonal spinel unit cell. After reduction at elevated temperatures, it transforms into a cubic unit cell.[103,104] Also, higher the degree of reduction, more the presence of epitaxially bound copper metal on the oxide surface.[100,101] Once a metallic copper layer is formed on the surface, it is stabilized by protons.[104]

As indicated previously, copper chromite catalysts are commonly used in the industry to hydrogenate fatty acids and esters to produce alcohols.[54,79] In upgrading biomass derived

compounds, such as pentanoic acids, to petrochemical intermediates, copper chromite catalysts are used as shown in Chapters 1 and 2. This catalyst was successful in converting pentanoic acid directly to pentanol. Also, it was successful in accelerating the pentanol production rate when an alcohol was cofed with pentanoic acid to form an ester intermediate. In this paper, we present results that propose the location of the active site for these reactions.

Reactions were performed in a liquid phase batch reactor and the reaction species were quantified using a gas chromatography equipped with a flame ionization detector (GC-FID). Using the copper chromite catalyst, temperature programmed reduction (TPR), X-ray diffraction (XRD), thermogravimetric analysis (TGA), scanning electron microscopy (SEM), transmission electron microscopy (TEM), and Brunauer-Emmett-Teller (BET) characterizations were performed. Barium promoters are commonly used in this catalyst to increase activity and selectivity of hydrogenation products. It was able to increase acidity of the catalyst by forming a $BaC_rO_4$ phase which was able to stabilize large particles of metallic copper.[97] In order to see if any promoters are present in this catalyst, Energy-dispersive X-ray spectroscopy (EDX) was also performed.

## 4.2 Experimental

### *4.2.1 Catalyst preparation*

The 3%, 5%, 10% $Cu/SiO_2$ catalysts were prepared using the incipient wetness impregnation method. The precursor, copper(II) nitrate hemi-(pentahydrate) (Alfa Aesar, 98%), was impregnated on the silica support (Davisil silicon dioxide, 99.8%).

The 3%, 5%, 10% $Cu/ZrO_2$ catalysts were prepared using the incipient wetness impregnation method. The precursor, copper(II) nitrate hemi-(pentahydrate) (Alfa Aesar,

98%), was impregnated on the $ZrO_2$ support (Aldrich, 99% trace metal basis). Zirconium dioxide was pre-treated in air at 100 °C for 24 hours before impregnation.

3%, 5%, 10% $Cu/Cr_2O_3$ catalysts were prepared using the incipient wetness impregnation method. The precursor, copper(II) nitrate hemi-(pentahydrate) (Alfa Aesar, 98%), was impregnated on the chromia support (Sigma-Aldrich, 99.9% trace metal basis).

The 10% $Cu/TiO_2$ catalyst was prepared using the incipient wetness impregnation method. The precursor, copper(II) nitrate hemi-(pentahydrate) (Alfa Aesar, 98%), was impregnated on the $TiO_2$ support (Aldrich, Aeroxide® P25, 21 nm, ≥99.5%).

All of the catalysts were dried overnight at 80 °C after impregnation. All of the catalysts were then calcined with an air flow of 150 mL/min. The system was ramped to 100 °C with a ramp rate of 2 °C /min and was held at 100 °C for 4 hours. Then, the system was again ramped to 400 °C with a ramp rate of 2 °C/min and was held at 400 °C for four hours.

*4.2.2 Catalyst characterization*

a. Temperature programmed-reduction (TPR)

TPR of the catalyst was performed in a custom-made system. A ¼" quartz tube packed with quartz wool and 50.0 mg of copper chromite catalyst was mounted vertically in a furnace. The tube and the sample were purged with nitrogen flow rate of 30 stcm for 30 minutes. After the signal stabilized, a flow rate of 35 sccm (5% hydrogen in argon) was passed through the sample. The thermal conductivity detector (TCD, SRI 110), measured the effluent gas that passed through the sample before entering the TCD. This was analyzed using 35 sccm of 5% hydrogen in argon mixture. The temperature was then

ramped to 900 °C at 10 °C/minute. The same procedure was followed for copper (II) oxide and 10% $Cu/SiO_2$ samples.

b. Brunauer-Emmett-Teller (BET)

BET surface area measurements were performed using Micromeritics ASAP 2010. A small sample was initially degassed at 200 °C for 6 hours before analysis.

c. Transmission electron microscopy (TEM)

Lawrence Barret performed TEM analysis at the Microbiology Department at OU.

The catalyst was pre-reduced at 280 °C for 2 hours under 100 stcm of hydrogen. After cooling it down to room temperature, a small sample was dispersed in heptane and sonicated to achieve a uniform suspension. A few drops of the suspension were then placed on TEM grids (polymer-coated copper). The TEM (ZEISS 10 model) was used to take images of the samples.

d. X-ray diffraction (XRD)

The XRD analysis was performed by the Geology Department at OU.

A small amount of fresh copper chromite catalyst was placed flat on a plastic slide. A curved crystal monochromator Rigaku automatic diffractor (model D-Max A) was used to analyze the sample. The equipment utilized 40 kV, 35 mA, and Cu Kα radiation source. After reaction from the liquid phase batch reactor, the reaction mixture was filtered via vacuum filtration. The catalyst in the Buchner funnel on the filtered paper was washed with pure acetone multiple times. This catalyst was then removed from the funnel and placed on a plate in an oven. The catalyst was dried over night at 80 °C and then cooled to room temperature before performing the XRD. The above parameters were used to analyze the sample.

e. Energy-dispersive X-ray spectroscopy (EDX)

Lawrence Barret performed EDX analysis at the Microbiology Department at OU.

A small sample of the copper chromite catalyst was pressed against the carbon tape on the stud. NEON ZEISS 40ESB was used to scan the sample for all elements of the periodic table. High, moderate, and low-resolution images were taken at various frames.

f. Thermogravimetric analysis (TGA)

Lawrence Barret performed TGA at the Chemical Engineering department at OU.

This technique was performed using STA 449 F1 Jupiter®, Netzsch and Quadrupole Mass Spectrometer (QMS) 403 C Aeolos®. Approximately 15 mg of copper chromite catalyst was reduced in hydrogen at 400 °C at a heating rate of 3 °C/min. The sample was then cooled down and passivated with nitrous oxide ($N_2O$) at 60 °C under constant flow of 60 mL/min for 4 hours. Afterwards, the sample was heated in hydrogen from 80 °C to 400 °C using the ramp rate of 3 °C/min.

## 4.3 Results and Discussion

### *4.3.1 Catalyst characterization results*

In order to find the reduction temperature of copper chromite, temperature programmed reduction (TPR) was performed. This is compared with 10% $Cu/SiO_2$. Results are shown in Figure 35. The bulk CuO is expected to reduce between 200-300 °C[73]. For the reaction conditions used in this study, at 280 °C, 350 psig of $H_2$ for 2 hours, a complete reduction of copper must have occurred. The 10% $Cu/SiO_2$ sample shows a shift in reduction temperature to the left compared to pure copper (II) oxide.

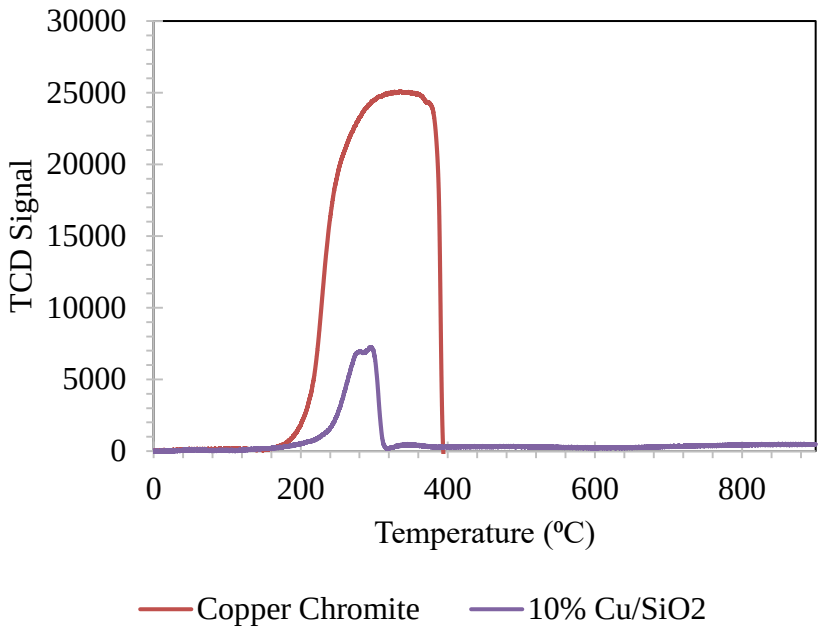



**Figure 35: Temperature programmed reduction (TPR) of the copper chromite and 10% Cu/$SiO_2$**

Transmission electron microscopy (TEM) was performed to calculate the copper particle diameters after reduction. However, the results showed extreme sintering of the copper and were not viable to calculate particle diameters.

To further confirm that under reaction conditions, there will be a complete reduction of copper, X-ray diffraction (XRD) analysis was performed after a liquid phase reaction. It was also done to understand the crystalline nature of the catalyst and the size of the copper particles in copper chromite. The resulting peaks in Figure 36 were identified according to XRD data obtained from literature.[74,78,79] The metallic copper peaks significantly increase in height after reduction and reaction, suggesting that there is a low dispersion and that the catalytic particles are not stable under reaction conditions. Therefore, the metallic copper particle size is higher due to sintering. $Cu^{2+}$ from CuO peak disappeared after reaction, suggesting that CuO was no longer present in the active phase of the

reaction and does not play a role. Because there is a large amount of metallic copper (due to sintering, etc.) at high particle diameters, this is likely the active site. More calculations are necessary to determine the exact plane where the reaction is taking place. However, planes (111) and (400) can be identified in Figure 36 according to literature[74,78,79].

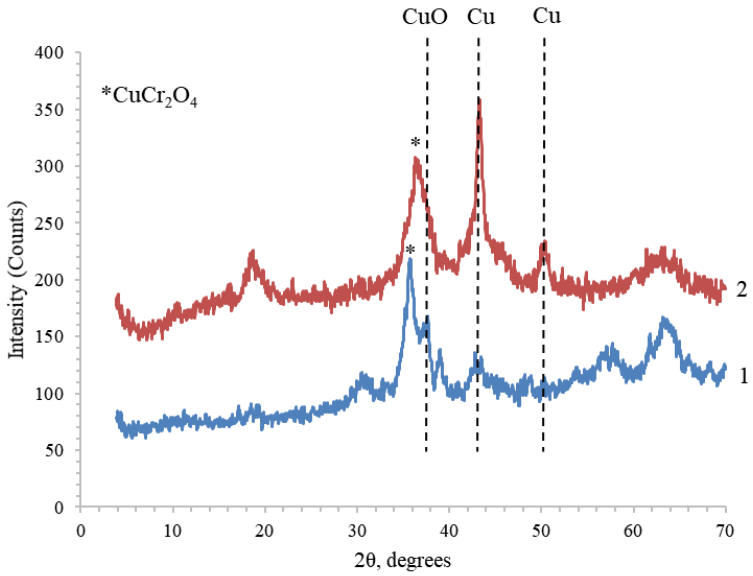



**Figure 36: The X-ray diffraction data for the copper chromite samples: 1 - fresh copper chromite, 2 - spent catalyst after reaction**

Applying the Scherrer equation (1)[75]:

$$D = \frac{K\lambda}{B\cos\theta} \quad (1)$$

Where, $K$ (dimensionless shape factor) = 0.89, $\lambda$ (X-ray wavelength) = 0.1542 nm, $B$ (line broadening at half the maximum intensity) = 0.680°, 2θ (Bragg angle) = 43.356°, the metallic copper particle diameter was calculated to be 12.44 nm. This value is comparable to the value accepted in literature (13.3 nm).[76]

Many commercial copper chromite catalysts were known to have promoters such as barium.[77,79] Thus, an energy-dispersive X-ray spectroscopy (EDX) was performed to scan

for various elements, impurities, or promoters in the sample for further confirmation. The results are shown below.

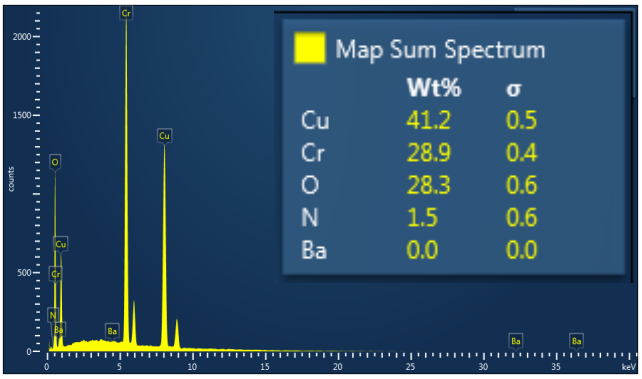



**Figure 37: Energy-dispersive X-ray spectroscopy (EDX) of copper chromite**

The copper chromite consists of 41 wt.% Cu, 29 wt.% Cr, and 28 wt.% O. Thus, the EDX further proved that the activity of the catalyst is only related to the copper and chromium mixed oxides present in the sample.

BET Surface Area of copper chromite was found to be 36.5 $m^2/g$. However, this may not be an accurate way to calculate the surface area of copper as it is not under reaction conditions. So, thermogravimetric analysis (TGA) was performed. However, the TGA results for copper chromite were not viable in calculating particle diameters. Our current experimental conditions must be altered because the weight loss of the sample showed a very high dispersion of copper particles with extremely low particle diameters. It is likely that the nitrous oxide may have penetrated deeper than simply the surface layer of the sample. Perhaps if the nitrous oxide was diluted and the passivation time was decreased, it would lead to more realistic results.

*4.3.2 Catalyst activity results*

The following graph shows results on various loadings of copper supported on silica. It can be concluded from this graph that particle size of metallic copper has an impact on the pentanol production rate. It requires more than 3% of metallic copper to begin seeing pentanol. Although it is likely that the GC-FID has reached detection limits for pentanol at such low concentrations, the pentanoic acid carbon balance is 100% without any conversion or formation of products for 3% $Cu/SiO_2$. Sintering of copper chromite from TEM results under reaction conditions also suggests that big particle sizes of copper are needed for the reaction to occur.

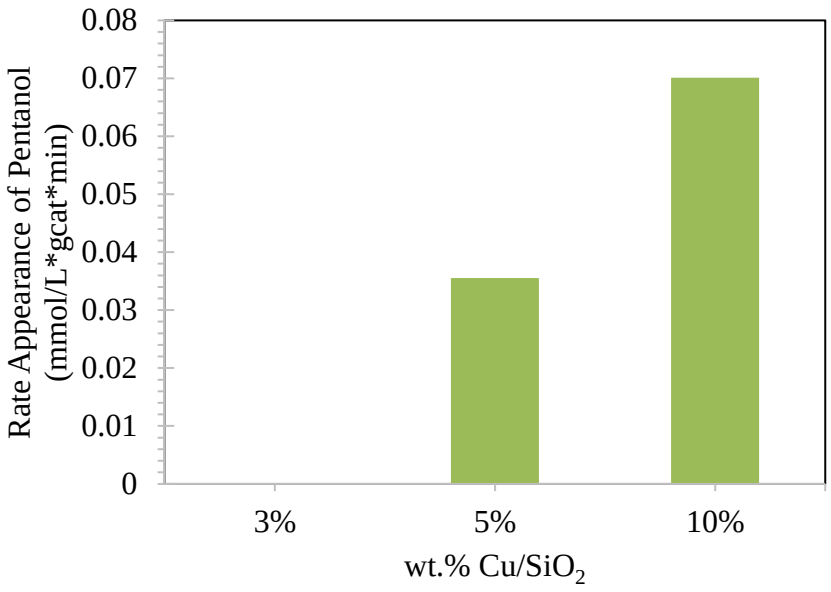



**Figure 38: Particle size effect of copper on pentanol production rate. Reduction: 300 mg x wt.% $Cu/SiO_2$ at 280 °C under 300 psi $H_2$ for 2 hrs. Reaction: 250 °C for 1 hr under 450 psi $H_2$. Feed: 0.101 M PEA. Carbon balances with respect to PEA: >90%.**

These results are compared with the activity of copper chromite in Figure 39. There is approximately 41.2 mg of copper in 100 mg of copper chromite according to the EDX in

Figure 37. There is roughly 30 mg of copper in 300 mg of 10% $Cu/SiO_2$ that was used in these reactions. The weight loading of metallic copper in both samples are close so the reactivity of both should be similar; however, there is a very radical change in pentanol production rates for both types of catalysts. Thus, Figure 39 suggests that support effects are present in reactions occurring on copper chromite.

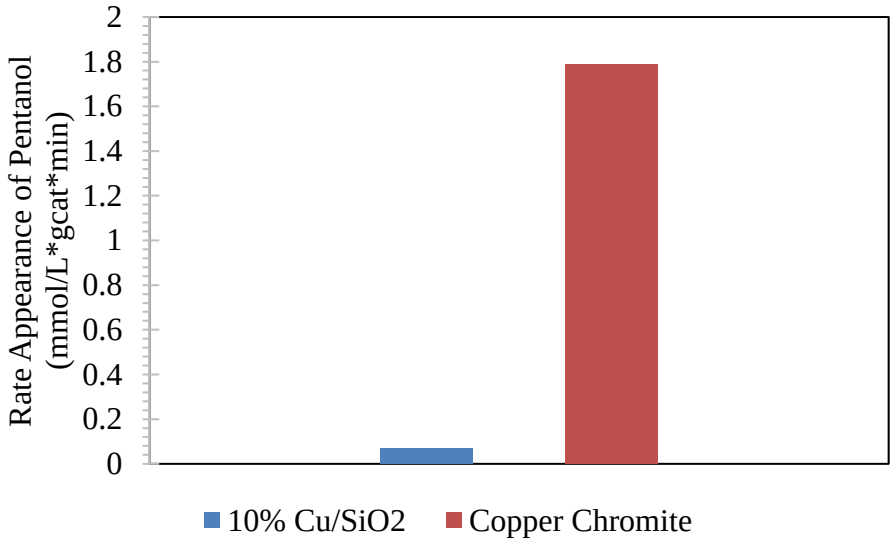



**Figure 39: Comparing activity of 10% Cu/SiO2 vs. copper chromite. Reduction: 300 mg 10% $Cu/SiO_2$ or 100 mg copper chromite at 280 °C under 300 psi $H_2$ for 2 hrs. Reaction: 250 °C for 1 hr under 450 psi $H_2$. Feed: 0.101 M PEA. Carbon balances with respect to PEA: >90%.**

Silica is a neutral support that does not have strong interactions with the metal.[105] Because of this, typically all the copper oxide is reduced to metallic copper in 10% $Cu/SiO_2$ under reduction conditions as calculated from the TPR in Figure 35. Some of the chromium oxide is also reduced in copper chromite as shown in the TPR. The reduction of chromia is known to generate Lewis acidic sites with high positive charge densities.[106] Therefore, the mixed oxide of copper and chromium oxides influence the reaction rate of converting pentanoic acid to pentanol. The metallic copper atoms that are released on the spinel

surface form a flat layer that is epitaxially bound to the surface of the oxide (particle sizes of ~100 angstroms).[101,104] In other words, the resulting copper metal particles sinter and come to the surface of the oxide.[96] In addition to this, it is likely that a small number of generated chromium Lewis acidic sites may also migrate to the surface and decorate the sintered metallic copper. Not only will this stabilize the copper particles, but it will also help form an ester when alcohols are cofed with pentanoic acids (Chapters 1 & 2). While it is still true that the ester cleavage will be occurring on metallic copper active sites, it is difficult to understand the location of the active site for PEA directly converting to alcohol.

### 4.4 Conclusion & Future Direction

A significantly different pentanol production rates were observed on 10% $Cu/SiO_2$ that is prepared via the incipient-wetness impregnation method versus copper chromite. These catalytic activity and characterization results suggest that there is an interaction of the support and/or mixed oxide with metallic copper in copper chromite. When copper chromite is initially reduced at 280 °C under 350 psi of $H_2$ for 2 hours, the metallic copper migrates to the surface of the oxide support.[93-95,102-104] The metallic copper atoms that are released on the spinel surface form a flat layer that is epitaxially bound to the surface of the oxide (particle sizes of ~100 angstroms).[101,104] In addition to this, we propose that some of the chromium atoms also reduces and migrates to the surface, decorating the largely sintered metallic of copper.

The results indicated in this study are only preliminary. More experiments are necessary to further confirm this claim. Perhaps TEM can be performed on copper chromite catalysts under various reduction conditions to observe the amount of sintering that

occurs. More careful characterization techniques must be employed to see if the sintered copper particles are decorated with chromium. Considering Chapters 1 and 2, the Lewis acidity contributes to the ester formation when alcohols are cofed with pentanoic acids. Also, it is still true that the ester cleavage occurs on metallic copper active sites. However, it is difficult to understand the location of the active site for PEA directly converting to alcohol. Thus, more experiments and characterization techniques are needed to locate the active site and the mechanism for the reduction of carboxylic acids (PEA) to alcohols (pentanol).

## Chapter 5: Concluding Remarks

Cofeeding small amounts of alcohols with pentanoic acid (PEA) accelerated the rate of pentanol produced in the liquid phase batch reactor. This is because the esters formed from these cofeeds have a much lower activation energy compared to carboxylic acids (PEA) alone.[51,52,72,90-92] While smaller molar ratios of alcohols to PEA accelerated the rate, high molar ratios had the opposite effect due to inhibition and species competing for sites. The results can be explained by using Langmuir-Hinshelwood kinetics and the competition for sites at zeroth order saturation conditions. Excessive amounts of water, alcohol, and heavy esters have an inhibitory effect. The reaction rate constants in Equations (8), (9), and (10) are expected to have the following trends: $k_1 < k_2 \leq k_{ester}$, where $k_1$ is for PEA → pentanol, $k_{ester}$ is for the formation of ester, and $k_2$ is for ester → pentanol. The equilibrium adsorption constants are expected to have the following trends: $K_{dodecanol} > K_{mcresol} > K_{ethanol}$. The rate constants for ester formations are expected to have the following trends: $k_{ethylvalerate} > k_{methylphenylvalerate} > k_{pentyldodecanoate}$. From equilibrium tests, it was proved that the enhancements observed in pentanol production rates are kinetic in nature and are not measured at equilibrium. Overall, it was possible to accelerate pentanol production rates with small addition of alcohol to the pentanoic acid feed on a copper chromite catalyst.

Cofeeding small amount of butanol with propionic acid (PrA) accelerated the rate of propanol produced in the gas phase flow reactor. This is because the ester formed from this cofeeds have a much lower activation energy compared to carboxylic acids (PEA) alone.[51,52,72,90-92]

In order to understand the effect of the mixed oxide copper chromite on the pentanol production rates, several characterization techniques were utilized. The catalytic activities were compared with 10% $Cu/SiO_2$. A significantly different pentanol production rates were observed on 10% $Cu/SiO_2$ that is prepared via the incipient-wetness impregnation method versus copper chromite. These catalytic activity and characterization results suggest that there is an interaction of the support and/or mixed oxide with metallic copper in copper chromite. When copper chromite is initially reduced at 280 °C under 350 psi of $H_2$ for 2 hours, the metallic copper migrates to the surface of the oxide support.[93-95,102-104] The metallic copper atoms that are released on the spinel surface form a flat layer that is epitaxially bound to the surface of the oxide (particle sizes of ~100 angstroms).[101,104] In addition to this, we propose that some of the chromium atoms also reduces and migrates to the surface, decorating the largely sintered metallic of copper. This decoration is responsible in producing the esters effectively when alcohols are cofed with pentanoic acids. The ester cleavage is still expected to occur on the active sites of metallic copper.

# Chapter 6: Future Direction

In the liquid phase, more experiments are required to understand what is happening between the data points collected in Figure 25. Furthermore, the role of the $Cr_2O_3$ in the mixed oxide copper chromite catalyst should be investigated in detail to understand the mechanism of this reaction. More studies need to be performed to verify that the metallic copper is the active site and that it is formed through an aldehyde intermediate. For strong support to explain the trends seen in Figure 25, DFT studies may be necessary to find the reaction rate constants and equilibrium adsorption constants to generate a working kinetic model.

In the gas phase, we still need to understand the effect of changing partial pressures of propionic acid on propanol production with alcohol cofeeds. The data presented above has been under zeroth order conditions where the catalyst surface is always saturated with the acid. To truly understand the effect of changing concentrations of acid, the reactant needs to be in a first order regime. After finding the first order regime with respect to the propionic acid, butanol can be added to enhance the rate while changing the concentration of the acid feed. This procedure will be followed for multiple alcohol cofeeds. DFT and experimental studies will need to be performed to generate a working kinetic model for these results also.

More careful characterization techniques must be employed to verify that the sintered copper particles are decorated with chromium. Finding the reason for copper chromite's catalytic behavior will allow us to understand the properties of the catalyst. This will help us fine tune other catalysts and manipulate certain characteristics to accomplish our goals.

Enhancing the pentanol, a product of the reduction of carboxylic acids and esters, production rates is just the beginning of this project. Future outlooks include modifying the liquid phase batch reactor to accommodate biphasic reactions. A biphasic reactor can be utilized to selectively remove pentanol from the oil phase as it is produced to increase the yield of pentanol even more. In the future, this pentanol will be dehydrated to form pentadiene to satisfy the goal of this project.

## References


1. J.Q. Bond, D. Martin Alonso, and J.A. Dumesic, Catalytic strategies for the conversion of lignocellulosic carbohydrates to fuels and chemicals, in Aqueous Pretreatment of Plant Biomass for Biological and Chemical Conversion to Fuels and Chemicals C.E. Wyman (Ed). Wiley Blackwell, Oxford, UK, 2013.

2. "Beyond the Ethylene Steam Cracker." American Chemical Society, www.acs.org/content/acs/en/pressroom/cutting-edge-chemistry/beyond-the-ethylene-steam-cracker.html.

3. Wade, L.G. (2006). *Organic Chemistry* (6th ed.). Pearson Prentice Hall. p. 309. ISBN 13 9780131478718.

4. Morrow, Norman L. "The industrial production and use of 1, 3-butadiene." Environmental health perspectives 86 (1990): 7.

5. Newton, Paul. "There Is a Business Opportunity to Satisfy the Increasing Demand for Butadiene." The High Price of Butadiene, www.duncanseddon.com/the-high-price-of-butadiene/.

6. Johann, Thorsten, et al. "Method for the production of butadiene and 1-butene." U.S. Patent No. 7,488,857. 10 Feb. 2009.

7. Marshall, Amanda-Lynn, and Peter J. Alaimo. "Useful products from complex starting materials: common chemicals from biomass feedstocks." Chemistry-A European Journal 16.17 (2010): 4970-4980.

8. Ezinkwo, G., Tretyakov, V., Aliyu, A., & Ilolov, A. (2014). Fundamental Issues of Catalytic Conversion of Bio-Ethanol into Butadiene. ChemBioEng Reviews, 1(5), 194-203.

9. Haas, T., et al. "New diol processes: 1, 3-propanediol and 1, 4-butanediol." Applied Catalysis A: General 280.1 (2005): 83-88.

10. Zhang, Chang, Wang, & Xu. (2007). Review of biomass pyrolysis oil properties and upgrading research. Energy Conversion and Management, 48(1), 87-92.

11. Yang, Yan, Chen, Lee, & Zheng. (2007). Characteristics of hemicellulose, cellulose and lignin pyrolysis. Fuel, 86(12), 1781-1788.

12. Bridgwater, Meier, & Radlein. (1999). An overview of fast pyrolysis of biomass. Organic Geochemistry, 30(12), 1479-1493.

13. Bridgwater, Anthony Victor. "Pyrolysis of biomass." Transformations to Effective Use: Biomass Power for the World" eds. W. van Swaaij, S. Kersten and W. Palz 6 (2015): 473-514.

14. Bridgwater, Anthony V. "Review of fast pyrolysis of biomass and product upgrading." Biomass and bioenergy 38 (2012): 68-94.

15. Prins, W. (2010). Fast pyrolysis technology development. Biofuels, Bioproducts and Biorefining, 4(2), 178-208.

16. Alonso, D., Wettstein, S., & Dumesic, J. (2013). Gamma-valerolactone, a sustainable platform molecule derived from lignocellulosic biomass. Green Chemistry, 15(3), 584-595.

17. Wettstein, Alonso, Gürbüz, & Dumesic. (2012). A roadmap for conversion of lignocellulosic biomass to chemicals and fuels. Current Opinion in Chemical Engineering, 1(3), 218-224.

18. Resasco, Daniel E., and Steven P. Crossley. "Implementation of concepts derived from model compound studies in the separation and conversion of bio-oil to fuel." Catalysis Today 257 (2015): 185-199.

19. Bals, Bryan, et al. "Evaluation of ammonia fibre expansion (AFEX) pretreatment for enzymatic hydrolysis of switchgrass harvested in different seasons and locations." Biotechnology for biofuels 3.1 (2010): 1.

20. Tao, Ling, et al. "Process and technoeconomic analysis of leading pretreatment technologies for lignocellulosic ethanol production using switchgrass." Bioresource technology 102.24 (2011): 11105-11114.

21. Zhao, Xuebing, Keke Cheng, and Dehua Liu. "Organosolv pretreatment of lignocellulosic biomass for enzymatic hydrolysis." Applied microbiology and biotechnology 82.5 (2009): 815.

22. Xing, Rong, Wei Qi, and George W. Huber. "Production of furfural and carboxylic acids from waste aqueous hemicellulose solutions from the pulp and paper and cellulosic ethanol industries." Energy & Environmental Science 4.6 (2011): 2193-2205.

23. Agbor, Valery B., et al. "Biomass pretreatment: fundamentals toward application." Biotechnology advances 29.6 (2011): 675-685.

24. Brandt, Agnieszka, et al. "Ionic liquid pretreatment of lignocellulosic biomass with ionic liquid–water mixtures." Green Chemistry 13.9 (2011): 2489-2499.

25. Tucker, Melvin P., et al. "Effects of temperature and moisture on dilute-acid steam explosion pretreatment of corn stover and cellulase enzyme digestibility." Biotechnology for Fuels and Chemicals. Humana Press, Totowa, NJ, 2003. 165-177.

26. Lee, Jae-Won, and Thomas W. Jeffries. "Efficiencies of acid catalysts in the hydrolysis of lignocellulosic biomass over a range of combined severity factors." Bioresource technology 102.10 (2011): 5884-5890.

27. Robinson, J. Michael, et al. "The use of catalytic hydrogenation to intercept carbohydrates in a dilute acid hydrolysis of biomass to effect a clean separation from lignin." Biomass and Bioenergy 26.5 (2004): 473-483.

28. Alonso, David Martin, Jesse Q. Bond, and James A. Dumesic. "Catalytic conversion of biomass to biofuels." Green Chemistry 12.9 (2010): 1493-1513.

29. Wright, William RH, and Regina Palkovits. "Development of heterogeneous catalysts for the conversion of levulinic acid to γ-valerolactone." ChemSusChem 5.9 (2012): 1657-1667.

30. Palkovits, Regina. "Pentenoic acid pathways for cellulosic biofuels." Angewandte Chemie International Edition 49.26 (2010): 4336-4338.

31. Bond, Jesse Q., et al. "Integrated catalytic conversion of γ-valerolactone to liquid alkenes for transportation fuels." Science 327.5969 (2010): 1110-1114.

32. R.T. Morrison and R. N. Boyd, *Organic Chemistry*, Allyn and Bacon, Boston, 1983, vol. 20, pp. 813-885.

33. Serrano-Ruiz, Juan Carlos, Ryan M. West, and James A. Dumesic. "Catalytic conversion of renewable biomass resources to fuels and chemicals." Annual review of chemical and biomolecular engineering 1 (2010): 79-100.

34. Turova, Olga V., et al. "Kinetic study of asymmetric hydrogenation of methyl levulinate using the (COD) Ru (2-methylallyl) 2–BINAP–HCl catalytic system." Journal of Molecular Catalysis A: Chemical 311.1-2 (2009): 61-65.

35. Gürbüz, Elif I., et al. "Reactive Extraction of Levulinate Esters and Conversion to γ-Valerolactone for Production of Liquid Fuels." ChemSusChem 4.3 (2011): 357-361.

36. Zhou, Yibo, L. Keith Woo, and Robert J. Angelici. "Solid acid catalysis of tandem isomerization-lactonization of olefinic acids." Applied Catalysis A: General 333.2 (2007): 238-244.

37. Akula, Shivaraju, et al. "Tandem isomerization–lactonization of olefinic fatty acids using the Lewis acidic ionic liquid, choline chloride· 2ZnCl2." Tetrahedron Letters 53.27 (2012): 3471-3473.

38. Manzer, Leo E. "Catalytic synthesis of α-methylene-γ-valerolactone: a biomass-derived acrylic monomer." Applied Catalysis A: General 272.1-2 (2004): 249-256.

39. Mehdi, Hasan, et al. "Integration of homogeneous and heterogeneous catalytic processes for a multi-step conversion of biomass: from sucrose to levulinic acid, γ-valerolactone, 1, 4-pentanediol, 2-methyl-tetrahydrofuran, and alkanes." Topics in Catalysis 48.1-4 (2008): 49-54.

40. Galletti, Anna Maria Raspolli, et al. "A sustainable process for the production of γ-valerolactone by hydrogenation of biomass-derived levulinic acid." Green Chemistry 14.3 (2012): 688-694.

41. Tukacs, József M., et al. "Efficient catalytic hydrogenation of levulinic acid: a key step in biomass conversion." Green Chemistry 14.7 (2012): 2057-2065.

42. Hengne, Amol M., and Chandrashekhar V. Rode. "Cu–ZrO 2 nanocomposite catalyst for selective hydrogenation of levulinic acid and its ester to γ-valerolactone." Green Chemistry 14.4 (2012): 1064-1072.

43. Bond, Jesse Q., Christian S. Jungong, and Anargyros Chatzidimitriou. "Microkinetic analysis of ring opening and decarboxylation of γ-valerolactone over silica alumina." Journal of Catalysis 344 (2016): 640-656.

44. Bond, Jesse Q., et al. "γ-Valerolactone ring-opening and decarboxylation over SiO2/Al2O3 in the presence of water." Langmuir 26.21 (2010): 16291-16298.

45. Bond, Jesse Q., et al. "Interconversion between γ-valerolactone and pentenoic acid combined with decarboxylation to form butene over silica/alumina." Journal of catalysis 281.2 (2011): 290-299.

46. Shell. Piperylene Product Stewardship Summary, https://www.shell.com/business-customers/chemicals/safe-product-handling-and-transportation/product-stewardship-summaries/piperylene-product-stewardship-summary-october-2012.pdf &cd=1&hl=en&ct=clnk&gl=us.

47. Tilman, David, et al. "Response—Biofuels." Science 326.5958 (2009): 1346-1346.

48. Tilman, David, et al. "Beneficial biofuels—the food, energy, and environment trilemma." Science 325.5938 (2009): 270-271.

49. Cheng, Shuiming, and Shengdong Zhu. "LIGNOCELLULOSIC FEEDSTOCK BIOREFINERY-THE FUTURE OF THE CHEMICAL AND ENERGY INDUSTRY." BioResources 4.2 (2009).

50. Carvalheiro, Florbela, Luís C. Duarte, and Francisco M. Gírio. "Hemicellulose biorefineries: a review on biomass pretreatments." Journal of Scientific & Industrial Research (2008): 849-864.

51. Santiago, MA Natal, M. A. Sanchez-Castillo, R. D. Cortright, and J. A. Dumesic. "Catalytic reduction of acetic acid, methyl acetate, and ethyl acetate over silica-supported copper." Journal of Catalysis 193.1 (2000): 16-28.

52. J. Clayden, N. Greeves, S. Warren and P. Wothers, Organic Chemistry, Oxford University Press, 2000.

53. Turek, T., D. L. Trimm, and N. W. Cant. "The catalytic hydrogenolysis of esters to alcohols." Catalysis Reviews—Science and Engineering 36.4 (1994): 645-683.

54. Adkins, Homer, and Karl Folkers. "The catalytic hydrogenation of esters to alcohols." Journal of the American Chemical Society 53.3 (1931): 1095-1097.

55. Adkins, H., *in* "Organic Reactions" (R. Adams, Ed.), Vol. 8. John Wiley & Sons, New York, 1954.

56. Folkers, Karl, and Homer Adkins. "The catalytic hydrogenation of esters to alcohols. II." Journal of the American Chemical Society 54.3 (1932): 1145-1154.

57. Lazier, Wilbur A. "Process for producing alcohols from esters of nonaromatic carboxylic acids." U.S. Patent No. 2,079,414. 4 May 1937.

58. Otto, Schmidt. "Catalytic hydrogenation of esters of aliphatic carboxylic acids." U.S. Patent No. 2,093,159. 14 Sep. 1937.

59. Case, Leslie C., and Yan Tsoung-Yuan. "Catalytic reduction of fluorinated esters." U.S. Patent No. 3,314,987. 18 Apr. 1967.

60. Evans, J. W., et al. "Hydrogenolysis of alkyl formates over a copper chromite catalyst." Applied Catalysis 7.1 (1983): 31-41.

61. Evans, J. W., et al. "Hydrogenolysis of ethyl formate over copper-based catalysts." Applied Catalysis 6.3 (1983): 355-362.

62. Stroupe, James D. "An X-ray diffraction study of the copper chromites and of the "copper-chromium oxide" catalyst." Journal of the American Chemical Society 71.2 (1949): 569-572.

63. Brands, Danny S., et al. "The relation between reduction temperature and activity in copper catalysed ester hydrogenolysis and methanol synthesis." Catalysis letters 36.3-4 (1996): 175-181.

64. van de Scheur, Frank Th, et al. "Structure-activity relation and ethane formation in the hydrogenolysis of methyl acetate on silicasupported copper catalysts." Applied Catalysis A: General 111.1 (1994): 63-77.

65. van de Scheur, Frank Th, et al. "Activity-enhanced copper-zinc based catalysts for the hydrogenolysis of esters." Applied Catalysis A: General 116.1-2 (1994): 237-257.

66. van de Scheur, Frank Th, and Leendert H. Staal. "Effects of zinc addition to silica supported copper catalysts for the hydrogenolysis of esters." Applied Catalysis A: General 108.1 (1994): 63-83.

67. Van Der Grift, C. J. G., et al. "Effect of the reduction treatment on the structure and reactivity of silica-supported copper particles." Journal of Catalysis 131.1 (1991): 178-189.

68. Kohler, M. A., et al. "The mechanism of the catalytic chemistry of ester hydrogenolysis on copper surfaces." 9th Int. Cong. Catal., Calgary 1043 (1988).

69. Agarwal, A. K., et al. "Catalytic hydrogenolysis of esters: a comparative study of the reactions of simple formates and acetates over copper on silica." Journal of molecular catalysis 43.1 (1987): 79-92.

70. Agarwal, A. K., et al. "Acetaldehyde hydrogenation over a Cu/SiO2 catalyst." Journal of molecular catalysis 45.2 (1988): 247-254.

71. Evans, J. W., et al. "Structural and reactivity effects in the copper-catalyzed hydrogenolysis of aliphatic esters." Journal of Catalysis 88.1 (1984): 203-213.

72. James Pritchard, Georgy A. Filonenko, Robbert van Putten, Emiel J. M. Hensen, and Evgeny A. Pidko. “Heterogeneous and homogeneous catalysis for the hydrogenation of carboxylic acid derivatives: history, advances and future directions.” Chemical Society Reviews. Royal Society of Chemistry, 05 May 2015.

73. Fierro, G., et al. "A study of anomalous temperature-programmed reduction profiles of Cu2O, CuO, and CuO-ZnO catalysts." Journal of catalysis 148.2 (1994): 709-721.

74. Khassin, Alexander A., et al. "The state of absorbed hydrogen in the structure of reduced copper chromite from the vibration spectra." Physical Chemistry Chemical Physics 11.29 (2009): 6090-6097.

75. Patterson, A. L. "The Scherrer formula for X-ray particle size determination." Physical review 56.10 (1939): 978.

76. Edrissi, M. (2011). Synthesis and characterisation of copper chromite nanoparticles using coprecipitation method. Micro & Nano Letters., 6(10), 836.

77. Turner, Keith, et al. "Process for producing a hydrogenation catalyst of copper chromite." U.S. Patent No. 5,030,609. 9 Jul. 1991.

78. Pimentel, Patrícia Mendonça, et al. "Pechini synthesis and microstructure of nickel-doped copper chromites." Materials Research 8.2 (2005): 221-224.

79. Santacesaria, E., et al. "Ethanol dehydrogenation to ethyl acetate by using copper and copper chromite catalysts." Chemical Engineering Journal 179 (2012): 209-220.

80. Yang, Feifei, et al. "Geometric and electronic effects of bimetallic Ni–Re catalysts for selective deoxygenation of m-cresol to toluene." Journal of Catalysis 349 (2017): 84-97.

81. Srivastava, Sanjay, G. C. Jadeja, and Jigisha Parikh. "A versatile bi-metallic copper–cobalt catalyst for liquid phase hydrogenation of furfural to 2-methylfuran." RSC Advances 6.2 (2016): 1649-1658.

82. Fogler, H. Scott. Elements of Chemical Reaction Engineering. Prentice Hall, Pearson Education, 2013.

83. Elliott, J. Richard., and Carl T. Lira. Introductory Chemical Engineering Thermodynamics. Prentice Hall, 2012.

84. Yan, T. Y., L. F. Albright, and L. C. Case. "Hydrogenolysis of esters, particularly perfluorinated esters." Industrial & Engineering Chemistry Product Research and Development 4.2 (1965): 101-107.

85. Claus, Peter, et al. "Selective hydrogenolysis of methyl and ethyl acetate in the gas phase on copper and supported group VIII metal catalysts." Applied Catalysis A: General 79.1 (1991): 1-18.

86. Kenvin, Jeffrey C., and Mark G. White. "Supported catalysts prepared from mononuclear copper complexes: catalytic properties." Journal of Catalysis 135.1 (1992): 81-91.

87. Normann, W. "Über die katalytische Reduktion der Carboxylgruppe." Angewandte Chemie 44.35 (1931): 714-717.

88. K. M. K. Mutzall and P.J. van den Berg, Hydrogenation of fatty acid esters to fatty alcohols, *Proc. 4$^{th}$ Eur. Symp. Chem. React. Eng.*, Pergamon Press, 1968, pp. 277-285.

89. Zhang, Shuangshuang, et al. "High-effective approach from amino acid esters to chiral amino alcohols over Cu/ZnO/Al 2 O 3 catalyst and its catalytic reaction mechanism." Scientific reports 6 (2016): 33196.

90. Lee, Jong-Min, et al. "Direct Hydrogenation of Biomass-Derived Butyric Acid to n-Butanol over a Ruthenium–Tin Bimetallic Catalyst." ChemSusChem 7.11 (2014): 2998-3001.

91. Tamura, Masazumi, et al. "Insight into the Mechanism of Hydrogenation of Amino Acids to Amino Alcohols Catalyzed by a Heterogeneous MoOx-Modified Rh Catalyst." Chemistry-A European Journal 21.7 (2015): 3097-3107.

92. Dub, Pavel A., and Takao Ikariya. "Catalytic reductive transformations of carboxylic and carbonic acid derivatives using molecular hydrogen." ACS Catalysis 2.8 (2012): 1718-1741.

93. Prince, E. "Crystal and magnetic structure of copper chromite." Acta Crystallographica 10.9 (1957): 554-556.

94. Dunitz, J. D., and L. E. Orgel. "Electronic properties of transition-metal oxides—I: Distortions from cubic symmetry." Journal of Physics and Chemistry of Solids 3.1-2 (1957): 20-29.

95. Kawamoto, Aparecida M., Luiz Claudio Pardini, and Luis Claudio Rezende. "Synthesis of copper chromite catalyst." Aerospace Science and technology 8.7 (2004): 591-598.

96. Minyukova, T. P., et al. "Dehydrogenation of methanol over copper-containing catalysts." Applied Catalysis A: General 237.1-2 (2002): 171-180.

97. Mane, R. B., et al. "Role of promoters in copper chromite catalysts for hydrogenolysis of glycerol." Catalysis today 164.1 (2011): 447-450.

98. Yurieva, T. M., et al. "State of copper-containing catalyst for methanol synthesis in the reaction medium." Reaction Kinetics and Catalysis Letters 51.2 (1993): 495-500.

99. Yurieva, T. M., et al. "Mechanisms for hydrogenation of acetone to isopropanol and of carbon oxides to methanol over copper-containing oxide catalysts." Journal of Molecular Catalysis A: Chemical 113.3 (1996): 455-468.

100. L.M. Plyasova, L.P. Soloviyova, T.A. Krieger, O.V. Makarova, T.M. Yurieva: *Kinet. Katal.*, 37, 622 (1996).

101. Simentsova, I. I., et al. "Kinetics of the medium-temperature reduction of copper chromite with hydrogen." Reaction Kinetics and Catalysis Letters 82.2 (2004): 355-361.

102. Simentsova, I. I., et al. "Adsorption of hydrogen on reduced copper chromite." Reaction Kinetics and Catalysis Letters 79.1 (2003): 85-92.

103. Plyasova, L. M., et al. "Interaction of Hydrogen with Copper-Containing Oxide Catalysts: V. Structural Transformations in Copper Chromite during Reduction–Reoxidation." Kinetics and catalysis 42.1 (2001): 126-131.

104. Plyasova, L. M., et al. "Redox Treatment Effects on the Magnetic Properties of Copper Chromite." Journal of Structural Chemistry 43.2 (2002): 252-256.

105. Copéret, Christophe, and Bruno Chaudret, eds. Surface and Interfacial Organometallic Chemistry and Catalysis. Vol. 16. Springer Science & Business Media, 2005.

106. Coulson, D. R., et al. "Chromium oxide-catalyzed disproportionation of chlorodifluoromethane: a mechanism study." Journal of Catalysis 140.1 (1993): 103-120.

# Appendix A1: Preliminary Studies

## A1.1 Literature Review

Esterification reactions are well studied in literature using Lewis and Bronsted acid catalysts. Lewis acid catalysts, milder than Bronsted acid catalysts, are electron-deficient and can activate electron-rich substrates. Duong *et al.*[1] studied acylation and esterification products of m-cresol and acetic acid reactions. The reactions were performed in the liquid phase using Bronsted acid catalysts: zeolites. It was found that the esterification between m-cresol and acetic acid was self-catalyzed but occurs at a much slower rate. As the amount of zeolite H-beta increased, larger amounts of acylation products were observed, indicating that the esterification was further catalyzed by the zeolite. The aromatic ester was then used as an intermediate to acylate. Thus, the esterification product was formed first which then converted to the acylation product over time.[1]

The hydrogenation of esters is also well-studied in literature and has been receiving more attention in upgrading biofuels. As indicated by Clayden *et al.*[2], esters are slightly more reactive than carboxylic acids based on the -R group attached. Deshpande *et al.*[3] showed that methyl oleate can be reduced to oleyl alcohol in the presence of Ru-Sn-B/$Al_2O_3$ (Ru/Sn = 1:2) catalysts. They believe that boron enhanced the electron density of ruthenium while tin helped increase the dispersion of ruthenium on the support. Dos Santos *et al.*[6] examined Ru-Sn catalysts on various supports in the hydrogenation of dimethyl adipate to diols. The diols selectivity decreased in the following order of the supports: $TiO_2$ > $CeO_2$ > $SiO_2$ > $Nb_2O_5$ > $Al_2O_3$.[4]

Studies were also performed in directly converting aliphatic carboxylic acids to alcohols. Tahara *et al.*[5] found that the type of tin precursor affected the yield of rosin alcohol from

rosin on Ru-Sn/$Al_2O_3$ and that the alkali metals promoted the C=O hydrogenation. The group also found that calcining Ru-Sn/$Al_2O_3$ at 650 $^oC$ and reducing at 450 $^oC$ provided an active catalyst that could selectively hydrogenate C=O without hydrogenating C=C.[6] This is done by polarizing the carbonyl group by interacting with the Lewis acidic Sn sites. Mendes *et al.*[7] studied the hydrogenation of oleic acid on various ruthenium catalysts. The Ru/$TiO_2$ catalyst prepared by the impregnation method showed a high selectivity towards saturated alcohols than unsaturated alcohols. However, the bimetallic Ru-Sn catalyst on $TiO_2$ showed a high activity and selectivity towards unsaturated alcohols than alumina supported Ru-Sn catalyst.[7]

Adkins-type catalysts such as CuO and $CuCr_2O_4$ were discovered in the 1930s are used to hydrogenate esters.[8] These catalysts are still used in the industry to manufacture alcohols even though they exhibit low activity and require harsh operating conditions. This is because their catalytic structure is resistant to the free fatty acids. Thus, the composition of these catalysts has remained unchanged since they were discovered.[7]

Norman[11] has a patent for dehydrating alcohols and ethers on ternary mixed oxides. A V-Ti-P mixed oxide was effectively able to dehydrate 2-methyl-tetrahydrofuran (2-MTHF) to pentadiene with a 63% yield. N-pentanol was dehydrated at a 100% conversion and 81% selectivity to pentenes. 1,5-pentanediol was dehydrated at a 100% conversion and 38% selectivity to pentadiene.[11] Abdelrahman *et al.*[10] studied the ring-opening and dehydration of tetrahydrofuran (THF) to form 1,3-butadiene using a phosphorus zeolite catalyst called P-SPP (phosphorus self-pillared pentasil). Using this catalyst, they obtained a high selectivity to diolefins such as hexadiene and pentadiene.[10] A clear reaction mechanism and catalyst characterization studies have not been published but

would have been useful. Regardless, P-SPP seems to be a promising catalyst for this project in the dehydration of ester's corresponding alcohols.

### A1.2 Preliminary Results and Discussion

In the liquid phase batch reactor, zeolite H-beta catalyzed the esterification between pentanoic acid and m-cresol to produce 3-methylphenyl valerate (ester product) and 1-(2-hydroxy-4-methylphenyl)pentan-1-one (acyl product). Figure below shows the yield of products over different amounts of zeolite H-Beta with pentanoic acid conversions.

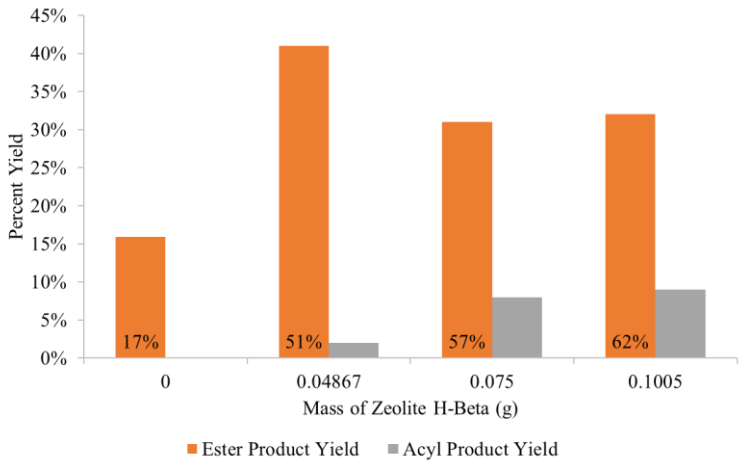



**Figure 40: Yield of products and conversion of pentanoic acid (indicated in the bars) over different amounts of zeolite H-Beta. Reaction conditions: 0.5 M pentanoic acid, 6 M m-cresol, 250 °C, 3 hours, under 500 psi $N_2$**

Figure 36 shows the selectivity of products over different amounts of zeolite H-Beta. The reaction conditions are: 0.5 M pentanoic acid, 6 M m-cresol, 250 °C, 3 hours, under 500 psi $N_2$. The ester product results directly from the addition of heat without any catalyst. However, the yield of ester and the conversion of acid is lower. In the presence of a catalyst, the conversion of acid and yield of ester is higher; however, an acyl product is made in the side reactions. As the amount of catalyst increases, the ester yield decreases while the acyl yield increases. This result supports the study published by Duong *et al.*[1],

that the esterification is a primary product which later converts into the acylation product. Although the ester can be formed, a 100% conversion of pentanoic acid to the ester will take a lot of time. Achieving a 100% conversion with a 100% selectivity to the ester would be difficult because it also catalyzes the acylation reaction. In addition, the ester is not commercially available. Thus, alternative alcohol that is highly abundant and forms an ester that is commercially available is used in the subsequent experiments.

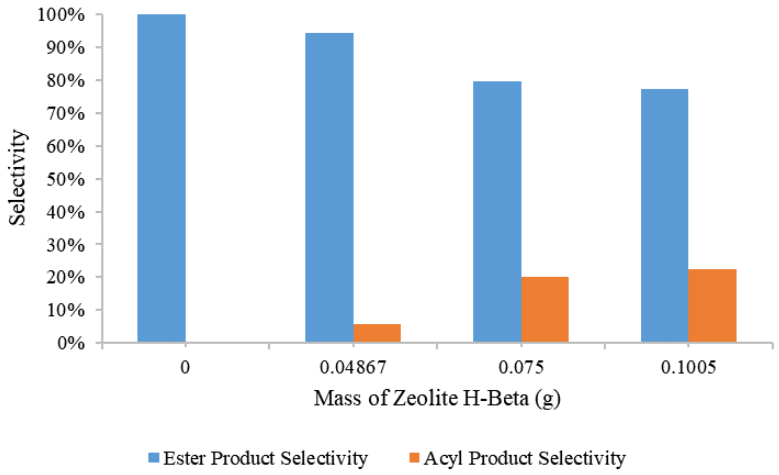



**Figure 41: Selectivity of products over different amounts of zeolite H-Beta. Reaction conditions: 0.5 M pentanoic acid, 6 M m-cresol, 250 $^{o}$C, 3 hours, under 500 psi $N_2$**

Ethanol is a highly abundant alcohol. Figure 37 shows the yield of ethyl-valerate and conversion of pentanoic acid from the esterification of pentanoic acid and ethanol on various Lewis acidic catalysts. The reactions were run using 50 mg of catalyst, 0.381 M ethanol, 0.569 M pentanoic acid (1:1.5 acid to alcohol molar ratio) in decalin. The reaction took place at 250 $^{o}$C for 1 hour. This suggest that the Lewis acidic catalysts accelerated the ethyl-valerate yield from 43% (no catalyst) to as high as 49.5%, but heat was sufficient in generating this ester.

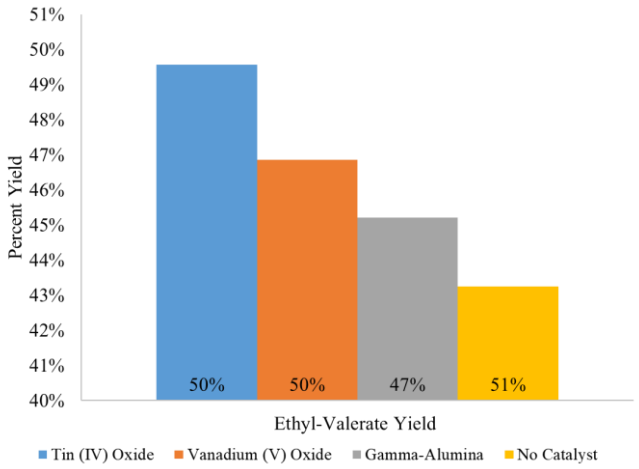



**Figure 42: Yield of ethyl-valerate and conversion of pentanoic acid (indicated in the bars) from the esterification of pentanoic acid and ethanol on various Lewis acidic catalysts. 50 mg of catalyst, 0.569 M pentanoic acid, 0.381 M ethanol (1:1.5 acid to alcohol molar ratio) in decalin. Reaction conditions: 250 °C for 1 hour**

Further experiments were done to reduce the ester to its corresponding alcohols. Figure 38 shows the selectivity to products on 5% Ru on carbon and titania supports.

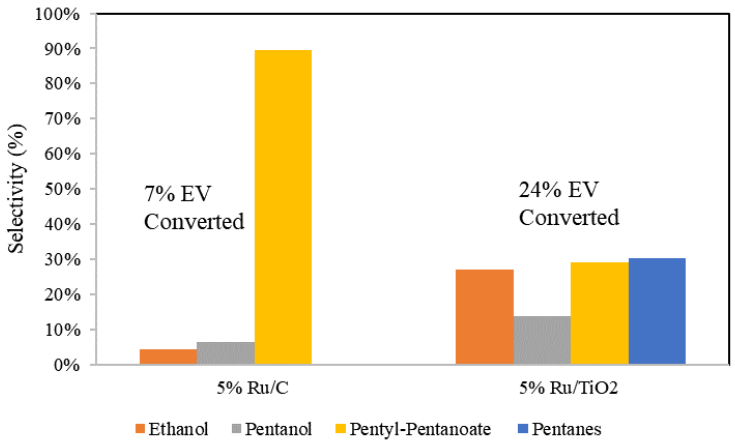



**Figure 43: Selectivity to products on 5% Ru on various supports. 100 mg of catalyst, reduced at 280 °C under 300 psi $H_2$ for 3 hours, and 0.4 M ethyl-valerate reacted at 250 °C for 4 hours.**

These reactions were performed using 100 mg of catalyst, reduced at 280 °C under 300 psi $H_2$ for 3 hours, and 0.381 M ethyl-valerate reacted at 250 °C for 4 hours. On 5% Ru/C,

the conversion of ethyl-valerate was only 7%; however, the selectivity towards pentyl-pentanoate, a transesterification product, was very high. On 5% $Ru/TiO_2$, the conversion of ethyl-valerate was 24% with higher selectivity to alcohols, but the side products also had high selectivity.

Experiments at different reaction times were also performed using 5% $Ru/TiO_2$ catalyst. The percent yields for ethanol and pentanol achieve constant values over time while the yields for pentyl-pentanoate and pentanes increase. This is due to pentanol dehydrating to form pentanes and reacting with ethyl-valerate to form pentyl-pentanoate. While the selectivity to ethanol and pentanol decreases over time, the selectivity to pentyl-pentanoate and pentanes increase. It is possible that the reduction of pentyl-pentanoate to pentanols is much slower than the reduction of ethyl-valerate.

In order to study solvent effects on 5% $Ru/TiO_2$, 1 mL of water was added to the feed. Results are shown below.

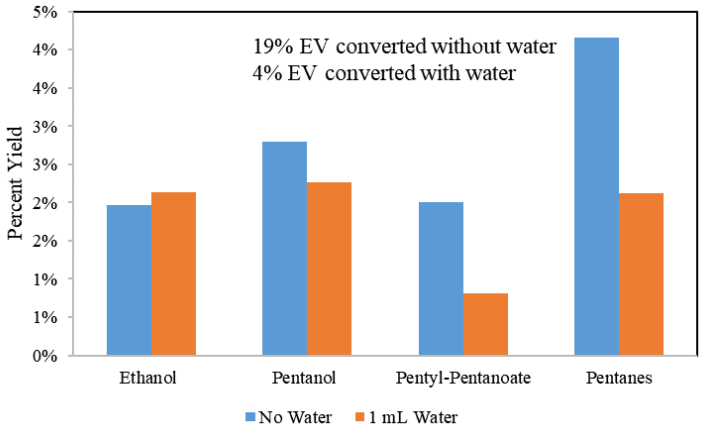



**Figure 44: Solvent effects on the reduction of ethyl-valerate on 100 mg 5% Ru/TiO2. Reduced at 280 °C under 300 psi $H_2$ for 2 hours, and 0.4 M ethyl-valerate reacted at 250 °C for 1 hour.**

Water lowered the conversion of ethyl-valerate from 19% to 4%, and significantly decreased the yield of pentyl-pentanoate and pentanes. In order to test if it is better to convert pentanoic acid directly to alcohols or to intercept the process by using an ester, two different reactions were performed on 5% $Ru/TiO_2$. When pentanoic acid was injected into the reactor, 17% of the reactant converted where a major product was pentyl-pentanoate. When ethyl-valerate was injected, 19% of the reactant converted where there was an even distribution between the alcohol yields. The pentanol product yields were comparatively the same in both reactions.

Another set of experiments were performed to compare the selectivity of products on 5% $Ru/TiO_2$ to a copper chromite catalyst (Adkins catalyst)[8]. Ethanol selectivity was not shown in this chart.

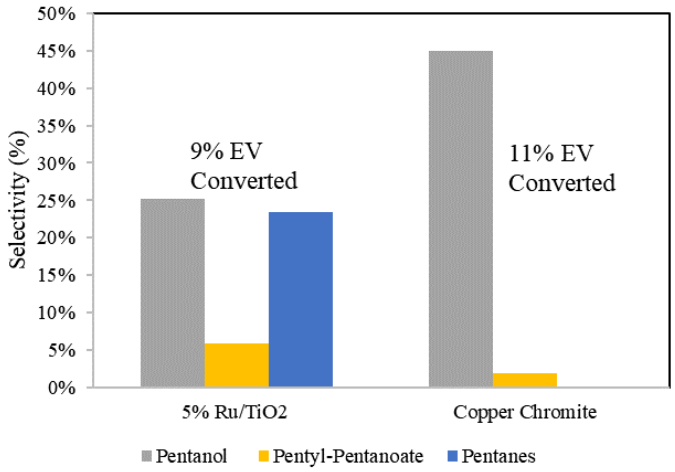



**Figure 45: Comparing selectivity of products on 5% $Ru/TiO_2$ to a copper chromite catalyst. 100 mg 5% $Ru/TiO_2$ reduced at 280 ºC under 300 psi $H_2$ for 2 hours, reacted at 250 ºC for 30 min. 100 mg $2CuO{\cdot}Cr_2O_3$ reduced at 280 ºC under 300 psi $H_2$ for 2 hours, reacted at 250 ºC for 30 min.**

Copper chromite showed a very high selectivity to alcohols and seemed to be a promising catalyst because there was a low selectivity towards pentyl-pentanoate and pentanes.

Therefore, copper is more selective in the process and we can optimize this reaction by finding a good support. From these results, this research direction took a turn in that the remainder of the studies focused on copper-based catalysts.

Figures 41 & 42 present the yields and selectivity based on the reactants fed onto copper chromite catalyst. Although the yield of alcohols is low when PEA with excess alcohol is fed, the selectivity towards alcohols is very high. This may be because ethanol adsorbs more strongly onto copper than ethyl-valerate. This saturates the surface with alcohol, selectively reacting pentanoic acid. When only PEA is fed, there is a high selectivity towards pentyl-pentanoate. This could be because pentyl-pentanoate reduction to pentanols occurs at a much slower rate than pentanoic acid to pentanols. When only ethyl-valerate is fed, there is a high selectivity towards alcohols but not as high when PEA with ethanol is fed. These results further served as the basis for the studies and experiments conducted in Chapters 1 and 2.

## Appendix A2: Supporting information for Chapter 1: Enhancing pentanol production rate by cofeeding alcohols in the presence of pentanoic acid in the liquid phase

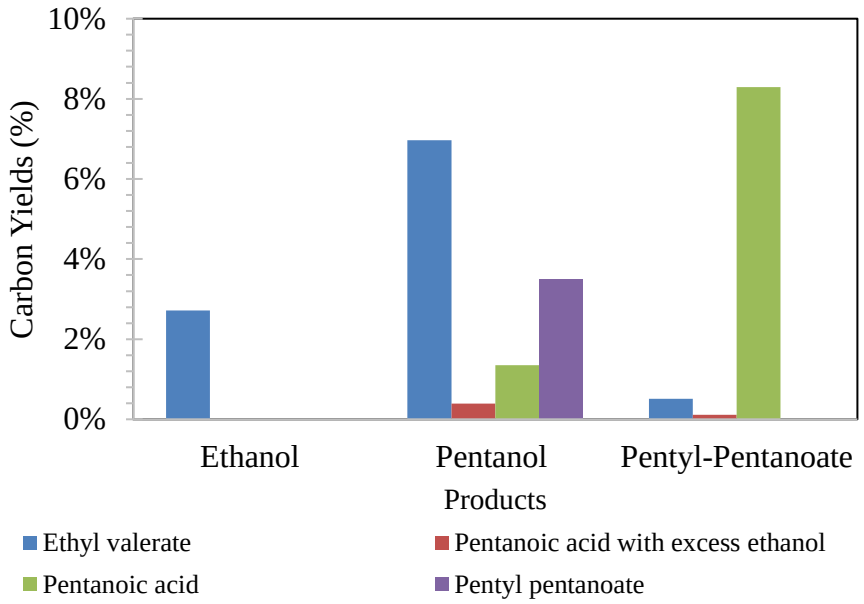



**Figure 46: Product distribution on copper chromite catalyst using various feeds. Reduction: 100 mg $2CuO{\cdot}Cr_2O_3$ at 280 °C under 300 psi $H_2$ for 2 hrs. Reaction: 250 °C for 2 hrs under 450 psi $H_2$. Feeds include: 0.421 M Ethyl-Valerate, 0.453 M Pentanoic Acid + excess ethanol (1:5 molar ratio), 0.424 M Pentanoic Acid, and 0.465 M Pentyl-Pentanoate**

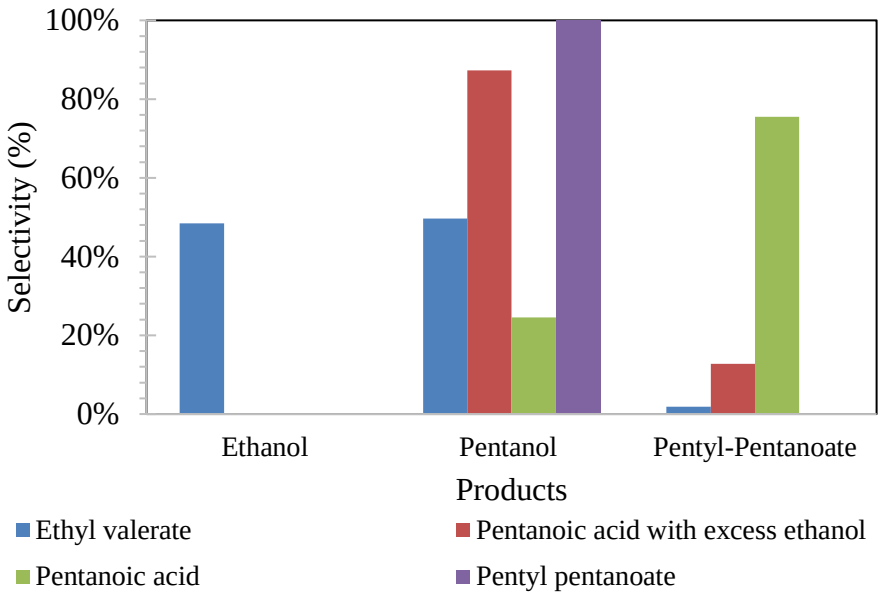



**Figure 47: Selectivity of products on copper chromite catalyst using various feeds. Conversion of reactants are shown in Section 2.3. 100 mg $2CuO{\cdot}Cr_2O_3$ reduced at 280 °C under 300 psi $H_2$ for 2 hours, reacted at 250 °C for 2 hours. Feeds include: 0.421 M Ethyl-Valerate, 0.453 M Pentanoic Acid + excess ethanol (1:5 molar ratio), 0.424 M Pentanoic Acid, 0.465 M Pentyl-Pentanoate**

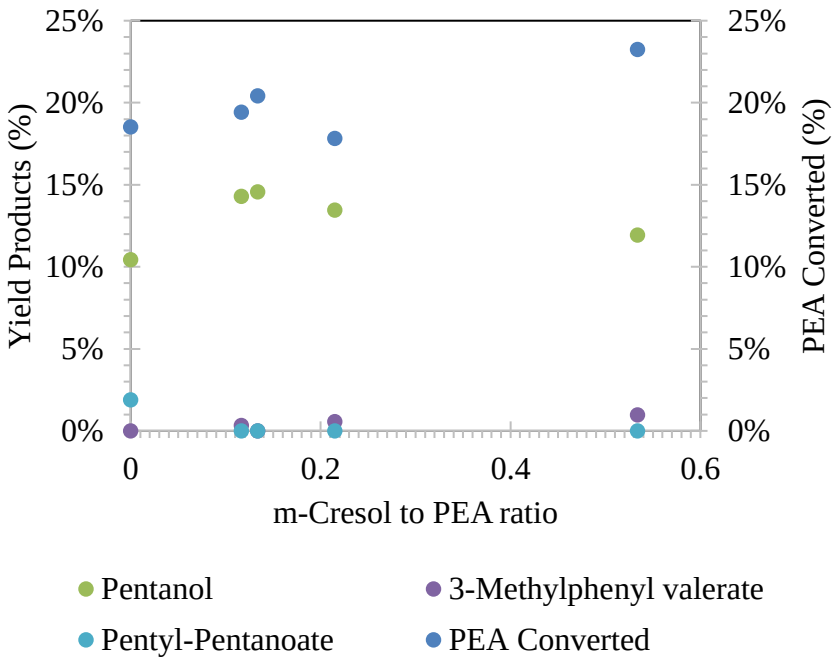



**Figure 48: Yield of products and conversion of PEA (%) at various molar ratios of m-cresol to PEA**

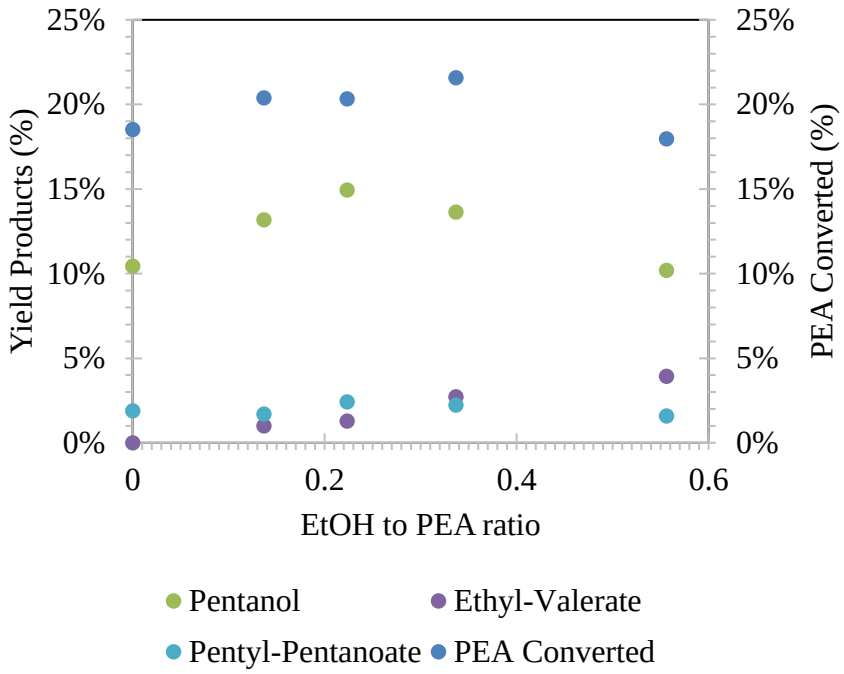



**Figure 49: Yield of products and conversion of PEA (%) at various molar ratios of ethanol to PEA**

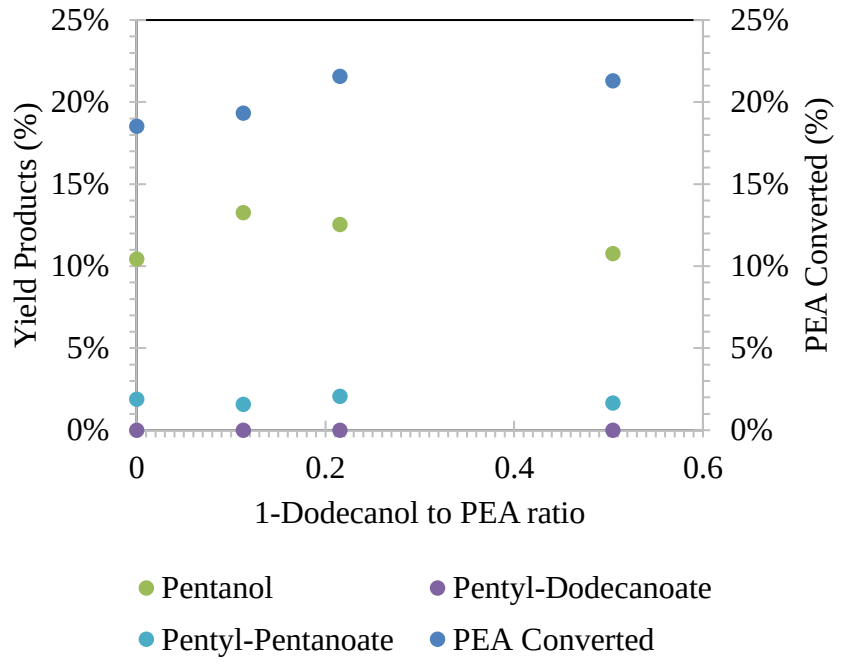



**Figure 50: Yield of products and conversion of PEA (%) at various molar ratios of 1-dodecanol to PEA**

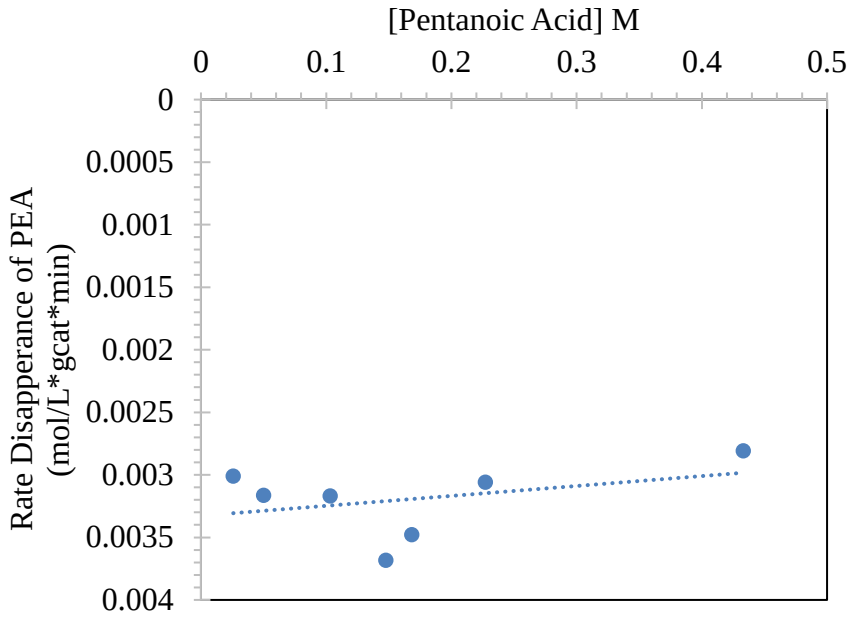



**Figure 51: Rate disappearance of PEA vs. concentration of PEA, zeroth order regime, reaction rate = k**

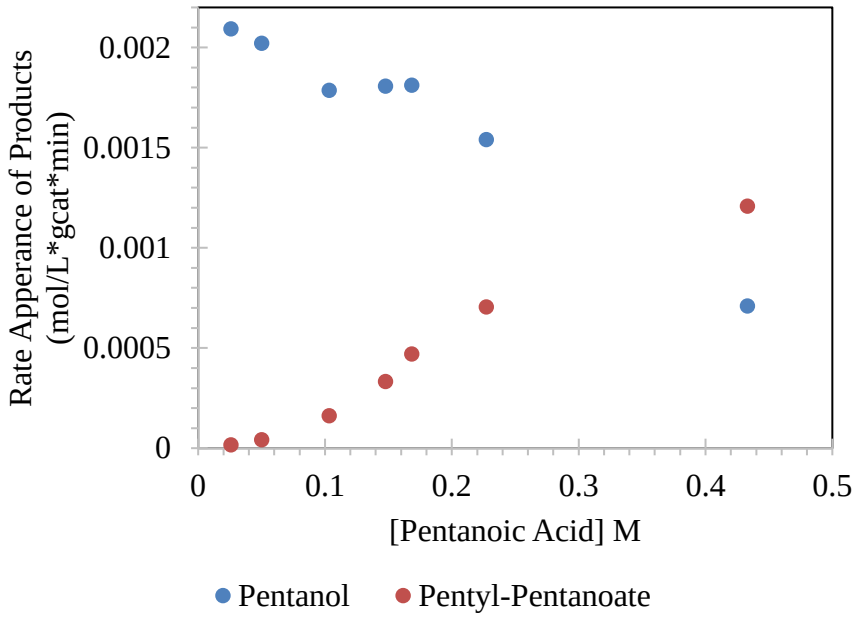



**Figure 52: Rate appearance of products vs. concentration of PEA at various concentrations of PEA, zeroth order regime with respect to PEA**

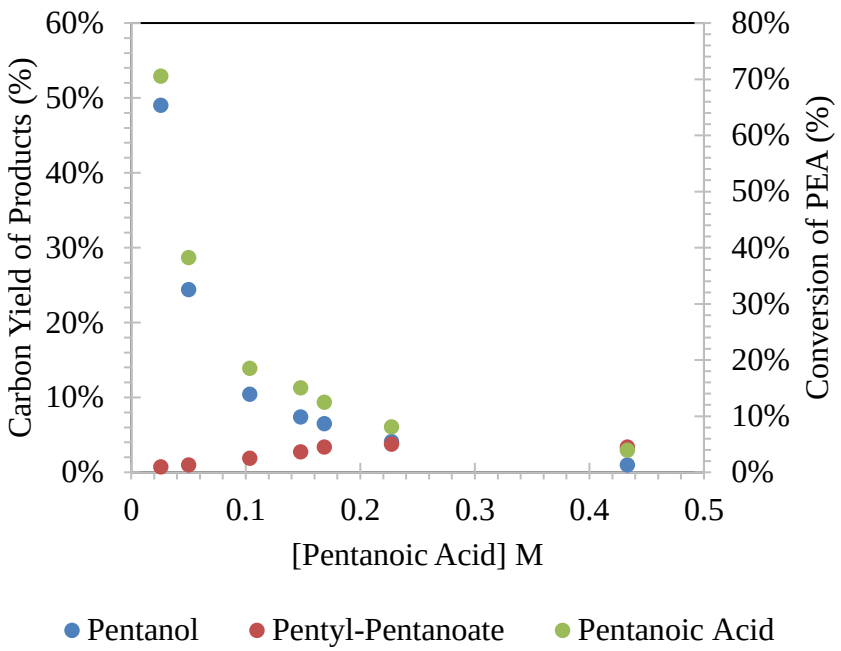



**Figure 53: Yield of products and conversion of PEA (%) at various concentrations of PEA, zeroth order regime with respect to PEA**

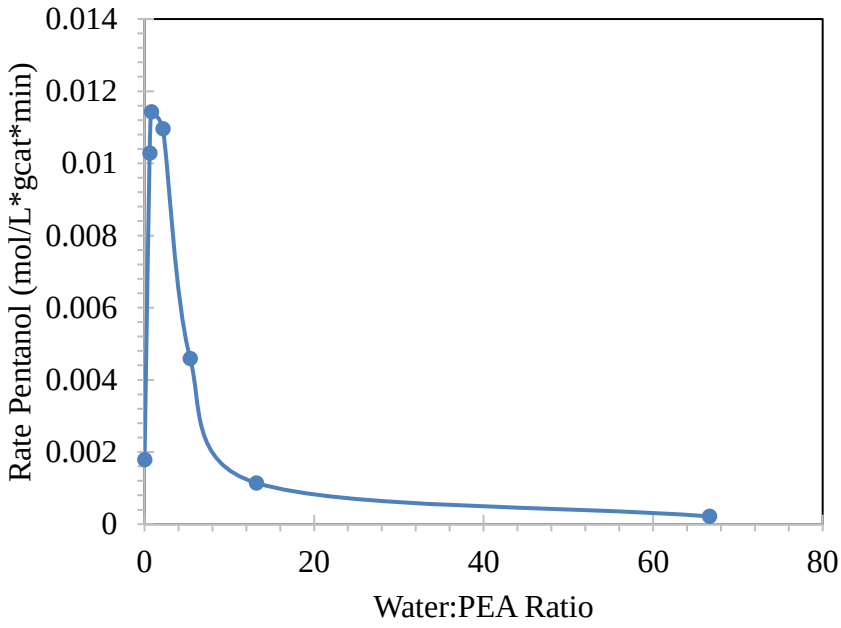



**Figure 54: Effect of various ratios of water to PEA on pentanol production rates**

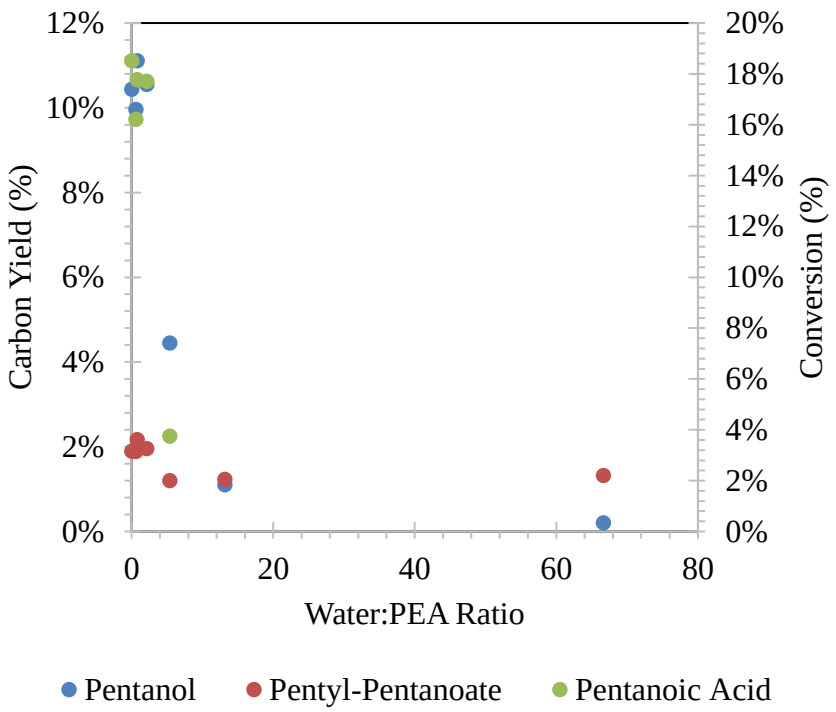



**Figure 55: Effect of various ratios of water to PEA on product yields and PEA conversion**

## Appendix A3: Supporting information for Chapter 2: Enhancing propanol production rate by cofeeding alcohols in the presence of propionic acid in the gas phase

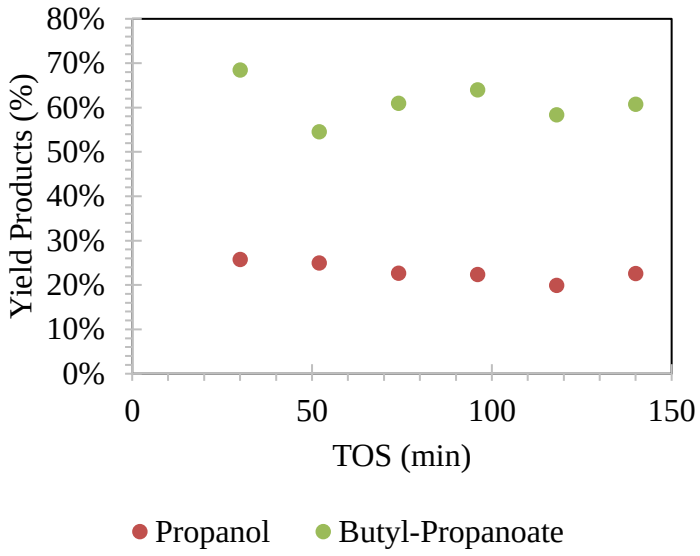



**Figure 56: Yield of products (%) when flowing 0.0013 mol/hr of propionic acid and 0.00067 mol/hr 1-butanol (1:0.5 molar ratio). Reduction: 50 mg of copper chromite, 400 °C, 1 hour, 100 stcm $H_2$. Reaction: 300 °C, 100 stcm $H_2$**

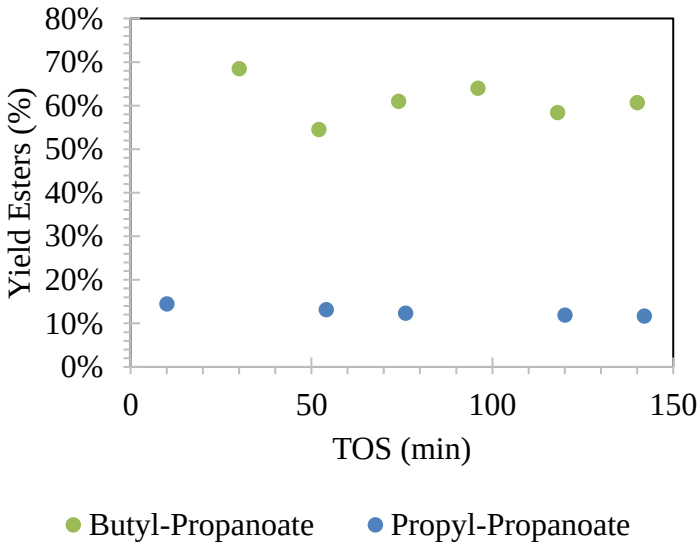



**Figure 57: Yield of propyl-propionate (%) when flowing 0.0013 mol/hr of propionic acid alone and yield of butyl-propionate (%) when flowing 0.0013 mol/hr of propionic acid and 0.00067 mol/hr 1-butanol (1:0.5 molar ratio). Reduction: 50 mg of copper chromite, 400 °C, 1 hour, 100 stcm $H_2$. Reaction: 300 °C, 100 stcm $H_2$**

## Appendix References


1. Duong, N. N., Wang, B., Sooknoi, T., Crossley, S. P., & Resasco, D. E. Enhancing the Acylation Activity of Acetic Acid by Formation of an Intermediate Aromatic Ester. *ChemSusChem* (2017).

2. J. Clayden, N. Greeves, S. Warren and P. Wothers, Organic Chemistry, Oxford University Press, 2000.

3. Deshpande, V. M., K. Ramnarayan, and Ch S. Narasimhan. "Studies on ruthenium-tin boride catalysts II. Hydrogenation of fatty acid esters to fatty alcohols." Journal of Catalysis 121.1 (1990): 174-182.

4. dos Santos, S. M., Silva, A. M., Jordão, E., & Fraga, M. A. (2005). Performance of RuSn catalysts supported on different oxides in the selective hydrogenation of dimethyl adipate. Catalysis today, 107, 250-257.

5. Tahara, K., Nagahara, E., Itoi, Y., Nishiyama, S., Tsuruya, S., & Masai, M. (1996). Liquid phase hydrogenation of carboxylic acid catalyzed by supported bimetallic Ru-Sn-alumina catalyst: effects of tin compounds in impregnation method. Journal of Molecular Catalysis A: Chemical, 110(1), L5-L6.

6. Tahara, K., Nagahara, E., Itoi, Y., Nishiyama, S., Tsuruya, S., & Masai, M. (1997). Liquid-phase hydrogenation of carboxylic acid on supported bimetallic Ru Sn-Alumina catalysts. Applied Catalysis A: General, 154(1), 75-86.

7. Mendes, M. J., Santos, O. A. A., Jordao, E., & Silva, A. M. (2001). Hydrogenation of oleic acid over ruthenium catalysts. Applied Catalysis A: General, 217(1), 253-262.

8. Adkins, Homer, and Karl Folkers. "The catalytic hydrogenation of esters to alcohols." Journal of the American Chemical Society 53.3 (1931): 1095-1097.

9. James Pritchard, Georgy A. Filonenko, Robbert van Putten, Emiel J. M. Hensen, and Evgeny A. Pidko. “Heterogeneous and homogeneous catalysis for the hydrogenation of carboxylic acid derivatives: history, advances and future directions.” *Chemical Society Reviews*. Royal Society of Chemistry, 05 May 2015.

10. Abdelrahman, O. A., Park, D. S., Vinter, K. P., Spanjers, C. S., Ren, L., Cho, H. J., ... & Dauenhauer, P. J. (2017). Biomass-Derived Butadiene by Dehydra-Decyclization of Tetrahydrofuran. ACS Sustainable Chemistry & Engineering, 5(5), 3732-3736.

11. Norman, David William. "Catalytic dehydration of alcohols and ethers over a ternary mixed oxide." U.S. Patent No. 8,981,172. 17 Mar. 2015.